

TECHNICAL REPORTS OF THE METEOROLOGICAL RESEARCH INSTITUTE No.37

Geochemical Study of the Atmosphere  
and Ocean in 1995 and 1996

by

Geochemical Research Department

気象研究所技術報告

第 37 号

大気と海洋の地球化学的研究  
(1995年及び1996年)

地球化学研究部



気 象 研 究 所

METEOROLOGICAL RESEARCH INSTITUTE, JAPAN

FEBRUARY 1999

# Meteorological Research Institute

Established in 1946

Director-General : Mr. Ryuji Hasegawa

Forecast Research Department	Director : Dr. Sadao Yoshizumi
Climate Research Department	Director : Mr. Hiroki Kondou
Typhoon Research Department	Director : Mr. Shouin Yagi
Physical Meteorology Research Department	Director : Mr. Kouichi Shirasaki
Atmospheric Environment and Applied Meteorology Research Department	Director : Dr. Tatsuo Hanafusa
Meteorological Satellite and Observation System Research Department	Director : Mr. Toyoaki Tanaka
Seismology and Volcanology Research Department	Director : Mr. Eishi Mochizuki
Oceanographical Research Department	Director : Dr. Takeshi Uji
Geochemical Research Department	Director : Dr. Katsuhiko Fushimi

1-1 Nagamine, Tsukuba, Ibaraki, 305-0052 Japan

## Technical Reports of the Meteorological Research Institute

Editor-in-chief : Hiroki Kondou

Editors : Masakatsu Kato      Nobuo Yamazaki      Akihiko Murata  
          Masashi Fukabori      Yukitomo Tsutsumi      Osamu Suzuki  
          Osamu Kamigaichi      Goro Yamanaka      Hidekazu Matsueda  
Managing Editors : Hiroshi Satoh, Takafumi Okada

The *Technical Reports of the Meteorological Research Institute* has been issued at irregular intervals by the Meteorological Research Institute since 1978 as a medium for the publication of technical reports, data reports and comprehensive reports on meteorology, oceanography, seismology and related earth sciences (hereafter referred to as reports) contributed by the members of the MRI and the collaborating researchers.

The Editing Committee reserves the right of decision on acceptability of manuscripts and is responsible for the final editing.

---

©1999 by the Meteorological Research Institute.

The copyright of reports in this journal belongs to the Meteorological Research Institute (MRI). Permission is granted to use figures, tables and short quotes from reports in this journal, provided that the source is acknowledged. Republication, reproduction, translation, and other uses of any extent of reports in this journal require written permission from the MRI.

In exception of this requirement, personal uses for research, study or educational purposes do not require permission from the MRI, provided that the source is acknowledged.

## 序

気象研究所地球化学研究部では、気候変動・地球環境問題の解明・予測への貢献を大きな目標として研究の推進を図っている。これは地球環境に関連する近年の諸問題の多くが地球上での化学物質の循環に関連して発生しており、これらの物質循環のメカニズムの解明が現在最も重要な課題となっているからである。

地球温暖化・気候変動をもたらす大気微量気体の増加、降水の広域酸性化、重金属・放射能汚染の拡大などのように、人類活動の大幅な増大に伴う人為起源物質の環境への大量導入によって、地球環境は最近の数十年間にかつてないほど急激で広範囲な化学的变化を起こしており、これが社会経済的に重大な影響をもたらしつつある。この変化の現状を時・空間的に正確にかつ総合的に把握し、変化のメカニズムの解明と、結果の予測を行うことは、国内外の社会的要請に応えるとともに、学問的にもきわめて重要である。

このため、地球化学研究部では、大気・海洋・地殻中の化学物質の濃度や挙動解析のための新しい手法を開発し、それに基づいて、各環境における化学物質の特性の把握や、環境間の物質交換過程などを含む物質循環の素過程の解明の研究を推進している。

特に、「温室効果気体を含む大気微量成分の挙動とそれを支配する要因の研究」、「大気・海洋間の物質交換に係わる諸過程の研究」及び「海洋における生物地球化学的諸過程の研究」に重点を置き、これらの研究に関連して「海洋と大気的人工放射性核種の動態に関する研究」も精力的に推進してきた。

地球化学研究部で推進するこれらの研究成果は、気象庁における大気、海洋の気候変動観測・監視業務や環境気象業務の推進・改善等に役立てられているとともに、世界気候研究計画（WCRP）や地球圏－生物圏国際協同研究計画（IGBP）などの国際的に推進されている重要な地球環境問題の研究計画にも寄与するものである。

得られた研究成果は、行政的報告書の他に、関連する内外の様々な学会誌等に個別に投稿されて論文として発表されているが、1年間の成果をまとめて概観できる年報的な英文報告物がこれまで作成されていなかった。1995年と1996年の最近の研究成果の概要をひとつの印刷物にまとめることによって、この間に行った研究の成果を一望してその足跡を確認し、今後の研究活動に役立たせるとともに、英文印刷物として地球化学研究部の研究成果の概要を広く内外に示すことにより、研究の一層の推進に役立てることができるものと考えている。

平成11年1月

地球化学研究部長 伏見克彦

Geochemical Study of the Atmosphere  
and Ocean in 1995 and 1996

by

Geochemical Research Department

大気と海洋の地球化学的研究  
(1995年及び1996年)

地球化学研究部

# Contents

FOREWORD .....	1
VOYAGE STATISTICS .....	2
Shipboard observations in 1995 .....	2
Shipboard observations in 1996 .....	3
Plane observations from Cairns/Sydney, Australia to Narita, Japan, since April 1993 .....	4
Radioactive fallout observations since 1958 .....	6
INTERNATIONAL/NATIONAL PROGRAMS .....	7
1995 ACTIVITIES .....	8
INTRODUCTION .....	8
GREENHOUSE GAS (CO <sub>2</sub> ) .....	8
1. Exchange of Chemical Substances Between Atmosphere and Ocean .....	8
1.1 Long-term trends in carbon dioxide partial pressure (pCO <sub>2</sub> ) in western North Pacific surface waters .....	8
1.2 Air-sea CO <sub>2</sub> exchange in central and western equatorial Pacific .....	10
1.3 Methods for dissolved inorganic carbon measurement in natural waters .....	12
2. Chemical Substance Exchange Between Atmosphere and Biosphere .....	12
2.1 Atmospheric CO <sub>2</sub> variations at the Meteorological Research Institute, Tsukuba, Japan .....	12
RADIOACTIVE NUCLIDES ( <sup>90</sup> Sr, <sup>137</sup> Cs, and Pu Isotopes) .....	14
3. Radioactive Materials in Air, Fallout, Rainwater, and Seawater .....	14
3.1 Geochemical studies on Chernobyl radioactivity in environmental samples .....	15
3.2 <sup>137</sup> Cs concentration temporal and spatial variation in western North Pacific and marginal seas from 1979 to 1988 .....	16
3.3 Recent <sup>90</sup> Sr and <sup>137</sup> Cs deposition observed in Tsukuba .....	18
3.4 Reference fallout material preparation for activity measurements .....	19
ORGANIC MATTER AND LIGANDS .....	21
4. Carbon and Nitrogen Biogeochemical Cycle at the Earth's Surface .....	21
4.1 Detection of dissolved protein molecules in oceanic waters and bacterial membranes: Possible source of major dissolved protein in seawater .....	21
4.2 Detection, characterization, and dynamics of dissolved organic ligands in oceanic waters .....	23
4.3 Relationship between particulate uranium .....	

and thorium-complexing capacity of oceanic particulate matter .....	24
ACID DEPOSITION .....	25
5. Acid Deposition at Summit of Mt. Fuji .....	25
IODINE .....	27
6. Iodine Determination in Natural and Tap Water	
Using Inductively Coupled Plasma Mass Spectrometry .....	27
1996 ACTIVITIES .....	30
INTRODUCTION .....	30
I. Field Observation Studies .....	30
GREENHOUSE GASES (CO <sub>2</sub> , CH <sub>4</sub> , and CO) .....	30
1. Studies on Greenhouse Gases in Upper Air Using Commercial Airlines .....	30
1.1 Atmospheric CO <sub>2</sub> and CH <sub>4</sub> measurements from 1993 to 1994 .....	30
1.2 CO <sub>2</sub> , CH <sub>4</sub> , and CO in the upper troposphere from 1993 to 1996 .....	34
2. Greenhouse Gas Behavior in Western and Central Pacific Ocean .....	36
2.1 Evaluation of CO <sub>2</sub> exchange at sea surface in western North Pacific:	
ΔpCO <sub>2</sub> distribution and CO <sub>2</sub> flux .....	36
2.2 Changes in longitudinal distribution of CO <sub>2</sub> partial pressure in central	
and western equatorial Pacific, west of 160°W .....	43
2.3 Temporal and spatial variations in atmospheric and oceanic CO <sub>2</sub>	
in western North Pacific from 1990 to 1993: Possible link to 1991/1992 ENSO event .....	45
2.4 Atmospheric methane over North Pacific from 1987 to 1993 .....	47
WATER MASS ANALYSIS .....	50
3. Western North Pacific .....	50
3.1 Water masses between Mindanao and New Guinea .....	50
3.2 Preliminary study of North Central Japan Sea temperature structure .....	52
RADIOACTIVE NUCLIDES .....	54
4. Anthropogenic Radionuclide Geochemical Studies and Analysis in Fallout Samples .....	54
ORGANIC MATTER AND LIGANDS .....	56
5. Ocean Biogeochemistry .....	56
5.1 Characterization of particulate protein in Pacific surface waters .....	56
5.2 Discrete dissolved and particulate proteins in oceanic waters .....	59

5.3 Abundance of viruses in deep oceanic waters .....	60
5.4 Extraction and characterization of organic ligands from oceanic water columns by immobilized metal ion affinity chromatography .....	62
5.5 Effects of ligand speciation on complexing abilities of strong ligands in natural waters .....	63
5.6 Determination of a strong organic ligand dissolved in seawater: Thorium-complexing capacity of organic matter dissolved in oceans .....	66
INTERNATIONAL ACTIVITIES .....	67
II. Participation in At-Sea Intercomparison of Underway pCO <sub>2</sub> System During <i>Meteor</i> Cruise 36-1 .....	67
III. Contribution to WOCE Hydrographic Program - Pacific Data QA Activity .....	67
1995 PUBLICATIONS .....	68
1996 PUBLICATIONS .....	69

# Geochemical Study of the Atmosphere and Ocean in 1995 and 1996

## Foreword

Contribution to society and science through geochemical study by clarifying the earth's changing climate and environment is the most important objective of the Geochemical Research Department (GRD) of the Meteorological Research Institute (MRI). Most recent environmental problems have occurred in connection with chemical substance cycling, and science's most important task is to clarify the mechanism of substance cycling.

The earth's chemical environment has changed rapidly in the last decades, due to the massive introduction of anthropogenic substances caused by the abrupt expansion of human activities, such as increasing atmospheric trace gases leading to global warming and climate change, the wide-ranging expansion of acid rain, heavy metals, and radioactive substances. This change has brought serious effects on society and economics. It is also scientifically important to meet the needs of society to understand the change precisely and comprehensively, temporally and spatially, and to clarify mechanisms to predict consequences.

To meet these scientific and social needs, scientists in the GRD have promoted the development of new methods for analyzing chemical substances in the atmosphere, ocean, and earth's crust, and the study of geochemical cycle processes of substances in the environment and exchange processes between environments. Our recent studies focus on the behavior of atmospheric trace components including greenhouse gases, gas and particle air/sea exchange processes, biogeochemical processes in the ocean, and in connection with these geochemical studies, behavior of artificial radioactive nuclides in the ocean and atmosphere.

These studies are expected to be useful for promoting and improving Japan Meteorological Agency (JMA) business in the fields of climate and environmental observation and monitoring and to contribute to international scientific studies such as the World Climate Research Program (WCRP) and International Geosphere-Biosphere Program (IGBP).

Our results are submitted to and published in numerous scientific papers and administrative documents. Annual English-language summaries remain to be published yet, however. Such summaries would, I believe, be very useful in providing a bird's-eye view of our studies in 1995 and 1996, and to make known our scientific prospects.

**Katsuhiko Fushimi**  
**Director, GRD**

# VOYAGE STATISTICS

## Shipboard observations in 1995

Cruise	Ship	Track/Sampling site	Substance
KH-90-2	R.V. <i>Hakuho Maru</i>	Tokyo (September 3, 1990) - Suva (Fiji) - Papeete (Tahiti) - Honolulu (October 25, 1990)	pCO <sub>2</sub>
KH-90-3	R.V. <i>Hakuho Maru</i>	Honolulu (October 31, 1990) - Rabaul (Papua New Guinea) - Guam - Tokyo (December 14, 1990)	pCO <sub>2</sub>
Ry-79-01	R.V. <i>Ryofu Maru</i>	137°E transect (January 1979)	<sup>137</sup> Cs
Ry-80-01	R.V. <i>Ryofu Maru</i>	137°E transect (January 1980)	<sup>137</sup> Cs
Ry-81-01	R.V. <i>Ryofu Maru</i>	137°E transect (Jan.-Feb. 1981)	<sup>137</sup> Cs
Ry-82-01	R.V. <i>Ryofu Maru</i>	137°E transect (January 1982)	<sup>137</sup> Cs
Ry-83-01	R.V. <i>Ryofu Maru</i>	137°E transect (January 1983)	<sup>137</sup> Cs
Ry-84-01	R.V. <i>Ryofu Maru</i>	137°E transect (Jan.-Feb. 1984)	<sup>137</sup> Cs
Ry-85-01	R.V. <i>Ryofu Maru</i>	137°E transect (January 1985)	<sup>137</sup> Cs
Ry-86-01	R.V. <i>Ryofu Maru</i>	137°E transect (January 1986)	<sup>137</sup> Cs
Ry-86-04	R.V. <i>Ryofu Maru</i>	31.5°N, 145.3°E (April 21, 1986)	<sup>137</sup> Cs
Ry-86-07	R.V. <i>Ryofu Maru</i>	34°N, 137°E (July 21, 1986)	<sup>137</sup> Cs
Ry-86-08	R.V. <i>Kofu Maru</i>	43°N, 138°E-45.3°N, 145°E (Aug. 1986)	<sup>134,137</sup> Cs
Ry-86-09	R.V. <i>Ryofu Maru</i>	35.3°N, 141°E-38.5°N, 145.5°E (Sep. 1986)	<sup>134,137</sup> Cs
Ry-87-01	R.V. <i>Ryofu Maru</i>	137°E transect (January 1987)	<sup>137</sup> Cs
NA-87-01	R.V. <i>Natsushima</i>	4°N, 180°E-6.2°N, 159.8°E (Feb. 1987)	<sup>134,137</sup> Cs
Ch-87-03	R.V. <i>Chofu Maru</i>	27.8°N-130.7°E (March 1987)	<sup>134,137</sup> Cs
Ry-87-04	R.V. <i>Ryofu Maru</i>	31.5°N, 145.7°E (April 1987)	<sup>134,137</sup> Cs
Ko-87-08	R.V. <i>Kofu Maru</i>	41.5°N, 147°E-44.2°N, 141°E (Aug. 1987)	<sup>134,137</sup> Cs
Ry-88-01	R.V. <i>Ryofu Maru</i>	137°E transect (January 1988)	<sup>137</sup> Cs
KH-93-4	R.V. <i>Hakuho Maru</i>	22.8°N, 158°W-45.2°N, 165.5°E (Oct.-Nov. 1993)	Protein

## Shipboard observations in 1996

Cruise	Ship	Track/Sampling site	Substance
NA-8701	R.V. <i>Natsushima</i>	Western and central equatorial Pacific (WCEP) (January-February 1987)	pCO <sub>2</sub> , CH <sub>4</sub>
NA-8901	R.V. <i>Natsushima</i>	WCEP (January-February 1989)	pCO <sub>2</sub> , CH <sub>4</sub>
NA-9001	R.V. <i>Natsushima</i>	WCEP (January-February 1990)	pCO <sub>2</sub> , CH <sub>4</sub>
NA-9101	R.V. <i>Natsushima</i>	WCEP (January-February 1991)	pCO <sub>2</sub> , CH <sub>4</sub>
LIDAR	R.V. <i>Kaiyo</i>	WCEP (November-December 1992)	pCO <sub>2</sub>
LIDAR	R.V. <i>Kaiyo</i>	WCEP (January-February 1994)	pCO <sub>2</sub>
TOCS	R.V. <i>Kaiyo</i>	WCEP (November-December 1992)	pCO <sub>2</sub>
TOCS	R.V. <i>Kaiyo</i>	WCEP (November-December 1994)	pCO <sub>2</sub>
KH-90-2	R.V. <i>Hakuho</i>	WCEP (September-December 1990)	pCO <sub>2</sub> , Protein, POC, PN, PCAA
KH-90-2	R.V. <i>Hakuho Maru</i>	Western, central North Pacific (WCNP) (September 1990)	Protein, POC, PN, PCAA
KH-90-3	R.V. <i>Hakuho Maru</i>	WCEP (September-December 1990)	pCO <sub>2</sub>
KH-91-3	R.V. <i>Hakuho Maru</i>	WCNP (May 1991)	Protein, POC, PN, PCAA
KH-93-4	R.V. <i>Hakuho Maru</i>	Western North and western equatorial Pacific (October- November 1993)	Protein
Ry-90-01	R.V. <i>Ryofu Maru</i>	137°E transect (January 1990)	Protein, POC, PN, PCAA
Ry-91-01	R.V. <i>Ryofu Maru</i>	137°E transect (January-February 1991)	pCO <sub>2</sub>
Ry-91-06	R.V. <i>Ryofu Maru</i>	137°E, 155°E transects (June-July 1991)	pCO <sub>2</sub>
Ry-92-01	R.V. <i>Ryofu Maru</i>	137°E transect (January-February 1992)	pCO <sub>2</sub>
Ry-92-06	R.V. <i>Ryofu Maru</i>	137°E, 155°E transects (June-July 1992)	pCO <sub>2</sub>
Ry-93-01	R.V. <i>Ryofu Maru</i>	137°E transect (January-February 1993)	pCO <sub>2</sub>
Ry-93-06	R.V. <i>Ryofu Maru</i>	137°E, 155°E transects (June-July 1993)	pCO <sub>2</sub>
Ry-87-01	R.V. <i>Ryofu Maru</i>	137°E transect (January-February 1987)	CH <sub>4</sub>
Ry-88-01	R.V. <i>Ryofu Maru</i>	137°E transect (January-February 1988)	CH <sub>4</sub>
Ry-89-01	R.V. <i>Ryofu Maru</i>	137°E transect (January-February 1989)	CH <sub>4</sub>
Ry-90-01	R.V. <i>Ryofu Maru</i>	137°E transect (January-February 1990)	CH <sub>4</sub>
Ry-91-01	R.V. <i>Ryofu Maru</i>	137°E transect (January-February 1991)	CH <sub>4</sub>
Ry-92-01	R.V. <i>Ryofu Maru</i>	137°E transect (January-February 1992)	CH <sub>4</sub>
Ry-93-01	R.V. <i>Ryofu Maru</i>	137°E transect (January-February 1993)	CH <sub>4</sub>
WOCE I	R.V. <i>Kaiyo</i>	Western equatorial Pacific (October 1992)	t, S, O <sub>2</sub> , Nutrients
WOCE II	R.V. <i>Kaiyo</i>	Western equatorial Pacific (February 1994)	t, S, O <sub>2</sub> , Nutrients
JKRJE	R.V. <i>Okean</i>	Japan Sea (March-April 1994)	t, S
JARE 34	I.B. <i>Fuji</i>	Indian and Southern Ocean (November 1992- March 1993)	Protein

Plane Observations From Cairns/Sydney, Australia, to Narita, Japan, Since April 1993

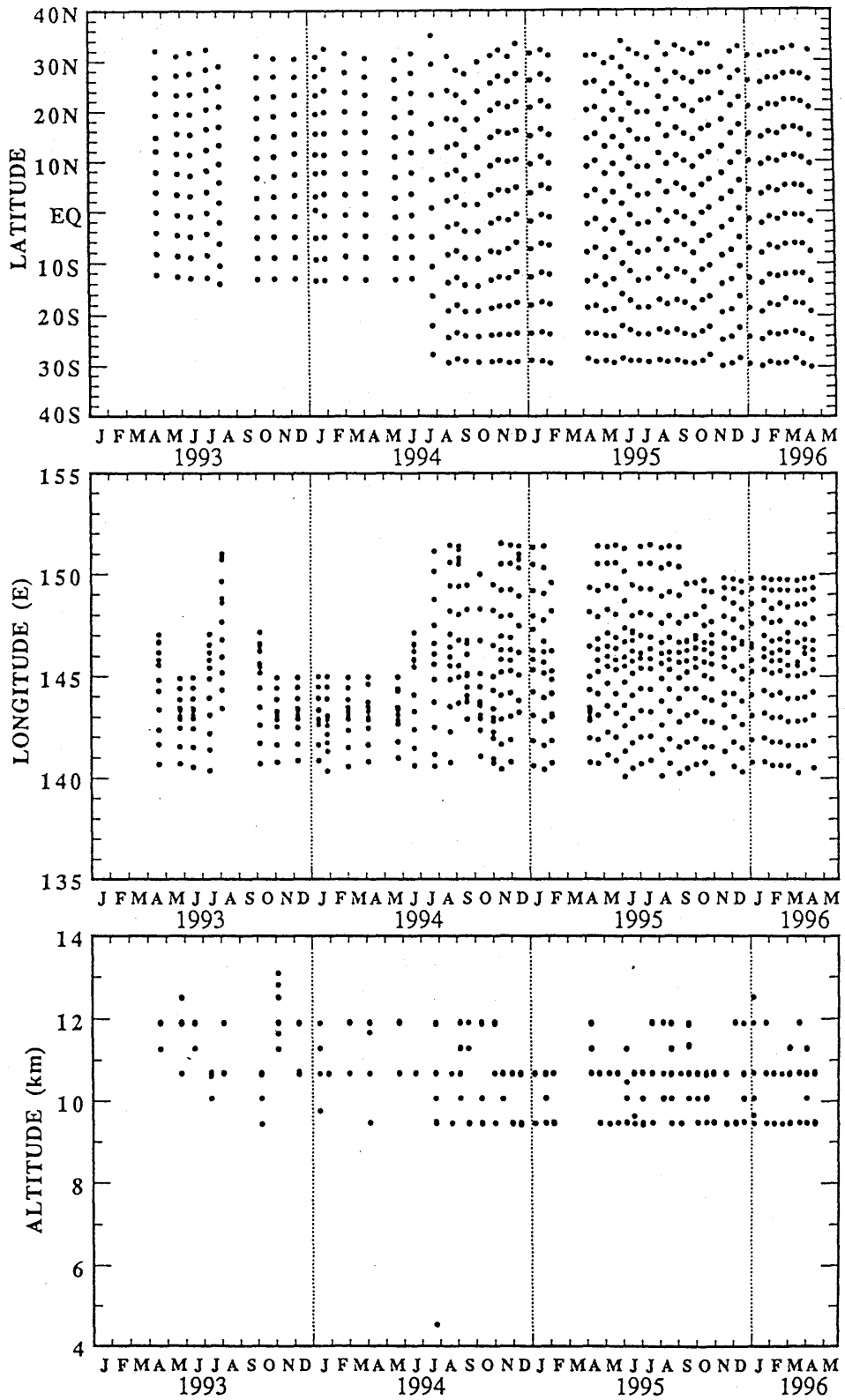
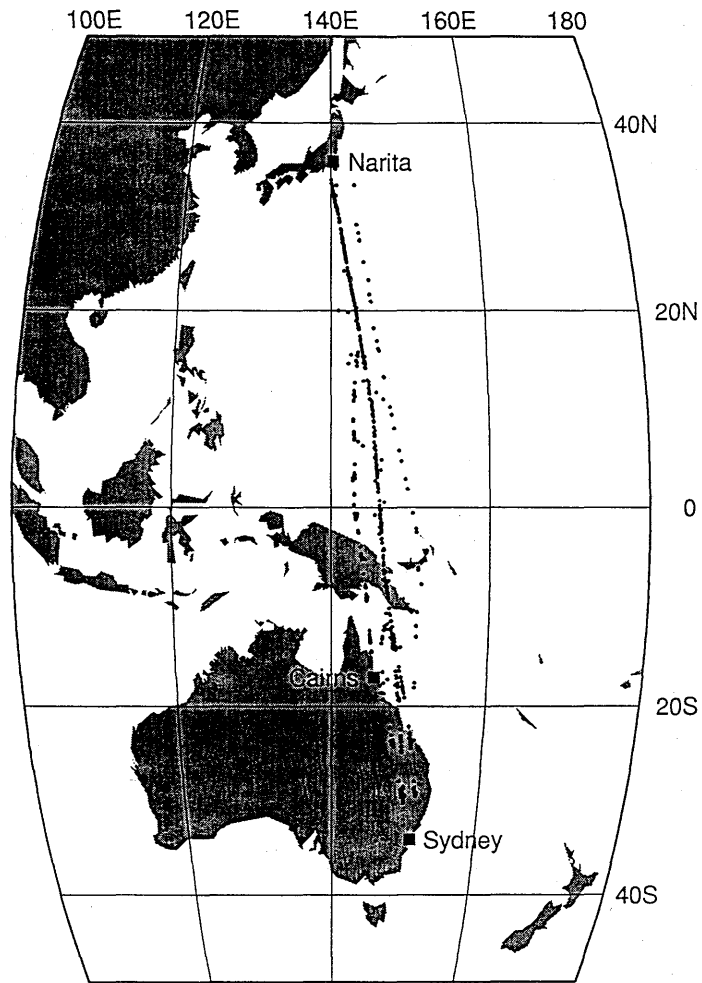


Fig. 1 Distributions of latitude(a), longitude(b) and altitude(c) of air samples collected from April 1993 to April 1996. (Matsueda *et al.*, 1997)



Sampling points (1993-1996)

Fig. 2 Sampling points of plane observations. (Matsueda *et al.*, 1997)

Radioactive fallout observations since 1958

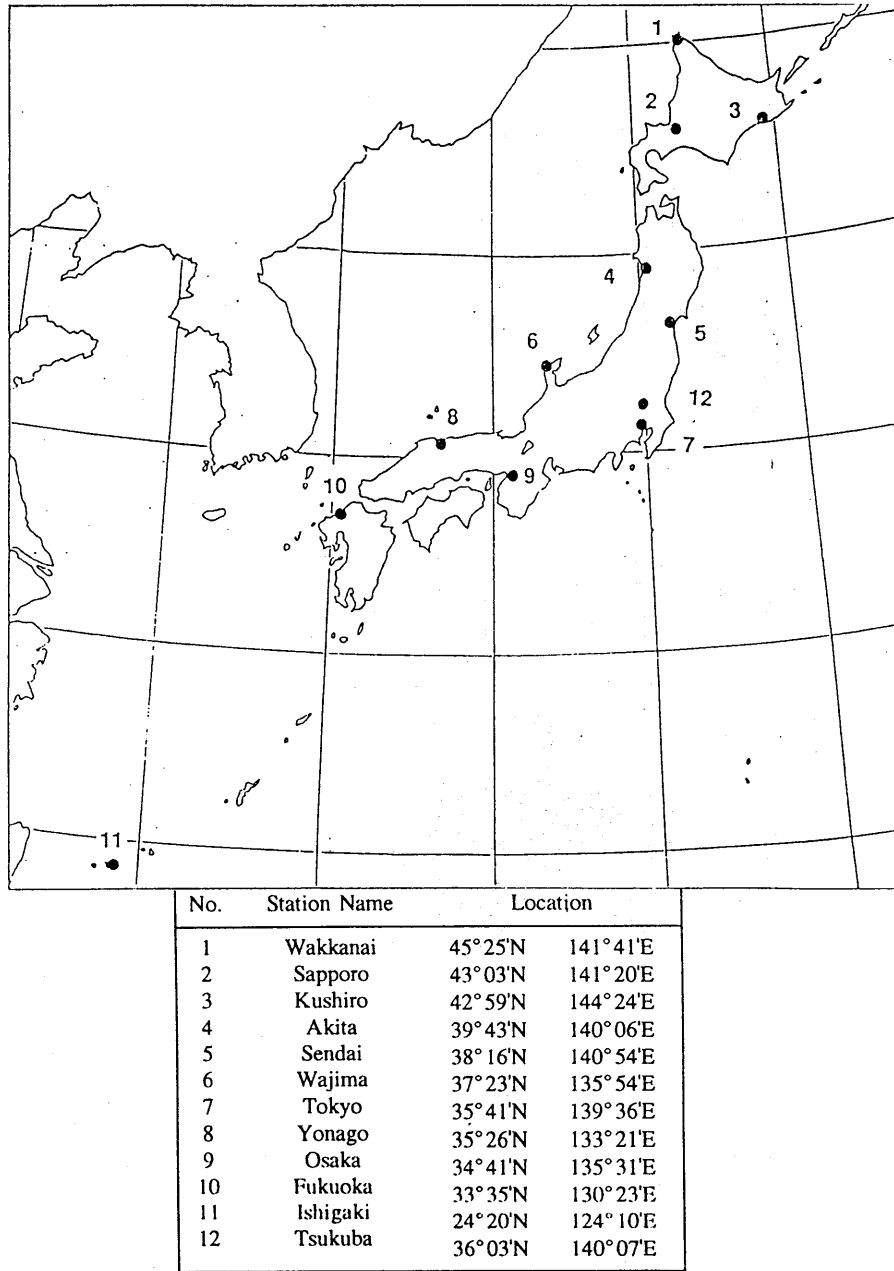


Fig. 3 Radioactive fallout sampling sites. (Hirose, 1995a)

## INTERNATIONAL/NATIONAL PROGRAMS

Table 1 1995 International/National Programs

International Study Number	
WCRP/WOCE	
IGBP/JGOFS	1.1, 1.2, 1.3, 4.1, 4.2, 4.3
IGBP/IGAC	2.1, 5
National Study Number	
JASRE (Reallocation fund from the Science and Technology Agency of Japan)	3.1, 3.2, 3.3, 3.4, 4.3, 6
JASBEGGA (Reallocation fund from the Science and Technology Agency of Japan)	1.1, 1.2, 1.3
GASREPA (Grant-in-Aid from Ministry of Education, Science and Culture of Japan)	4.1, 4.2
MRI/JMA operating funds	1.1, 1.2, 1.3, 2.1, 4.1, 4.2, 5

Table 2 1996 International/National Programs

International Study Number	
WCRP/WOCE	3.1, III
IGBP/JGOFS	2.1, 2.2, 2.3, 5.1, 5.2, 5.3, 5.4, 5.5, 5.6, II
IGBP/IGAC	1.1, 1.2, 2.4
National Study Number	
JASRE (Reallocation fund from the Science and Technology Agency of Japan)	3.2, 4
JASBEGGA (Reallocation fund from the Science and Technology Agency of Japan)	2.1, 2.2, 2.3
GASREPA (Grant-in-Aid from Ministry of Education, Science and Culture of Japan)	5.1, 5.2, 5.3, 5.4, 5.5
UAOCA (Fund supported by the JAL Foundation)	1.1, 1.2
MRI/JMA operating funds	1.1, 1.2, 2.1, 2.3, 2.4, 3.1, 5.1, 5.2, 5.3, 5.4, 5.5, 5.6

## 1995 ACTIVITIES

### INTRODUCTION

Clarifying the Earth's chemical environment is an important objective of the Geochemical Research Department (GRD). GRD scientists have studied the geochemical cycle of chemical substances found in the terrestrial environment – the atmosphere, the hydrosphere, and the lithosphere – since the 1940s.

With increasing human activity and the introduction of anthropogenic materials, the terrestrial chemical environment has been changing rapidly. Given the scientific and public considerations involved, our recent studies have been focused on obtaining precise, accurate information on the following subjects: temporal and spatial variation of greenhouse gases such as CO<sub>2</sub> in the atmosphere, carbon and nitrogen cycles in the marine environment, the exchange rate of chemical substances between the ocean and atmosphere as well as the biosphere and atmosphere, radioactive contamination of the ocean and atmosphere, and the behavior of natural and artificial chemicals in the air and ocean.

We are involved in many scientific projects related to large national and international programs such as the Japanese Study on the Radioactivity in the Environment (JASRE), Japanese Study on the Behavior of Greenhouse Gases and Aerosols (JASBEGGA), World Climate Research Program (WCRP)/World Ocean Circulation Experiment (WOCE), International Geosphere-Biosphere Program (IGBP)/Joint Global Ocean Flux Study (JGOFS) and International Global Atmospheric Chemistry Program (IGBP/IGAC).

At yearend, the department had 10 scientific staffers.

International/National scientific programs and budgetary funds for our studies are shown in Table 1.

### GREENHOUSE GAS (CO<sub>2</sub>)

#### 1. Exchange of Chemical Substances Between Atmosphere and Ocean

##### 1.1 Long-term trends in carbon dioxide partial pressure (pCO<sub>2</sub>) in western North Pacific surface waters

**Inoue, Matsueda, Fushimi, Hirota, Asanuma, and Takasugi (1995)**

Carbon dioxide in the atmosphere appears to play a major role in determining the earth's climate and habitability through its regulation of solar radiation balance. Atmospheric CO<sub>2</sub> levels have been increasing since the Industrial Revolution, mainly due to anthropogenic of CO<sub>2</sub> emissions.

Open oceans have been regarded as an important "sink" for processing anthropogenic CO<sub>2</sub>, but few measurements have confirmed oceanic CO<sub>2</sub> uptake. Inoue *et al.* (1995) studied the long-term trends of carbon dioxide partial pressure (pCO<sub>2</sub>) in surface waters of the western North Pacific, analyzing data in the western North Pacific and the overlying air measured regularly on board the Japan Meteorological Agency (JMA) research vessel "Ryofu Maru" (Fig. 95-1).

pCO<sub>2</sub> in surface seawater (pCO<sub>2</sub><sup>sea</sup>) observed every boreal winter from 1984 to 1993 gives a growth rate of  $1.8 \pm 0.6 \mu\text{atm yr}^{-1}$  north of 15°N and  $0.5 \pm 0.7 \mu\text{atm yr}^{-1}$  south of 14°N, averaging  $1.2 \pm 0.9 \mu\text{atm yr}^{-1}$ . The rate

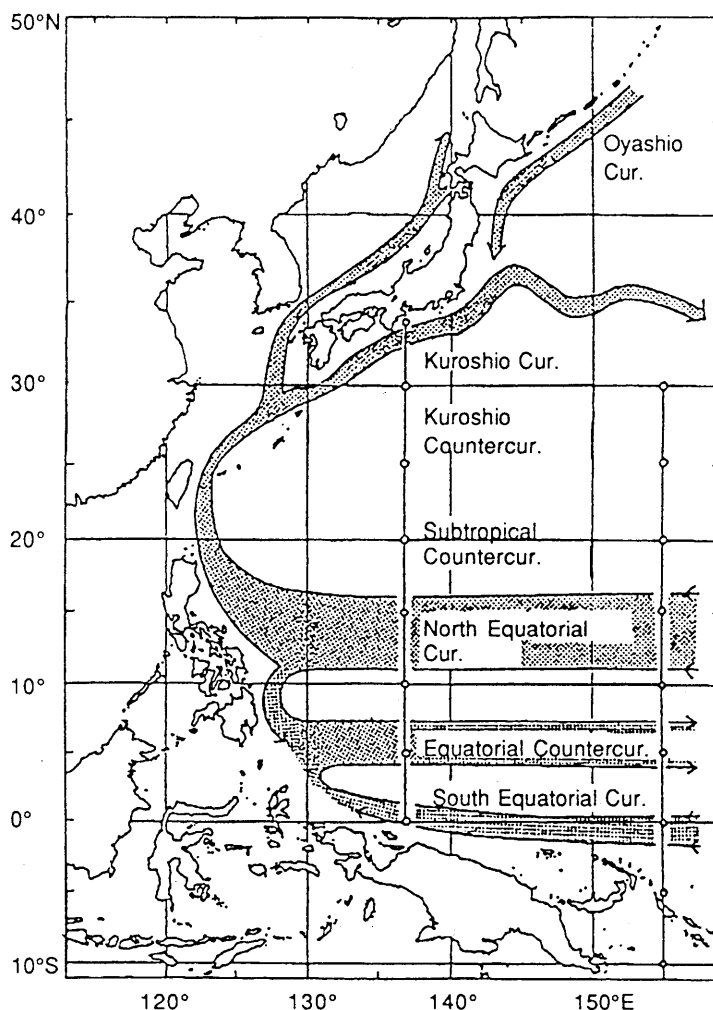


Fig. 95-1 Repeated transects where  $p\text{CO}_2^{\text{sea}}$  measurements were made since 1981. Open circles: oceanographic stations, where seawater samples from surface to the bottom were taken by CTD casts for measurement of oxygen,  $\text{TCO}_2$ , nutrients, salinity, etc. South of  $32^\circ\text{N}$  along  $137^\circ\text{E}$ , oceanographic stations were located every  $1^\circ$  and CTD casts to 1000 (or 2000) dbar were obtained. Typical major western North Pacific currents patterns are indicated.

of  $p\text{CO}_2^{\text{sea}}$  increase north of  $15^\circ\text{N}$  equals that of atmospheric  $\text{CO}_2$  ( $1.8 \mu\text{atm yr}^{-1}$ ) during the same period although that south of  $14^\circ\text{N}$  is lower (Fig. 95-2).

They estimated the annual  $\text{CO}_2$  flux between the sea and air based on monthly mean  $\Delta p\text{CO}_2$  and the gas transfer coefficient calculated according to Liss and Merlivat (1986), Tans *et al.* (1990), and Wanninkhof (1992). Large  $\text{CO}_2$  influx occurred off the coast of Japan ( $-16 \text{ mmol m}^{-2}\text{day}^{-1}$ , based on Tans *et al.*, 1990) because of the large negative  $\Delta p\text{CO}_2$  ( $-60 \mu\text{atm}$ ) and strong wind during winter. In the sink area, the annual mean air-sea  $\text{CO}_2$  flux ranged from  $-8 \text{ mmol m}^{-2}\text{day}^{-1}$  at  $31^\circ\text{N}$  to  $-1 \text{ mmol m}^{-2}\text{day}^{-1}$  at  $11^\circ\text{N}$ .

The  $p\text{CO}_2^{\text{sea}}$  increase rate is therefore high where the ocean acts as a strong sink for atmospheric  $\text{CO}_2$ . South of  $10^\circ\text{N}$ , the ocean acts as a source ( $0.2\text{--}0.7 \text{ mmol m}^{-2}\text{day}^{-1}$ ), but  $\text{CO}_2$  evasion flux is considerably smaller than in the central and eastern equatorial Pacific.

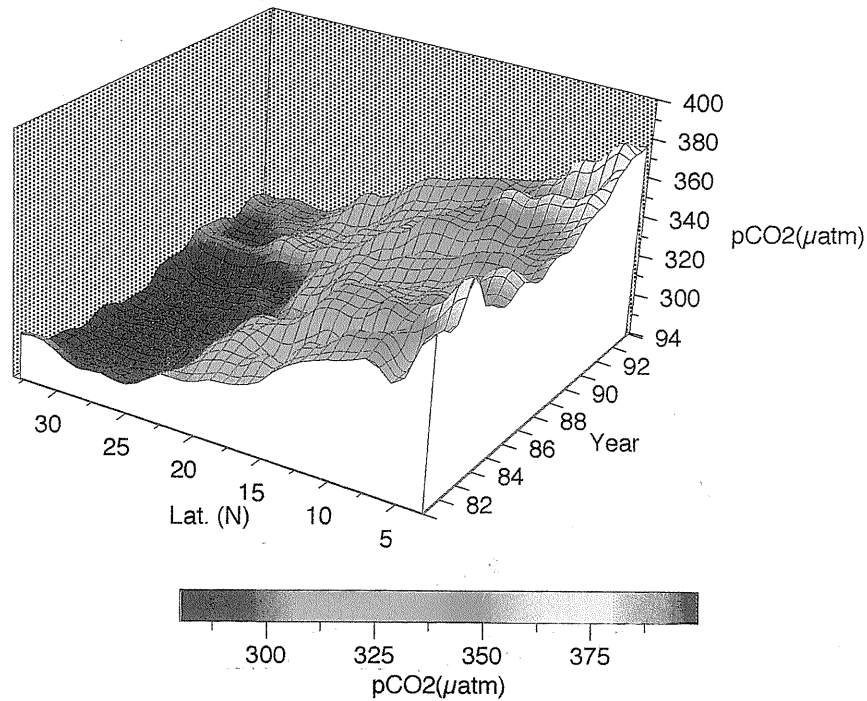


Fig. 95-2 Temporal variations in pCO<sub>2</sub> along 137°E observed in late January.

## 1.2 Air-sea CO<sub>2</sub> exchange in central and western equatorial Pacific

Ishii and Inoue (1995)

Ishii and Inoue (1995) studied the air-sea exchange of CO<sub>2</sub> in the central and western equatorial Pacific. They made measurements of CO<sub>2</sub> in marine boundary air and in surface seawater of the central and western Pacific west of 150°W from September to December 1990 (Fig. 95-3). They observed a steep decrease in pCO<sub>2</sub><sup>sea</sup> from 400 μatm to 350 μatm between 179°E and 170°E along with a decrease in salinity (Fig. 95-4). West of 170°E, where salinity is low due to heavy rainfall, pCO<sub>2</sub><sup>sea</sup> was nearly equal to pCO<sub>2</sub><sup>air</sup>. They evaluated the net CO<sub>2</sub> flux from the sea to the atmosphere in the region (15°S-10°N, 140°E-150°W) from the pCO<sub>2</sub> distribution and several gas transfer coefficients reported so far (Table 95-1). It ranged from 0.13 GtC year<sup>-1</sup> to 0.29 GtC year<sup>-1</sup>. This CO<sub>2</sub> evasion flux is thought to almost disappear during an El Niño event.

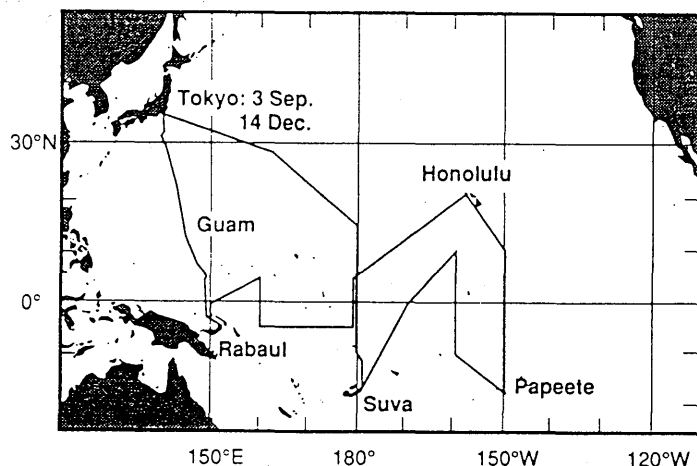


Fig. 95-3 Tracks of KH-90-2 and KH-90-3 of the R.V. *Hakuho Maru*. KH-90-2 is from Tokyo (September 3, 1990) to Honolulu (Hawaii) (October 25, 1990) via Suva (Fiji) and Papeete (Tahiti). KH-90-3 is from Honolulu (October 31, 1990) to Tokyo (December 14, 1990) via Rabaul (Papua New Guinea) and Guam.

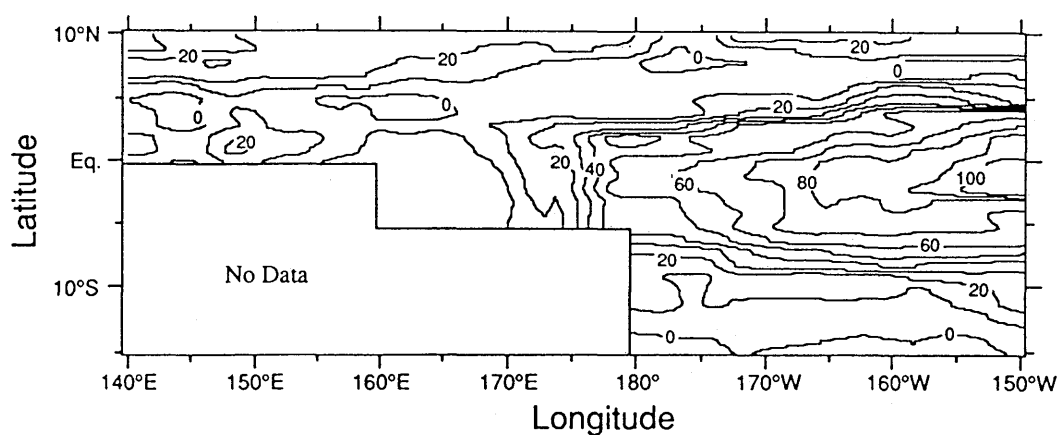


Fig. 95-4 Distribution of  $\Delta p\text{CO}_2$  in central and western equatorial Pacific in September 1990.

Table 95-1  $\text{CO}_2$  flux (MtC) in the central and western equatorial Pacific in September-November 1990

Eq.	Flux (15°S-1°S) (MtC)	Flux (0°-10°N) (MtC)		Total flux (MtC)
<i>(Flux accumulated twice-daily flux over a month)</i>				
	GANAL	GANAL		GANAL
Liss and Merlivat	19.5	13.1		32.6
Wanninkhof (short)	30.2	21.1		51.3
Wanninkhof (short, chem)	36.6	26.8		63.4
Wanninkhof (long)	38.0	26.5		64.5
Tans et al.	42.3	29.0		71.3
<i>(Flux calculated by using monthly mean wind speed)</i>				
	GANAL	GANAL	WSCLI	GANAL
Liss and Merlivat	19.5	12.9	11.4	32.4
Wanninkhof (short)	28.9	19.8	18.5	48.7
Wanninkhof (short, chem)	35.4	25.6	24.4	61.0
Wanninkhof (long)	36.4	24.9	23.3	61.3
Tans et al.	42.2	29.0	25.7	71.2

Table 95-2 DIC ( $\mu\text{mol} \cdot \text{dm}^{-3}$ ) of natural water standards prepared with lake or sea water as measured by both the TOC-5000 and coulometer. Lake standards 1 and 2 were prepared from surface water collected at station 9 in the middle of Lake Kasumigaura in November 1993 and April 1994, respectively. Sea water standard 1 was prepared from surface water collected from the Western North Pacific at 20°N, 130°E in February 1992. Sea water standard 2 was prepared from a mix of surface waters collected from the Western North Pacific at 20°N, 137°E in January 1993 and at 19°N, 137°E in January 1994.

standard	instrument	mean [DIC]	std. dev.	bottles	reps/bottle
Lake 1	TOC-5000	997.1	4.8	2	6 & 10
Lake 1	Coulometer	994.2	0.6	4	1
Lake 2	TOC-5000	1013.9	3.0	5	4 to 8
Lake 2	Coulometer	1011.2	0.7	3	1
Sea 1	TOC-5000	2028.3	2.2	2	10
Sea 1	Coulometer	2026.5	0.6	4	1
Sea 2	TOC-5000	2048.4	6.2	3	6 to 16
Sea 2	Coulometer	2053.1	2.0	2	1 or 2

### 1.3 Methods for dissolved inorganic carbon measurement in natural waters

Weisburd, Ishii, Fukushima, and Otsuki (1995)

Knowing the concentrations of dissolved inorganic carbon (DIC) in natural waters is important in studies of ecology and biogeochemistry. The available measurement methods remain relatively difficult and imprecise. Weisburd *et al.* (1995) demonstrated that a commercially available, nondispersive infrared (ND-IR) organic carbon analyzer could provide relatively accurate, precise ( $\pm 2-3 \mu\text{mol dm}^{-3}$ ) DIC measurements (Table 95-2). This precision, though less than the  $0.5-1 \mu\text{mol dm}^{-3}$  for the state-of-the-art instrument ( $\text{CO}_2$  Coulometer), is adequate for many applications and is easier to use. For DIC transects and profiles in systems with moderate to large DIC variations or for discrete DIC productivity measurements, the TOC-5000's precision is generally sufficient. The precision of the coulometer remains necessary, however, for marine DIC surveys.

## 2. Chemical Substances Exchange Between Atmosphere and Biosphere

### 2.1 Atmospheric $\text{CO}_2$ variations at Meteorological Research Institute, Tsukuba, Japan

Inoue and Matsueda (1996)

The  $\text{CO}_2$  exchange between the air and biosphere is an important process controlling the level of atmospheric  $\text{CO}_2$  on a time scale of hours to decades. To get a better understanding of  $\text{CO}_2$  exchange between the air and terrestrial biosphere, measurements of the  $\text{CO}_2$  concentration in the surface air have been conducted at the Meteorological Research Institute (MRI, 36°04'N, 147°07'E, 25 m above sea level) in Tsukuba, 50 km northeast of Tokyo, Japan, since April 1986 (Fig.95-5).

Inoue and Matsueda (1996) began continuous measurements of  $\text{CO}_2$  in the air 1.5 m above the earth's surface in April 1986 and studied variations in atmospheric  $\text{CO}_2$  at the Meteorological Research Institute, Tsukuba, Japan (Fig. 95-6). At the end of February 1992, they added measurements of atmospheric  $\text{CO}_2$  at 200 m on a meteorological tower, 213 m high, 250 m from the 1.5 m sampling site. They selected  $\text{CO}_2$  data observed at MRI in daytime with hour-to-hour variation less than 1 ppmv and compared data with that of Ryori (39°02'N, 141°50'E), a continental station operated by the JMA. They showed that the selected  $\text{CO}_2$  record provided a representative  $\text{CO}_2$  level in surface air on spatial scales of at least a few hundred kilometers.

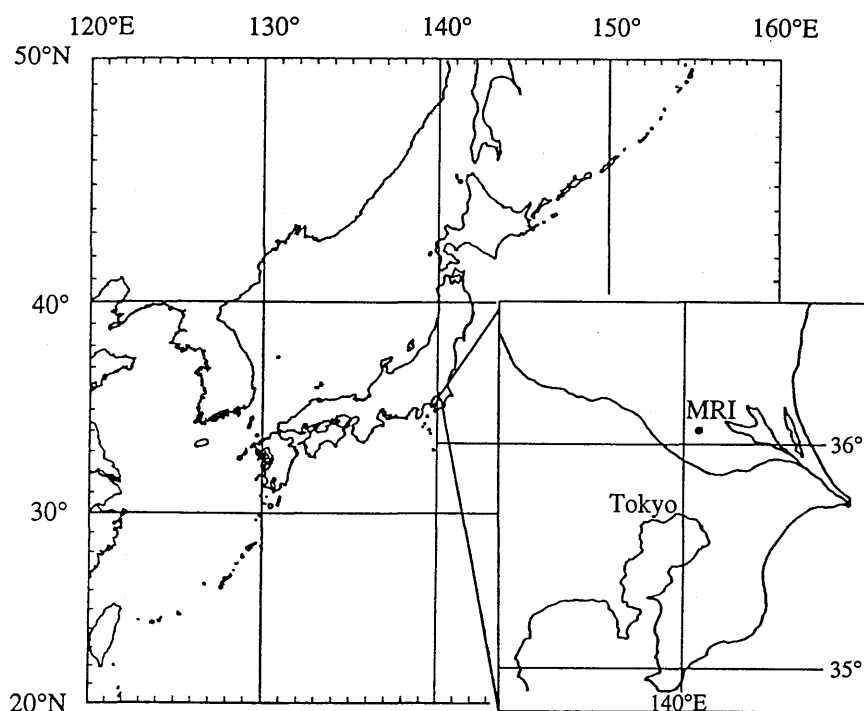


Fig. 95-5 MRI atmospheric CO<sub>2</sub> sampling site.

Reprinted from *J. Atmospher. Chem.*, **23** (1996), 137-161, Variations in atmospheric CO<sub>2</sub> at the Meteorological Research Institute, Tsukuba, Japan, Inoue and Matsueda, fig. 1 (©1996 Kluwer Academic Publishers. Printed in the Netherlands.) with kind permission from Kluwer Academic Publishers.

They also studied the interannual changes in photosynthesis/respiration against changes in climatological parameters. They found that respiration was sensitive to the temperature change within a small temperature anomaly (ca. 1°C), while photosynthesis was less sensitive. When the temperature anomaly is large, however, photosynthesis and respiration tend to be competitive. The decrease in respiration due to cooling (-0.7°C) could play an important role in determining the 1992 CO<sub>2</sub> level, which did not increase compared to that of 1991 in the Northern Hemisphere.

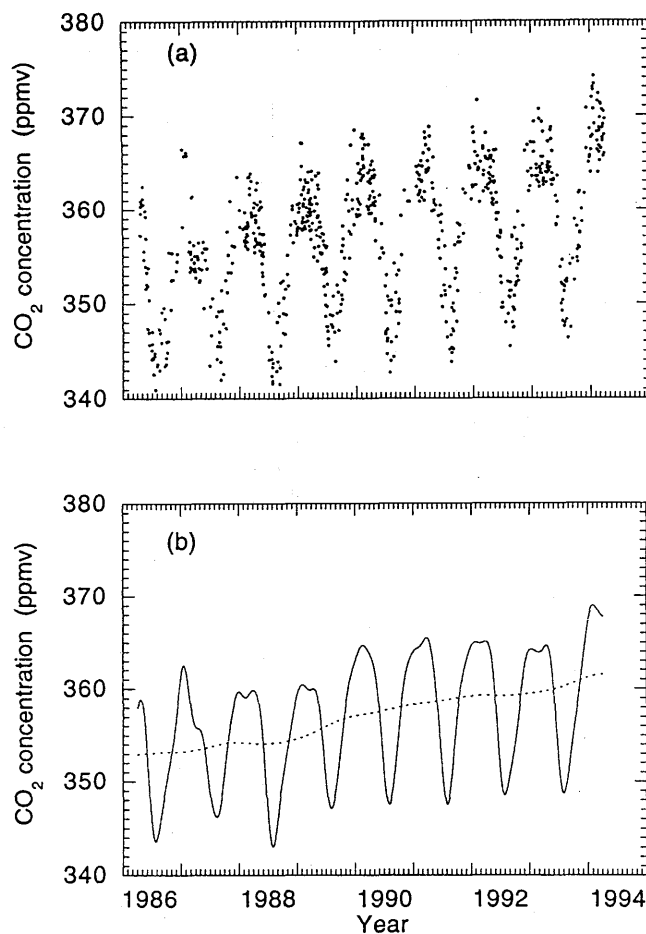


Fig. 95-6 Temporal variations in daily average when hour-to-hour changes are less than 1 ppmv (C<sub>p</sub>) between 11:00 JST and 16:00 JST. (a) displays all raw data from April 13, 1986, to March 31, 1994. The solid curve in (b) is for a low-pass filter with cutoff at 100 days and the dashed curve is for cutoff at 667 days. Reprinted from *J. Atmospher. Chem.*, **23** (1996), 137-161, Variations in atmospheric CO<sub>2</sub> at the Meteorological Research Institute, Tsukuba, Japan, Inoue and Matsueda, fig. 7 (©1996 Kluwer Academic Publishers. Printed in the Netherlands.) with kind permission from Kluwer Academic Publishers.

## RADIOACTIVE NUCLIDES (<sup>90</sup>Sr, <sup>137</sup>Cs, and Pu Isotopes)

### 3. Radioactive Materials in Air, Fallout, Rainwater, and Seawater

Global radioactive contamination derived from the fallout of nuclear weapon tests, waste disposal, or accidents at nuclear facilities has brought about scientific and social consequences. To evaluate the feedback effect on society and to trace the fate in the global environment, meteorological and oceanographic studies on the environmental radioactivity have been conducted for the last 40 years.

### 3.1 Geochemical studies on Chernobyl radioactivity in environmental samples

Hirose (1995a)

The Chernobyl accident on April 26, 1986, contaminated a wide area of the Northern Hemisphere. GRD scientists have comprehensively studied the environmental effect of Chernobyl fallout. Pronounced, high-level radioactivity has been observed in surface air and rainwater in Japan since May 3, 1986 and higher concentrations of Chernobyl radionuclides in surface air continued until early July 1986 (Aoyama *et al.*, 1986). Chernobyl fallout caused partly increasing  $^{137}\text{Cs}$  concentrations in surface water and riverwater (Hirose *et al.*, 1990). They obtained some new evidence about the transport of Chernobyl radioactivity to the stratosphere, dry deposition, and wet deposition (Aoyama *et al.*, 1987; Aoyama *et al.*, 1991; 1992; Hirose *et al.*, 1993).

Hirose (1995a) described the deposition of  $^{137}\text{Cs}$ ,  $^{90}\text{Sr}$ , and plutonium isotopes at Tsukuba in 1986 and summarized geochemical studies of Chernobyl fallout in Japan (Table 95-3). Artificial radionuclides in deposition and airborne dust samples in 1986 were measured at Tsukuba and 11 stations in Japan. Significant amounts of  $^{238}\text{Pu}$  and  $^{241}\text{Pu}$  were detected in deposition samples in May 1986 at Tsukuba.  $^{238}\text{Pu}/^{239,240}\text{Pu}$  and  $^{241}\text{Pu}/^{238}\text{Pu}$  ratios in monthly deposition show that meaningful amounts of Chernobyl-derived plutonium isotopes were transported to Japan, about 8,000 km distant from Chernobyl. Hirose found that the  $^{241}\text{Pu}/^{239,240}\text{Pu}$  activity ratio was useful as a geochemical marker because its isotopic ratios changed significantly for different sources of plutonium.

The Chernobyl  $^{90}\text{Sr}$  and plutonium isotopes, especially Pu, were preferentially scavenged from the atmosphere by wet and dry deposition, compared to volatile radionuclides such as  $^{131}\text{I}$  and  $^{137}\text{Cs}$ . This is due to the particle size difference between radionuclide-bearing aerosols; the order of particle size was Pu isotopes >  $^{90}\text{Sr}$  >  $^{137}\text{Cs}$  (Fig. 95-7). These findings suggest that large amounts of actinides were deposited near the accident site. This will require an assessment of the environmental effects of actinides because of their high toxicity and long radioactive life.

Table 95-3 Monthly Deposition of  $^{137}\text{Cs}$ ,  $^{90}\text{Sr}$ , and Plutonium Isotopes at Tsukuba in 1986

Month	$^{137}\text{Cs}$	$^{90}\text{Sr}$	$^{239,240}\text{Pu}$	$^{238}\text{Pu}$
	(Bq m <sup>-2</sup> )		(mBq m <sup>-2</sup> )	
January	0.036±0.010	0.021±0.003	0.065±0.013	-
February	0.083±0.016	0.027±0.004	0.343±0.060	-
March	0.080±0.016	0.094±0.011	1.02±0.11	0.061±0.020
April	0.097±0.013	0.024±0.002	0.155±0.023	-
May	131±13	1.24±0.14	0.650±0.045	0.107±0.020
June	2.51±0.27	0.164±0.019	0.075±0.014	0.021±0.010
July	0.783±0.084	0.015±0.002	0.069±0.012	0.020±0.010
August	0.369±0.045	0.018±0.002	0.133±0.019	0.010±0.007
September	0.087±0.014	0.011±0.002	0.148±0.021	0.017±0.009
October	0.106±0.020	0.016±0.002	0.266±0.027	0.030±0.010
November	0.071±0.012	0.019±0.002	0.129±0.019	0.025±0.010
December	0.078±0.016	0.010±0.001	0.150±0.020	0.025±0.009

The data of monthly  $^{137}\text{Cs}$  and  $^{90}\text{Sr}$  were cited from the results of Aoyama, *et al.*, 1991.

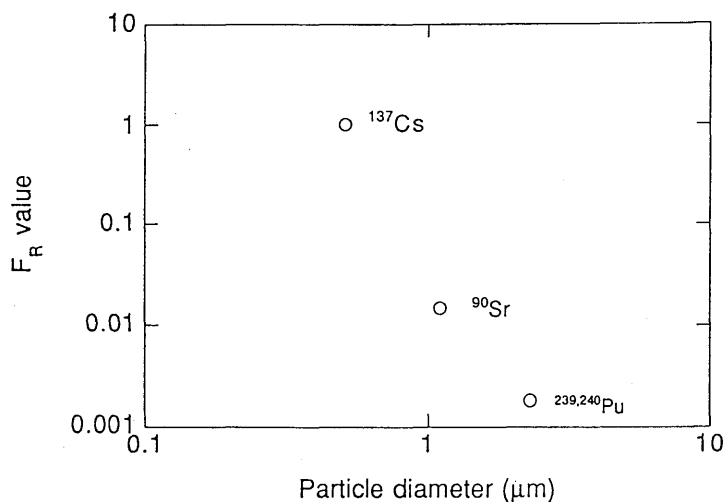


Fig. 95-7 F<sub>R</sub> and particle size of radionuclide-bearing particles.

### 3.2 <sup>137</sup>Cs concentration temporal and spatial variation in western North Pacific and marginal seas from 1979 to 1988

Aoyama and Hirose (1995)

After the Chernobyl accident in May 1986, intensified observation was conducted to study the geographical distribution of Chernobyl radioactivity. Aoyama and Hirose (1995) studied temporal and spatial variation of <sup>137</sup>Cs concentration in the western North Pacific and its marginal seas during the period from 1979 to 1988. <sup>137</sup>Cs concentrations in surface water along the 137°E transect from 1979 to 1988 were 5.0–10.6 mBq l<sup>-1</sup> between 30°N and 24°N, 3.4–7.8 mBq l<sup>-1</sup> between 24°N and 7°N, and 2.1–6.9 mBq l<sup>-1</sup> between 7°N and the Equator (Fig. 95-8). <sup>137</sup>Cs concentrations at stations between 30°N and 7°N did not show clear temporal variation, while those at stations south of 7°N increased from 1986 to 1988.

The <sup>137</sup>Cs concentration south of 7°N became the same magnitude as those in two latitude bands between 30°N and 7°N in 1987 and 1988. Chernobyl-derived <sup>134</sup>Cs was detected in surface water of marginal seas around Japan north of about 30°N, which reflects the meridional distribution of Chernobyl-derived <sup>134</sup>Cs in surface air over the western North Pacific (Fig. 95-9). The particulate cesium isotope concentration ranged from 0.1 to 1.0 % of the total cesium isotope concentration in 1986 and 1987.

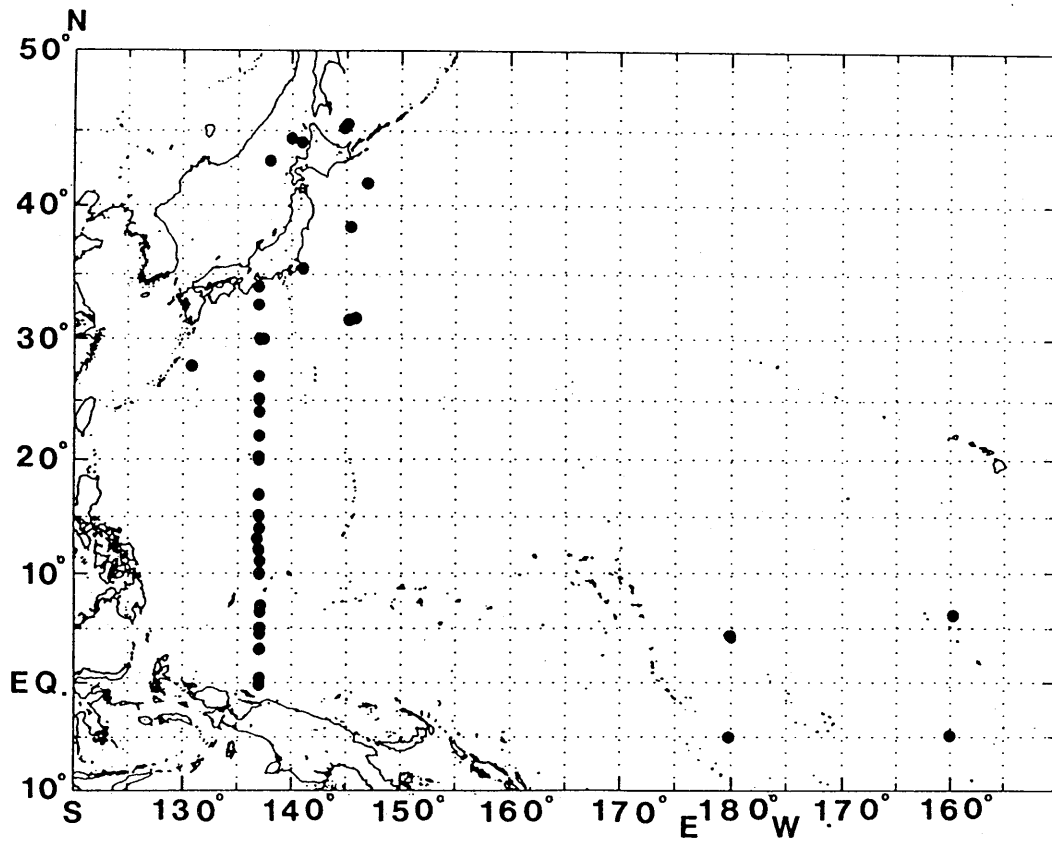


Fig. 95-8 Sampling sites.

Reprinted from *J. Environ. Radioactivity*, 29, Aoyama and Hirose, The temporal and spatial variation of  $^{137}\text{Cs}$  concentration in the western North Pacific and its marginal seas during the period from 1979 to 1988, 57-74, Copyright (1995), with permission from Elsevier Science.

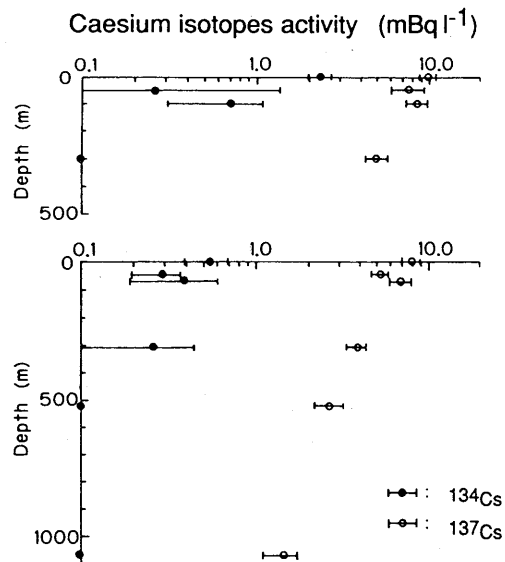


Fig. 95-9 Vertical distribution of  $^{137}\text{Cs}$  and  $^{134}\text{Cs}$  on August 22, 1986, at  $44^{\circ}30'N$ ,  $140^{\circ}00'E$  (upper panel) and on August 26, 1987, at  $44^{\circ}15'N$ ,  $140^{\circ}58'E$  (lower panel). Reprinted from *J. Environ. Radioactivity*, 29, Aoyama and Hirose, The temporal and spatial variation of  $^{137}\text{Cs}$  concentration in the western North Pacific and its marginal seas during the period from 1979 to 1988, 57-74, Copyright (1995), with permission from Elsevier Science.

### 3.3 Recent $^{90}\text{Sr}$ and $^{137}\text{Cs}$ deposition observed in Tsukuba

Igarashi, Otsuji-Hatori, and Hirose (1996)

Igarashi *et al.* (1996) studied recent deposition of  $^{90}\text{Sr}$  and  $^{137}\text{Cs}$  observed in Tsukuba. Referring to the trend in annual radioactivity deposition observed at the MRI since 1957, they showed the annual deposition of  $^{90}\text{Sr}$  in 1990s to be as low as around  $0.15 \text{ Bqm}^{-2}$  and that of  $^{137}\text{Cs}$  to be  $0.3 \text{ Bqm}^{-2}$  (Fig. 95-10). This is because no atmospheric nuclear weapons tests have been conducted since 1981. Although the Chernobyl accident brought a significant amount of  $^{137}\text{Cs}$  to Japan, no long-term effect seems to have continued in radioactivity deposition in Japan (Fig. 95-11). The present activity level is lower than that in 1985 when minimum annual radioactivity deposition was recorded.

Although a spring peak was found in deposition, it is difficult to explain this seasonal pattern only by stratospheric fallout. The variation in ratios of the radioactivity to corresponding stable elements did not show

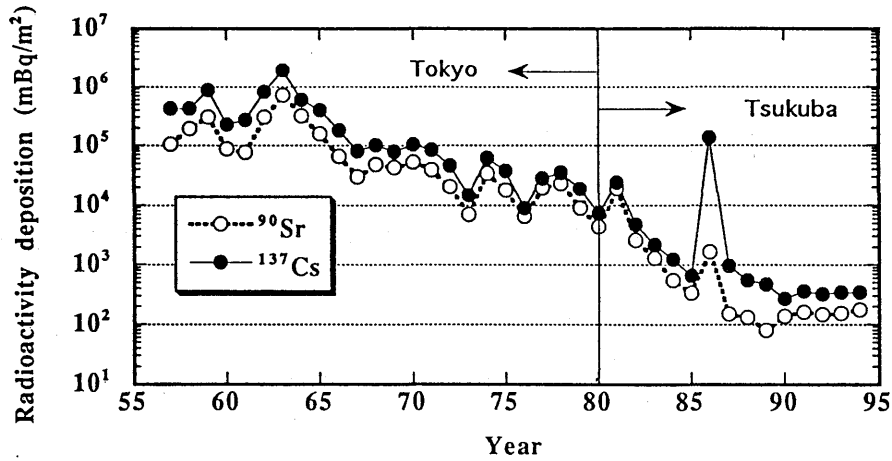


Fig. 95-10 Temporal variation in annual radioactivity deposition observed at MRI. Reprinted from *J. Environ. Radioactivity*, 31, Igarashi *et al.*, Recent deposition of  $^{90}\text{Sr}$  and  $^{137}\text{Cs}$  observed in Tsukuba, 157-169, Copyright (1996), with permission from Elsevier Science.

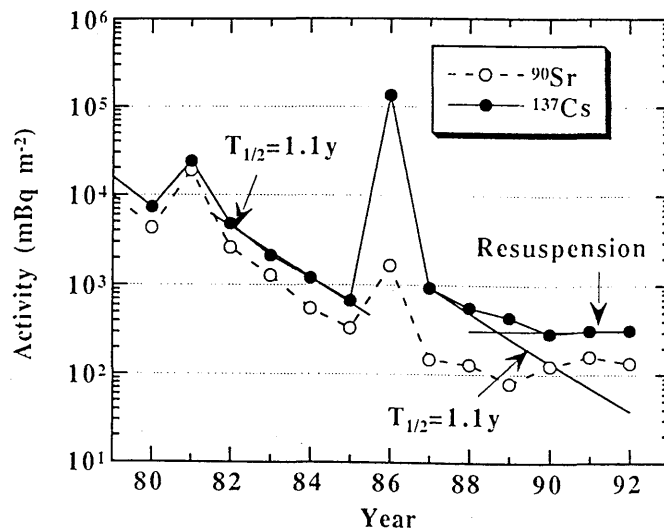


Fig. 95-11 Influence of the stratospheric component on the annual deposition of  $^{137}\text{Cs}$  and  $^{90}\text{Sr}$ . Reprinted from *J. Environ. Radioactivity*, 31, Igarashi *et al.*, Recent deposition of  $^{90}\text{Sr}$  and  $^{137}\text{Cs}$  observed in Tsukuba, 157-169, Copyright (1996), with permission from Elsevier Science.

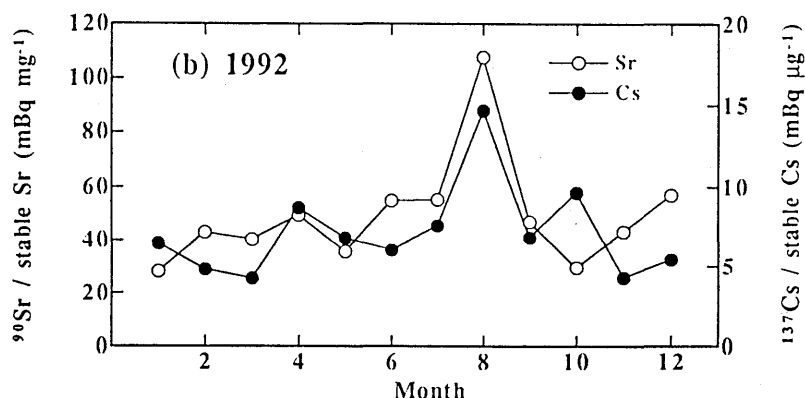


Fig. 95-12 Seasonal r/s ratio variation.

Reprinted from *J. Environ. Radioactivity*, 31, Igarashi *et al.*, Recent deposition of  $^{90}\text{Sr}$  and  $^{137}\text{Cs}$  observed in Tsukuba, 157-169, Copyright (1996), with permission from Elsevier Science.

the maximum in deposition peak months in spring (Fig. 95-12). It was concluded that most  $^{90}\text{Sr}$  and  $^{137}\text{Cs}$  deposits are of resuspended soil origin. The activity ratio ( $^{137}\text{Cs}/^{90}\text{Sr}$ ) suggests that plural sources are present for resuspended radioactivity in Japan.

### 3.4 Reference fallout material preparation for activity measurements

Otsuji-Hatori, Igarashi, and Hirose (1996)

Since the present environmental radioactivity level is becoming extremely low, quality control in determining fallout has become more important, despite the dearth of reference material for fallout activity determination. Otsuji-Hatori *et al.*(1996) attempted to prepare reference fallout material for activity measurements by using deposition samples collected at 14 stations over Japan in 1963-1979, preserved after gamma-activity measurement (Fig. 95-13). With this reference material,  $^{90}\text{Sr}$ ,  $^{137}\text{Cs}$ , and Pu isotopes were determined by several independent institutions. Results show good accord among individual institutions, meaning that the sample can be used as a reference for the measurement of fallout (Table 95-4). At present, this reference is being effectively used in quality control of radiochemical analysis.

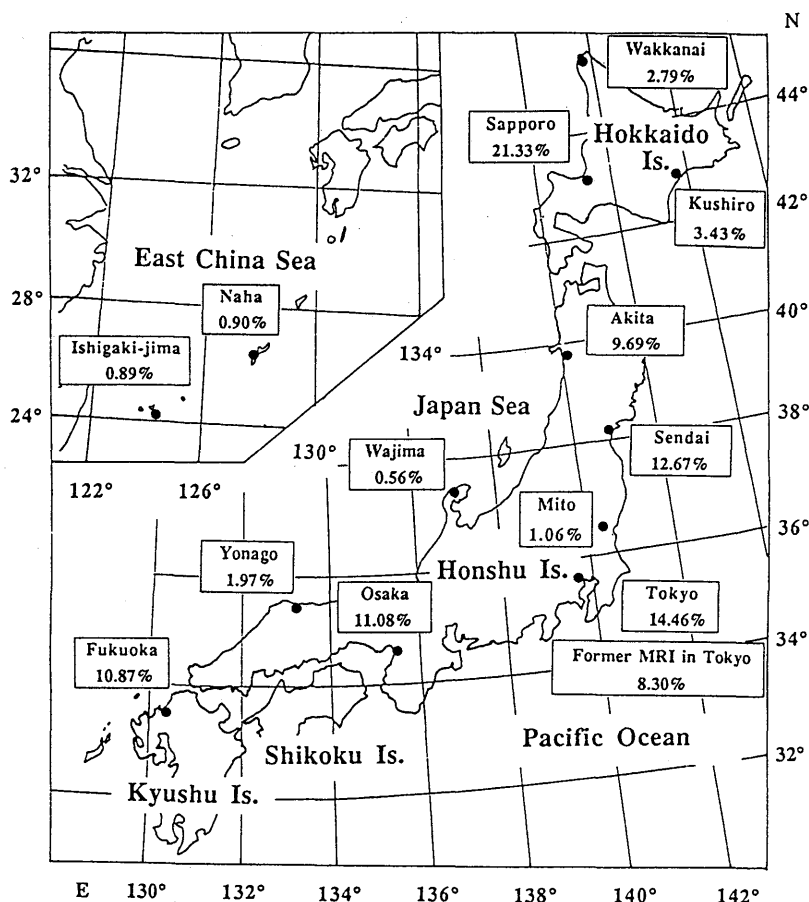


Fig. 95-13 Sampling station site and weight percentage of fallout from each station composing "reference fallout material". Reprinted from *J. Environ. Radioactivity*, 31, Otsuji-Hatori *et al.*, Preparation of a reference fallout material for activity measurements, 143-155, Copyright (1996), with permission from Elsevier Science.

Table 95-4 Reported Concentrations of Radionuclides in the 'Reference Fallout Material' (mBq g<sup>-1</sup>)

Institution	Sample (n)	<sup>137</sup> Cs	<sup>90</sup> Sr	<sup>239,240</sup> Pu	<sup>238</sup> Pu	<sup>210</sup> Pb	<sup>226</sup> Ra
A	5	298 ± 3 <sup>a</sup>	186 ± 3	6.32 ± 0.10	0.25 ± 0.03		
B	5	304 ± 11					
C	5	328 ± 11					
D	5	314 ± 6					
E	5	342 ± 11	248 ± 7	7.23 ± 0.54	0.40 ± 0.08		
F	5	314 ± 9					
G	5			6.41 ± 0.15	0.27 ± 0.01		
H	5	290 ± 9					
I	4 <sup>b</sup>	305 ± 3				661 ± 15	15 ± 2
MRI	5(16) <sup>c</sup>	309 ± 6	198 ± 8	6.49 ± 0.30	0.14 ± 0.08		
Average		312 ± 16	211 ± 33	6.61 ± 0.42	0.27 ± 0.11	661	15
Weighted mean		311	211	6.52	0.28		

<sup>a</sup>Errors indicated in this table show the unbiased SD for each data set.

<sup>b</sup>Although the five bottles were provided, one was broken during transportation. For <sup>226</sup>Ra, one sample showed a value below the detection limit.

<sup>c</sup>The figure in parentheses is for <sup>137</sup>Cs.

Reprinted from *J. Environ. Radioactivity*, 31, Igarashi *et al.*, Recent deposition of <sup>90</sup>Sr and <sup>137</sup>Cs observed in Tsukuba, 157-169, Copyright (1996), with permission from Elsevier Science.

## ORGANIC MATTER AND LIGANDS

### 4. Carbon and Nitrogen Biogeochemical Cycle at Earth's Surface

The abundance of carbon at the earth's surface potentially exchangeable with atmospheric carbon dioxide is approximately  $43 \times 10^{18}$  gC. The ocean holds about 90% of this "active" carbon, in either inorganic or organic form. Carbon and nitrogen are incorporated into the biogeochemical cycle in the ocean and buffer the level of atmospheric carbon dioxide.

Improved knowledge of the carbon and nitrogen biogeochemical cycle is of critical importance to understanding and responding effectively to issues on regional and global climatic change. Our research focused on clarifying the dynamics of chemical compounds in the ocean and their relationship to the global carbon cycle.

#### 4.1 Detection of dissolved protein molecules in oceanic waters and bacterial membranes: Possible source of a major dissolved protein in seawater

Tanoue (1995)

Tanoue, Nishiyama, Kamo and Tsugita (1995)

Dissolved organic matter (DOM) in seawater is one of the three reactive reservoirs of organic matter on the planet; the other two are living plants and organic matter in soil on land. Although evidence indicates that the majority of DOM originated in marine environments, only less than 30% of the component molecules, such as combined amino acids, carbohydrates, and solvent-extractable lipids, have been identified so far. To date, there is a gap in our understanding of organic constituents between those of marine organisms (sources of organic matter) and those of the inanimate organic (DOM) pool in both classes and quality.

Tanoue (1995) and Tanoue *et al.* (1995) developed a new method for extraction and detection of dissolved protein molecules in oceanic waters and studied bacterial membranes as a possible source of a major dissolved protein in seawater. They measured dissolved protein at a variety of depths at three stations in the Pacific, ranging from the tropics to the subarctic. Most dissolved protein is distributed over a wide range of molecular masses, but consists of fewer than 30 individual proteins. One, with an apparent molecular mass of 48 kDa, is a major constituent at all stations (Fig. 95-14). Its N-terminal amino acid sequence was found to be a homologue of porin P, a trans-outer-membrane channel protein of gram-negative bacteria.

The correspondence of N-terminal amino acid sequences and apparent molecular masses between this dissolved protein and porin P indicates that almost the complete homologue of porin P, from the N-terminus to (probably) the C-terminus, survives without modification in the water column (Table 95-5). Persistence of appreciable amounts of an identifiable protein suggests a pathway for the production of dissolved organic matter whereby enzyme-resistant biopolymers survive and accumulate in the sea. The accumulation of appreciable amounts of a relatively limited number of proteins leads to the hypothesis that particulate proteins that make up the majority of dissolved protein components in seawater are derived from specific sources and contribute quantitatively to the oceanic organic nitrogen pool.

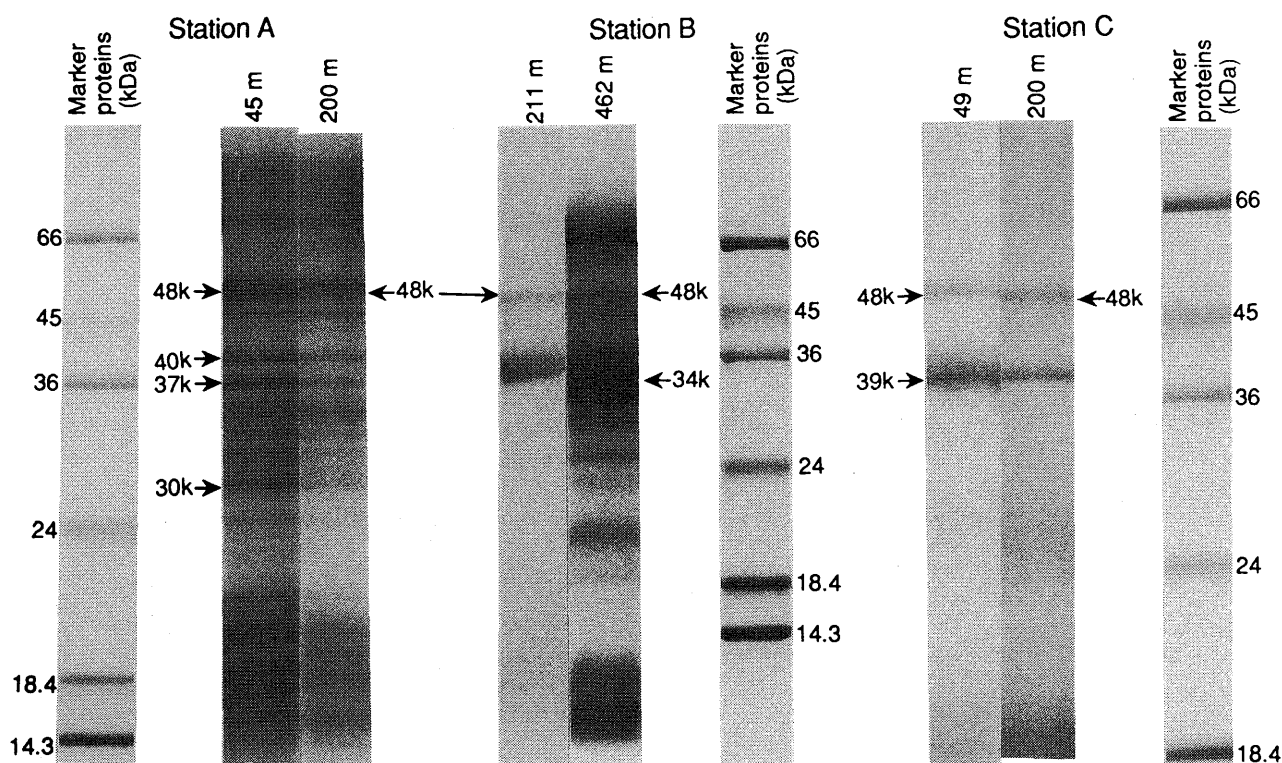


Fig. 95-14 Electrophoresis of dissolved proteins extracted from surface and intermediate waters at three stations: subarctic Station A (45°10.3'N, 165°34.4' E); subtropical Station B (24°35.0'N, 170°00.1' E); and tropical Station C (22°47.1'N, 158°04.6' W). Standard marker proteins are shown for all stations. Proteins in certain bands (arrows) on gels were subjected to N-terminal amino acid sequencing (Table 95-5). Amounts of samples loaded on gels were equivalent to 1 liter of original seawater at Stations A and C, and 0.25 liters of original seawater at Station B. Each marker protein was loaded at 1 µg for Stations A and C, and at 2 µg for Station B. Reprinted from *Geochim. et Cosmochim. Acta*, 59, Tanoue *et al.*, Bacterial membranes: Possible source of a major dissolved protein in seawater, 2643-2648, Copyright (1995), with permission from Elsevier Science.

Table 95-5 N-terminal amino acid sequences of the proteins in the dissolved phase. "Xaa" indicates that an identifiable phenylhydantoin derivative was not recovered.

Cycle	mol.mass of protein	1	2	3	4	5	6	7	8	9	10	11	12	13	14	15
Station A (45°10.3'N, 165°34.4'E; depth, 5,934 m)																
45 m	48 kDa	Gly	Thr	Val	Thr	Thr	Asp	Gly	Ala	Asp	Ile	Val	Ile	Lys	Thr	
	40 kDa	Thr	Val	Thr	Val	Thr	Pro	Leu	Met	Leu	Gly	Tyr	Thr	Phe	Gln	Leu
	37 kDa	Ala	Asp	Val	Lys	Ile	Tyr	Gly	Arg	Ala	His	Val	Ser	Leu	Asp	Tyr
	30 kDa	Thr	Gln	Ala	Glu	Val	Gly	Ala	Ser	Ala	Gly	Leu	Ile	Asp	Pro	Asp
200 m	48 kDa	Gly	Thr	Val	Thr	Thr	Asp	Gly	Thr**	Asp	Ile	Val	Ile	Lys	Thr	Lys
		Ala*														
Station B (24°35.0'N, 170°0.1'E; depth, 5,966 m)																
211 m	48 kDa	Gly	Thr	Val	Thr	Thr	Asp	Gly	Ala	Asp	Leu**	Val	Ile	Lys	Thr	Lys
462 m	48 kDa#	Gly	Thr	Val	Thr	Thr	Asp	Gly	Ala	Asp	Xaa	Val	Ile	Lys	Thr	Lys
		Met	Lys	Asp	Gly	Leu	Val	Glu	Arg	Thr	Gln	Gly	Ser	Glu	Val	Asp
	34 kDa	Val	Thr	Gly	Gly	Tyr	Ala	Arg	Leu	Pro	Val	Glu	Leu	Tyr	Lys	
Station C (22°47.1'N, 158°4.6'W; depth, 4744 m)																
49 m	48 kDa	Gly	Thr	Val	Thr	Thr	Asp	Gly	Xaa	Asp	Ile	Val	Ile	Lys	Thr	Lys
	39 kDa	Ala	Val	Val	Gly	Gly	Gly	Ala	Thr	Leu	Pro	Gln	Asn	Leu	Tyr	Asn
200 m	48 kDa	Gly	Thr	Val	Thr	Thr	Asp	Gly	Xaa	Asp						
		Porin P##														
		Gly	Thr	Val	Thr	Thr	Asp	Gly	Ala	Asp	Ile	Val	Ile	Lys	Thr	Lys

\* This amino acid was also detected, \*\* The amino acid was detected but not at a significant level. # The protein in this sample with a molecular mass of 48 kDa was a mixture of two proteins, and two amino acids were detected at every step. One protein was identified as a homologue of porin P and no sequence resembling that of the other protein was found in the PIR database. ## After Worobec *et al.* (1988) and Siehnel *et al.* (1990). Reprinted from *Geochim. et Cosmochim. Acta*, 59, Tanoue *et al.*, Bacterial membranes: Possible source of a major dissolved protein in seawater, 2643-2648, Copyright (1995), with permission from Elsevier Science.

## 4.2 Detection, characterization, and dynamics of dissolved organic ligands in oceanic waters

Tanoue and Midorikawa (1995)

In the last two decades, increased attention has been paid to the chemistry of metalorganic compounds. The ability of dissolved organic matter to form complexes with metal ions in natural water is of interest because of associated biological implications, such as the bioavailability and toxicity of metals to living organisms, and because of its relevance to efforts to understand geochemical cycles of metals in the environments.

Tanoue and Midorikawa (1995) studied the detection, characterization and dynamics of dissolved organic ligands in oceanic waters, focusing on interaction with copper. Three classes of organic ligands —  $L_1$ ,  $L_2$  and  $L_N$  — concentrated by repeated lyophilization and dialysis, were distinguished by differences in their copper complexing.  $L_1$  and  $L_2$  appear to belong to the group of weak ligands in the literature (Table 95-6). The conditional stability constant of ligand  $L_N$  for Cu(II) was extremely high and comparable to that of EDTA (Table 95-7).

Two types of ligand similar to weak ligands  $L_1$  and  $L_2$  were extracted directly from seawater using immobilized metal ion affinity chromatography (IMAC). IMAC gave new insights in showing that the weak ligands were a mixture of at least two types of different organochemical ligands and that their dynamics may be active in the water column.

Table 95-6 Conditional stability constants ( $K'_{ML}$ ) and concentrations ( $C_L$ ) of natural ligands in samples of seawater at pH8.15 (EPPS), at an ionic strength of 0.7 M ( $KNO_3$ ), and at a temperature of 25.0°C. The concentration of ligand has been converted to that in seawater. The volume of the original sample of seawater used was about 5l, except in the case of site S-1, 0 m (+: 1.7l, #: 1.0l)

Site <sup>a</sup>	Depth (m)	Cu(II)								Cd(II)	
		$C_{L1}$ (nM)		$\log K'_{ML1}$		$C_{L2}$ (nM)		$\log K'_{ML2}$		$C_L$ (nM)	$\log K'_{ML}$
		B	A	B	A	B	A	B	A	A	A
S-1	0+	9.4	8.6	8.34	8.61	62	19	6.38	7.25	-	-
	0#	7.9	7.0	8.48	8.68	45	17	6.57	7.30	-	-
P	0	-	2.2	-	8.89	-	7.3	-	7.09	2.7	6.81
	191	5.1	3.9	8.26	8.41	20	5.5	6.55	7.75	3.8	6.74
J	0	1.9	1.2	9.36	9.60	7.6	6.5	7.50	7.57	1.2	7.21
	523	1.3	1.1	9.20	9.44	5.4	4.0	7.59	7.94	1.4	6.75
	1071	*	3.5	*	9.05	14	11	7.15	7.77	4.5	6.82

<sup>a</sup>Site S-1: at 34°56' N, 138°41' E on Apr. 26, 1988. Site P: at 41°32' N, 147°00' E on Aug. 13, 1987. Site J: at 44°15' N, 130°58' E on Aug. 26, 1987.

Key: \*, not detected; -, not determined; B, before demetallization; A, after demetallization.

Table 95-7 Estimated lower limits for the concentration of the undemetallizable ligand,  $L_N$ , and the conditional stability constant for copper in various samples of seawater at an ionic strength below  $10^{-5}$  M, at pH5.71 and at 4°C.

Site	Depth (m)	Lower limit	
		$C_{LN}^a$ (nM)	$\log K'_{CuL_N}$
S-1 <sup>b</sup>	0	$0.79 \pm 0.04$	$13.9 \pm 0.2$
	0	$0.77 \pm 0.04$	$14.0 \pm 0.2$
	0	$0.80 \pm 0.06$	$14.2 \pm 0.2$
	0	$0.74 \pm 0.15$	$14.0 \pm 0.3$
	ave.	$0.78 \pm 0.04$	$14.1 \pm 0.1$
S-2 <sup>b</sup>	0	$1.08 \pm 0.20$	$14.2 \pm 0.3$
	0	$1.04 \pm 0.18$	$13.5 \pm 0.3$
	ave.	$1.06 \pm 0.13$	$14.0 \pm 0.2$
A	0	$0.31 \pm 0.03$	$13.8 \pm 0.3$
P	0	$0.200 \pm 0.004$	$14.3 \pm 0.3$
	191	$0.071 \pm 0.004$	$14.0 \pm 0.3$
J	0	<0.01	*
	523	$0.050 \pm 0.002$	$13.9 \pm 0.3$
	1071	$0.170 \pm 0.004$	$14.0 \pm 0.3$

\*Not estimated.

<sup>a</sup>Concentration of ligand is that in seawater. The values of  $[Cu]_{ex}$  was taken as the lower limit for  $C_{LN}$  (MIDORIKAWA and TANOUE, 1994a).

<sup>b</sup>Values estimated from multiple subsamples of seawater from Suruga Bay are averaged.

#### 4.3 Relationship between particulate uranium and thorium-complexing capacity of oceanic particulate matter

Hirose (1995b)

Chemical characterization of particulate organic matter (POM) surfaces in their metal complexing is of importance to understanding oceanographic roles of particulate matter (PM). Hirose (1995b) studied the relationship between particulate uranium and thorium-complexing capacity of oceanic particulate matter. Thorium-complexing capacity (ThCC), defined as the amount of thorium adsorption onto PM in  $0.1 \text{ mol l}^{-1}$  HCl by complexing, has been introduced as a new oceanographic parameter. ThCC implies the concentration of a strong organic ligand in PM.

To specify chemically strong ligands in PM, Hirose compared ThCC in PM with that of particulate uranium, which exists as an organic complex in sea water. ThCC in PM correlated with particulate uranium, and this relationship enables the conditional stability constant of the organic uranium complex in PM to be calculated based on mass action law. The estimated conditional stability constant of the uranium complex in seawater ( $10^{14.5} \text{ l mol}^{-1}$ ) is greater than that determined for organic copper complexes, whose order of magnitude coincides with the result of the metal adsorption on microorganisms (Table 95-8). These findings suggest that the strong ligand corresponding to ThCC in PM, which is directly related to the complexation of metals in PM, originates in marine organisms.

Table 95-8a The thorium-complexing capacity in particulate matter and particulate uranium in seawater: surface waters

Sampling date	Location	ThCC (nmol l <sup>-1</sup> )	Particulate U (μBq l <sup>-1</sup> )
The western North Pacific			
Apr. 1991	32°00'N 140°15'E	3.41 ± 0.19	2.90 ± 0.42
Apr. 1991	30°00'N 140°07'E	2.30 ± 0.13	2.13 ± 0.38
May 1991	28°00'N 137°00'E	5.84 ± 0.32	4.96 ± 0.35
May 1991	18°00'N 137°00'E	3.37 ± 0.16	2.79 ± 0.22
May 1991	10°00'N 137°00'E	7.31 ± 0.42	6.07 ± 0.36
May 1991	3°00'N 144°00'E	9.47 ± 0.42	8.24 ± 0.58
May 1991	7°00'N 144°00'E	3.22 ± 0.16	2.17 ± 0.15
May 1991	22°00'N 144°00'E	4.63 ± 0.21	3.29 ± 0.23
The Japan Sea			
May 1993	38°09'N 134°27'E	13.5 ± 0.5	11.3 ± 0.6
May 1993	38°36'N 143°03'E	9.92 ± 0.48	

Table 95-8b The thorium-complexing capacity in particulate matter and particulate uranium in seawater: vertical distribution (location: 39°25'N 133°25'E)

Depth(m)	Temp. (°C)	Salinity (‰)	ThCC	Particulate U
0	13.06	34.51	11.4 ± 0.6	10.5 ± 0.7
10	12.99	34.50	9.67 ± 0.48	
25	10.92	34.44	6.89 ± 0.48	
50	9.05	34.13	4.49 ± 0.31	
100	6.08	34.04	3.05 ± 0.21	2.83 ± 0.40
200	1.63	34.05	1.62 ± 0.21	
300	0.78	34.06	1.42 ± 0.18	
500	0.38	34.07	1.28 ± 0.16	1.22 ± 0.22
750	0.29	34.07	1.23 ± 0.16	1.25 ± 0.22
1000	0.23	34.07	1.06 ± 0.14	1.16 ± 0.21

Reprinted from *The Science of the Total Environment*, 173/174, Hirose, The relationship between particulate uranium and thorium-complexing capacity of oceanic particulate matter. 195-201, Copyright (1995), with kind permission of Elsevier Science - NL, Sara Burgerhartstraat 25, 1055 KV Amsterdam, The Netherlands.

## ACID DEPOSITION

### 5. Acid Deposition at Summit of Mt. Fuji

**Dokiya, Tsuboi, Sekino, Hosomi, Igarashi, and Tanaka (1995)**

The summit of Mt. Fuji, the highest mountain in Japan, is a solitary 3,776m peak considered to be in the free atmosphere and presumably free from local pollution. The JMA has run a weather station at the summit since 1932. Because of severe meteorological conditions, no data is available on the amount of precipitation and only a few studies have been made on the chemical species in precipitation at the summit.

Dokiya *et al.* (1995) have measured chemical species in precipitation since August 1990 to evaluate the site as a background air quality station and to obtain information on the long-range transport of chemical species. They conducted intensive observations of chemical species in aerosols, gases, and other samples at the summit of Mt. Fuji and at Tarobo (1,300m up on the mountain's southern slope) during summer 1993 and 1994 to evaluate the sources of chemical species in precipitation.

From July 26 to August 3, 1993, concentrations of gaseous HCl and SO<sub>2</sub> were low and comparable to those at remote sites. The concentration of NH<sub>3</sub> during this period was higher with diurnal variation, however,

suggesting some influence of mountain climbers. Similar tendencies were found for gases from July 26 to 30, 1994.

The concentration of sulfate in aerosols increased abruptly after a typhoon passed on July 30, 1993 (Fig. 95-15). Aerosols with high sulfate concentrations were found to be acidic and back-trajectory analysis indicated that they advected to Mt. Fuji from the west. In contrast, the higher sulfate concentrations observed during the first half of July 1994 seemed to originate from local sources, presumably in the Kanto metropolitan area (Fig. 95-16).

Further intensive studies of atmospheric chemistry at the summit of Mt. Fuji (Summer Campaign 1997) are planned in 1997 by MRI scientists, including those from our laboratory.

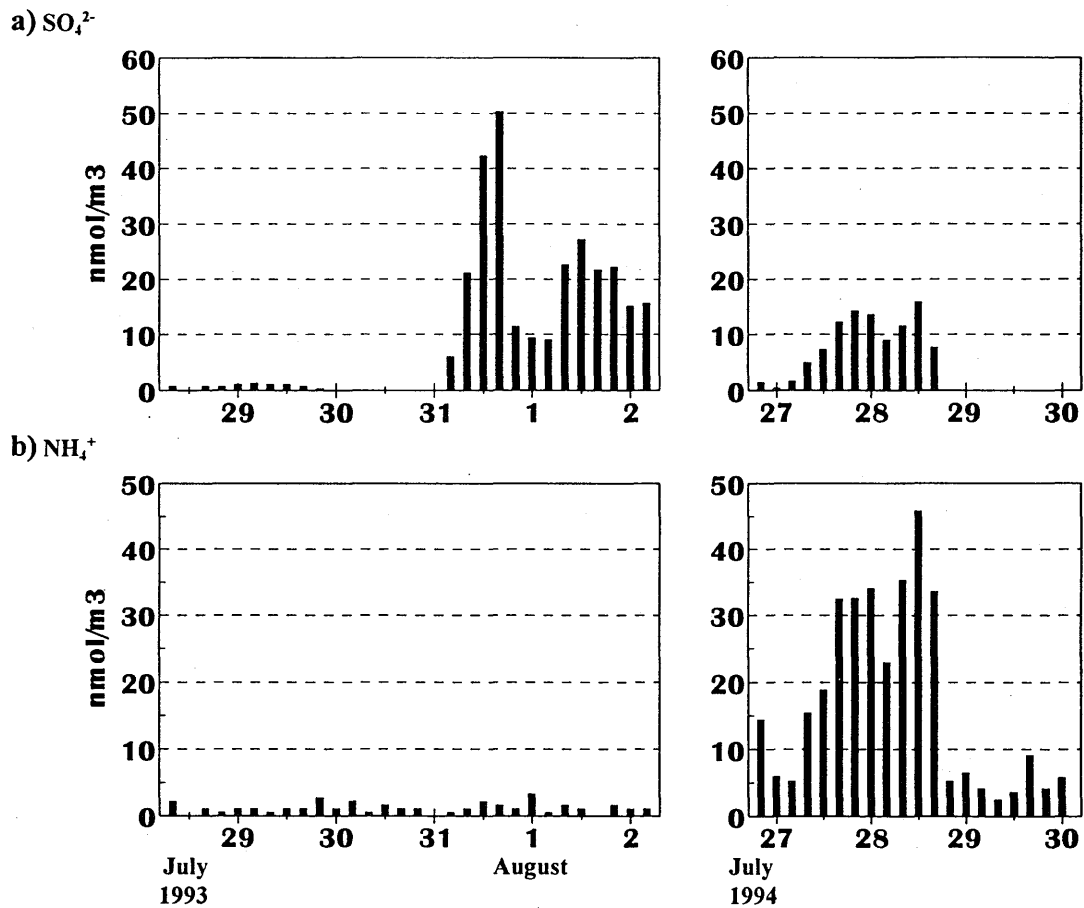


Fig. 95-15 Sulfate and ammonium concentration in aerosols a)  $\text{SO}_4^{2-}$ ; b)  $\text{NH}_4^+$ . Reprinted from *Water, Air and Soil Pollution*, 85 (1995), 1967-1972, Acid deposition at the summit of Mt. Fuji: Observations of gases, aerosols, and precipitation in summer, 1993 and 1994, Dokiya *et al.*, fig. 1 (©1995 Kluwer Academic Publishers. Printed in the Netherlands.) with kind permission from Kluwer Academic Publishers.

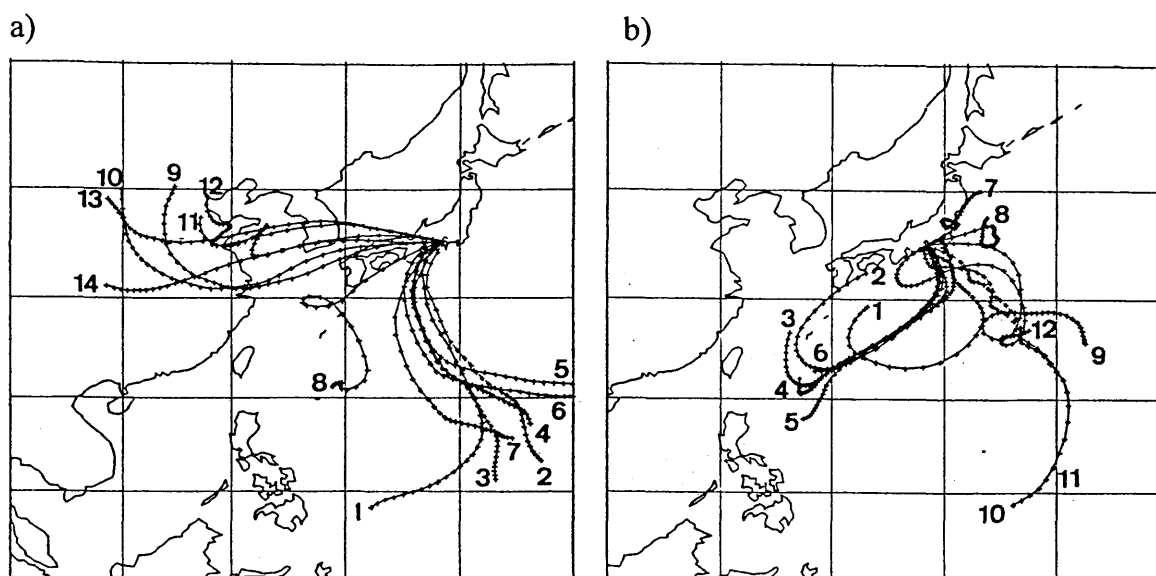


Fig. 95-16 Back trajectory analyses for air sampled on Mt. Fuji.

a) July 27 to August 2, 1993: 1: July 27, 9:00 (local time); 2: July 27, 21:00; 3: July 28, 9:00; 4: July 28, 21:00; 5: July 29, 9:00; 6: July 29, 21:00; 7: July 30, 9:00; 8: July 30, 21:00; 9: July 31, 9:00; 10: July 31, 21:00; 11: August 1, 9:00; 12: August 1, 21:00; 13: August 2, 9:00; 14: August 2, 21:00;

b) July 25 to 30, 1994: 1: July 25, 9:00; 2: July 25, 21:00; 3: July 26, 9:00; 4: July 26, 21:00; 5: July 27, 9:00; 6: July 27, 21:00; 7: July 28, 9:00; 8: July 28, 21:00; 9: July 29, 9:00; 10: July 29, 21:00; 11: July 30, 9:00; 12: July 30, 21:00. Each small tick on the line indicates 6 hours.

Reprinted from *Water, Air and Soil Pollution*, 85 (1995), 1967-1972, Acid deposition at the summit of Mt. Fuji: Observations of gases, aerosols and precipitation in summer, 1993 and 1994, Dokiya *et al.*, fig 3 (©1995 Kluwer Academic Publishers. Printed in the Netherlands.) with kind permission from Kluwer Academic Publishers.

## IODINE

### 6. Iodine Determination in Natural and Tap Water Using Inductively Coupled Plasma Mass Spectrometry

Takaku, Shimamura, Masuda, and Igarashi (1995)

Takaku *et al.* (1995) examined the feasibility of iodine determination in natural and tap water, using inductively coupled plasma mass spectrometry (ICP-MS) to investigate the environmental behavior of iodine from the viewpoint of health science and public hygiene. Iodine is essential to the body, mainly the thyroid gland, and plays an important role in metabolism. It is also important to trace radioactive iodine ( $^{129}\text{I}$ ,  $^{131}\text{I}$ ,  $^{133}\text{I}$ , etc.) released to the environment from nuclear power plants and nuclear test sites.

Because iodine concentrations in environmental samples are usually very low, it is difficult to make a direct analysis by the traditional methods without preconcentration. Because iodine is highly volatile, however, the chemical yield of iodine during preconcentration is both low and variable. It is preferable to conduct direct analysis without preconcentration.

Takaku *et al.* (1995) easily determined iodine by ICP-MS without separation or preconcentration. The detection limit was 10 pg/ml. They obtained a stable iodine determination by adding an organic alkali to samples just before analysis to suppress iodine vaporization. They determined the iodine concentration of 42 natural water samples in the northern Kanto area, Japan (Fig. 95-17). The concentrations of iodine ranged from 0.65 to 35.9 ng/ml (Table 95-9).

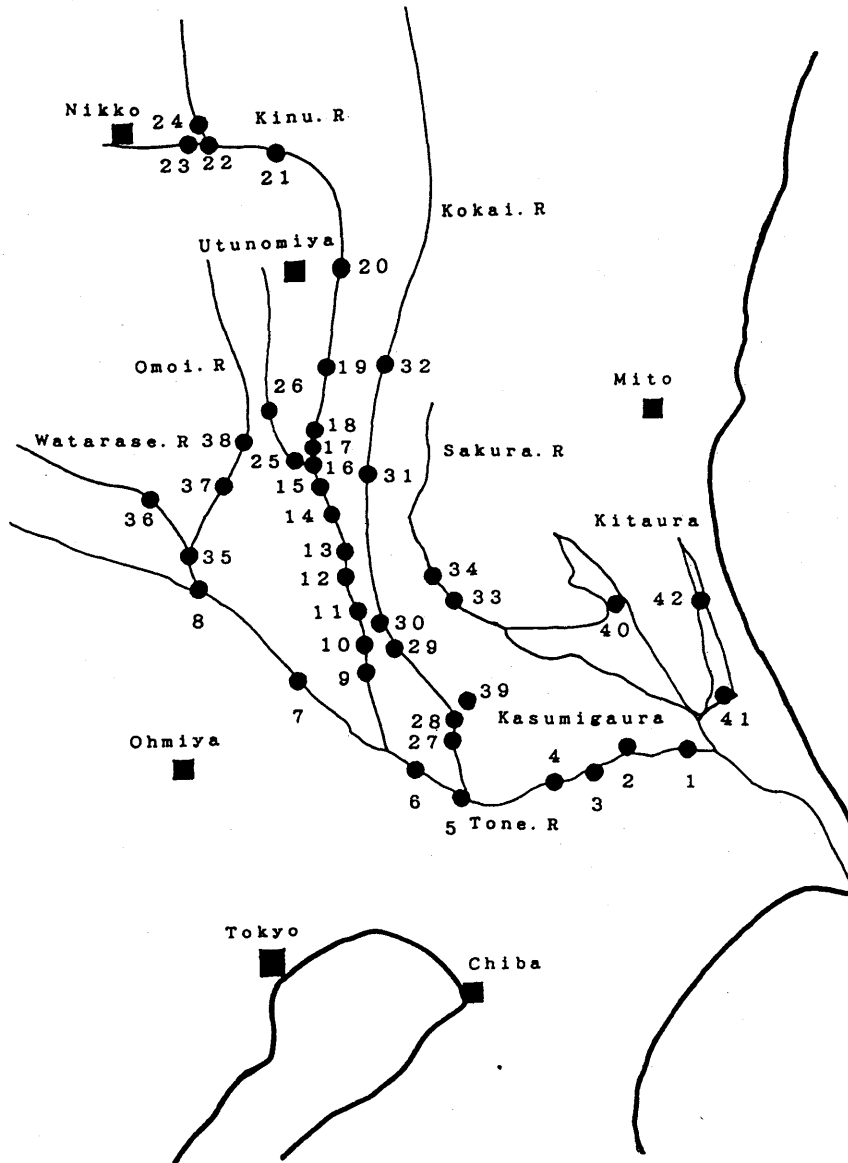


Fig. 95-17 River and lakewater sampling points.

Table 95-9 Concentrations of I in river- and lake-water samples

Name of river	City	Sample point Place	EC/ $\mu\text{S cm}^{-1}$	pH	Cl, ppm	NO <sub>3</sub> -N, ppm	SO <sub>4</sub> -S, ppm	I, ppb	
1	Tone	Sahara	Suigou-ohashi	311	7.4	46.2	2.4	10.5	35.9 ±0.2
2		Kanzaki	Kanzaki-ohashi	285	7.5	38.7	2.2	9.9	28.6 0.5
3		Shintone	Jyousou-ohashi	270	7.4	30.7	2.3	10.2	20.0 0.2
4		Kawachi	Nagatomi-hashhi	238	7.4	21.9	2.4	10.9	8.2 0.1
5		Abiko	Sakae-hashhi	223	7.5	19.1	2.1	10.6	7.9 0.1
6		Toride	Tone-ohashi	230	7.4	19.3	2.2	11.5	8.4 0.3
7		Iwai	Mebuki-ohashi	254	7.3	23.6	2.4	13.7	11.3 0.1
8		Koga	Tonegawa-hashhi	235	7.3	23.8	2.2	12.7	9.4 0.2
9	Kinu	Mitsukaidou	Housui-hashhi	178	7.0	11.4	1.7	8.6	4.04 0.04
10		Mitsukaidou	Mituma-hashhi	163	7.4	9.2	1.4	7.7	2.77 0.06
11		Moriya	Tamadai-hashhi	166	7.5	10.3	1.4	8.0	3.30 0.01
12		Ishige	Ishige-hashhi	154	7.4	8.6	1.2	7.1	2.46 0.02
13		Chiyokawa	Ogata-hashhi	157	7.4	9.5	1.3	7.2	2.54 0.05
14		Shimotsuma	Kinugawa-hashhi	159	7.5	9.7	1.3	7.6	2.49 0.09
15		Sekijyou	Komashiro-hashhi	162	7.5	10.1	1.2	7.9	2.42 0.03
16		Shimodate	Funadama-hashhi	151	7.5	8.9	1.1	6.9	2.43 0.07
17		Shimodate	Kawashima-hashhi	141	7.8	8.7	1.1	6.8	2.44 0.05
18		Shimodate	Nakajima-hashhi	143	7.9	8.3	1.0	6.5	2.34 0.06
19		Ninomiya	Daidousen-hashhi	110	8.7	6.0	0.63	4.2	1.56 0.04
20		Mouka	Miyaoka-hashhi	108	8.7	6.8	0.55	4.4	1.80 0.05
21		Utsunomiya	Yanagida-hashhi	93	8.8	4.7	0.4	3.8	1.76 0.04
22		Shioya	Kamihira-hashhi	120	8.4	5.4	0.89	4.2	1.55 0.09
23		Shioya	Onami-hashhi	75	8.1	2.7	0.36	3.3	1.12 0.02
24	Daiya	Imaichi	Kaishin-hashhi	117	7.8	4.3	0.46	5.7	2.25 0.03
25	Ta	Yuuki	Shin-tagawa-hashhi	298	7.3	22.7	3.1	16.0	3.66 0.05
26		Oyama	Funato-hashhi	281	7.6	17.5	2.3	17.9	5.14 0.09
27	Kokai	Fujishiro	Kokaigawa-ohashi	221	7.4	16.8	2.3	8.7	5.10 0.05
28		Yawahara	Yamato-hashhi	227	7.4	17.6	2.5	10.1	4.61 0.05
29		Mitsukaidou	Fukurai-hashhi	222	7.4	16.3	2.2	9.3	4.2 0.15
30		Shimotsuma	Iwai-hashhi	207	7.7	17.8	2.1	8.9	4.45 0.02
31		Shimodate	Ishida-hashhi	199	8.5	15.8	2.0	7.4	3.88 0.02
32		Mouka	Inonai-hashhi	167	9.1	11.8	1.4	6.2	2.50 0.06
33	Sakura	Tsukuba	Ota-hashhi	205	7.4	19.3	1.9	9.1	6.2 0.36
34		Tsukuba	Jyunmi-hashhi	171	7.6	18.2	1.9	8.6	5.9 0.23
34	Watarase	Koga	Mikuni-hashhi	225	7.2	17.9	2.3	11.0	4.4 0.11
36		Fujioka	Fujioka-ohashi	273	7.6	29.6	1.7	17.0	4.76 0.09
37	Omoi	Oyama	Kuromoto-hashhi	143	8.5	10.3	3.5	4.6	0.65 0.09
38		Oyama	Amito-hashhi	192	8.3	16.0	3.2	7.1	2.05 0.05
39	Ushikunuma	Ryugasaki	Sanuki	211	9.0	21.7	1.7	7.4	3.04 0.07
40	Kasumigaura	Dejima	Kasumigaura-ohashi	259	8.5	37.5	0.26	8.1	4.4 0.2
41	Kitaura	Itako	Jingu-hashhi	405	8.4	80.9	—	8.4	5.3 0.27
42		Taiyou	Kagyou-hashhi	243	7.8	31.5	2.2	6.5	2.4 0.24

# 1996 ACTIVITIES

## INTRODUCTION

In 1996, GRD scientists focused their study on atmospheric chemistry, biogeochemical oceanography, and environmental radioactivity.

International/National scientific programs and budgetary funds for our studies are shown in Table 2.

### I. Field Observation Studies

#### GREENHOUSE GASES (CO<sub>2</sub>, CH<sub>4</sub>, and CO)

##### 1. Studies on Greenhouse Gases in Upper Air Using Commercial Airliners

###### 1.1 Atmospheric CO<sub>2</sub> and CH<sub>4</sub> measurements from 1993 to 1994

**Matsueda and Inoue (1996)**

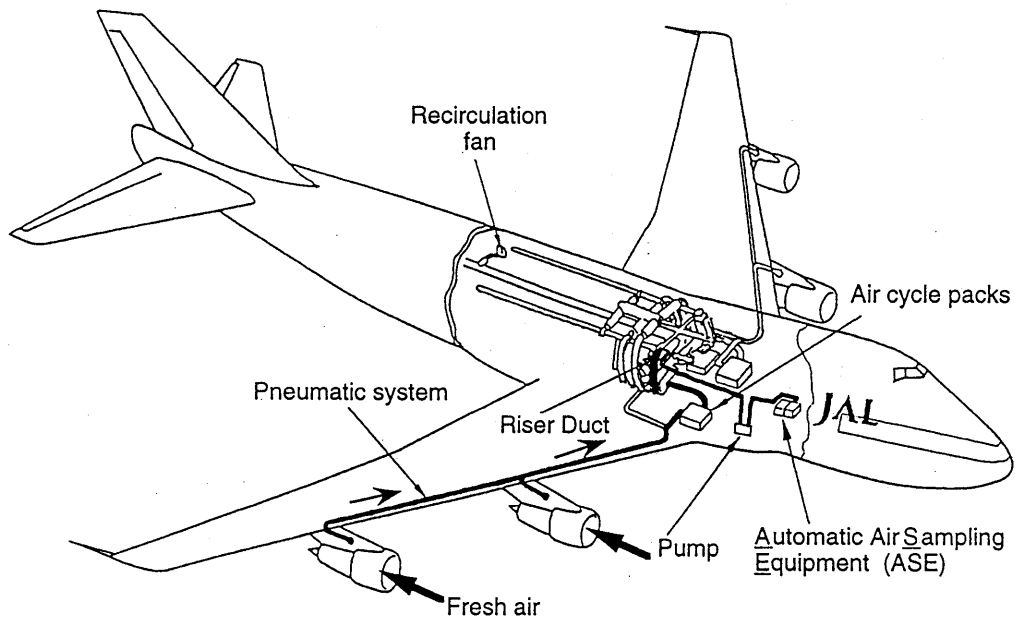
The increase of trace gases such as carbon dioxide in the atmosphere is expected to contribute to on-going global warming and to affect the chemical cycles in the atmosphere. Recent levels of greenhouse gases in surface air have been regularly observed at worldwide sampling networks such as NOAA/CMDL and GAW, but few systematic measurements have been made of greenhouse gases in the upper atmosphere.

Matsueda and Inoue (1996) developed a new automatic flask sampling system for the Boeing 747 commercial airliner in April 1993 to observe the mixing ratios of CO<sub>2</sub>, CH<sub>4</sub> and other trace gases in the upper atmosphere at altitudes of 9–13 km using regular commercial flights between Australia and Japan. This program was to clarify seasonal variations and secular trends in greenhouse gases in the upper atmosphere through cooperation supported by the JAL Foundation, Japan Airlines (JAL), the JMA, and Japan's Ministry of Transportation.

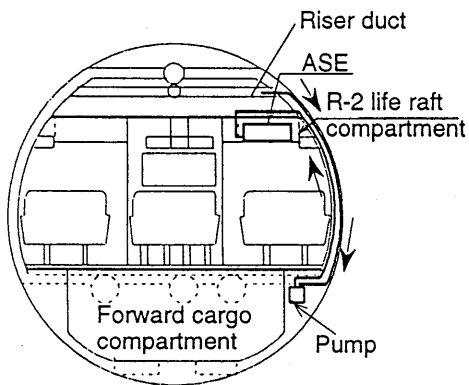
They described their sampling system and the results of CO<sub>2</sub> and CH<sub>4</sub> measurements in the upper troposphere for one year from 1993 to 1994 (Fig. 96-1). The air sampling system was developed to collect air samples automatically in 12 electrochemically buffed titanium flasks of automatic air sampling equipment (ASE) using a metal bellows pump. Engine bleed (fresh air outside the aircraft) was introduced into the ASE through a pneumatic system and a bypass intake using a metal bellows pump for flushing and compressing the air sample into flasks. Storage tests indicated no significant change of CO<sub>2</sub> and CH<sub>4</sub> mixing ratios in sample flask until analysis.

The air sample was analyzed for the CO<sub>2</sub> mixing ratio using an NDIR and for CH<sub>4</sub> mixing ratio using a GC-FID in the laboratory. Analytical precision for measurement was less than  $\pm 0.02$  ppm for CO<sub>2</sub> and less than  $\pm 0.12\%$  for CH<sub>4</sub>.

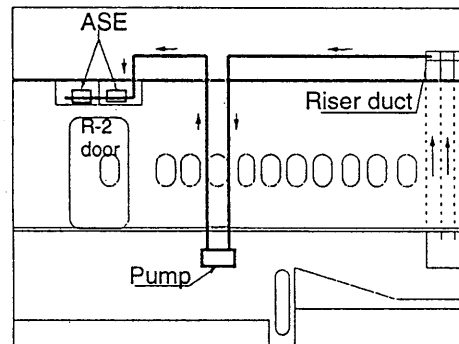
The CO<sub>2</sub> and CH<sub>4</sub> mixing ratios in the air sample were referenced to five working standard gases of CO<sub>2</sub> in air and CH<sub>4</sub> in air. Working standards were calibrated regularly by primary standards. No significant drift of mixing ratio was found in any of the working standards in high-pressure aluminum cylinders for one year. All mixing ratios are reported in ppm or ppb by mole fraction in dry air based on the WMO x85 scale for CO<sub>2</sub> and the MRI/GRD scale for CH<sub>4</sub>.



(a) Bird's-eye view



(b) Rear view



(c) Side view

Fig. 96-1 Air flow diagrams of flask sampling system developed for Boeing 747 commercial airliner. Bold lines indicate sample airstream in the aircraft by bird's-eye view (a), rear view (b), and side view (c). Reprinted from *Atmospheric Environment*, 30, Matsueda and Inoue, Measurements of atmospheric CO<sub>2</sub> and CH<sub>4</sub> using a commercial airliner from 1993 to 1994, 1647-1655, Copyright (1996), with kind permission from Elsevier Science.

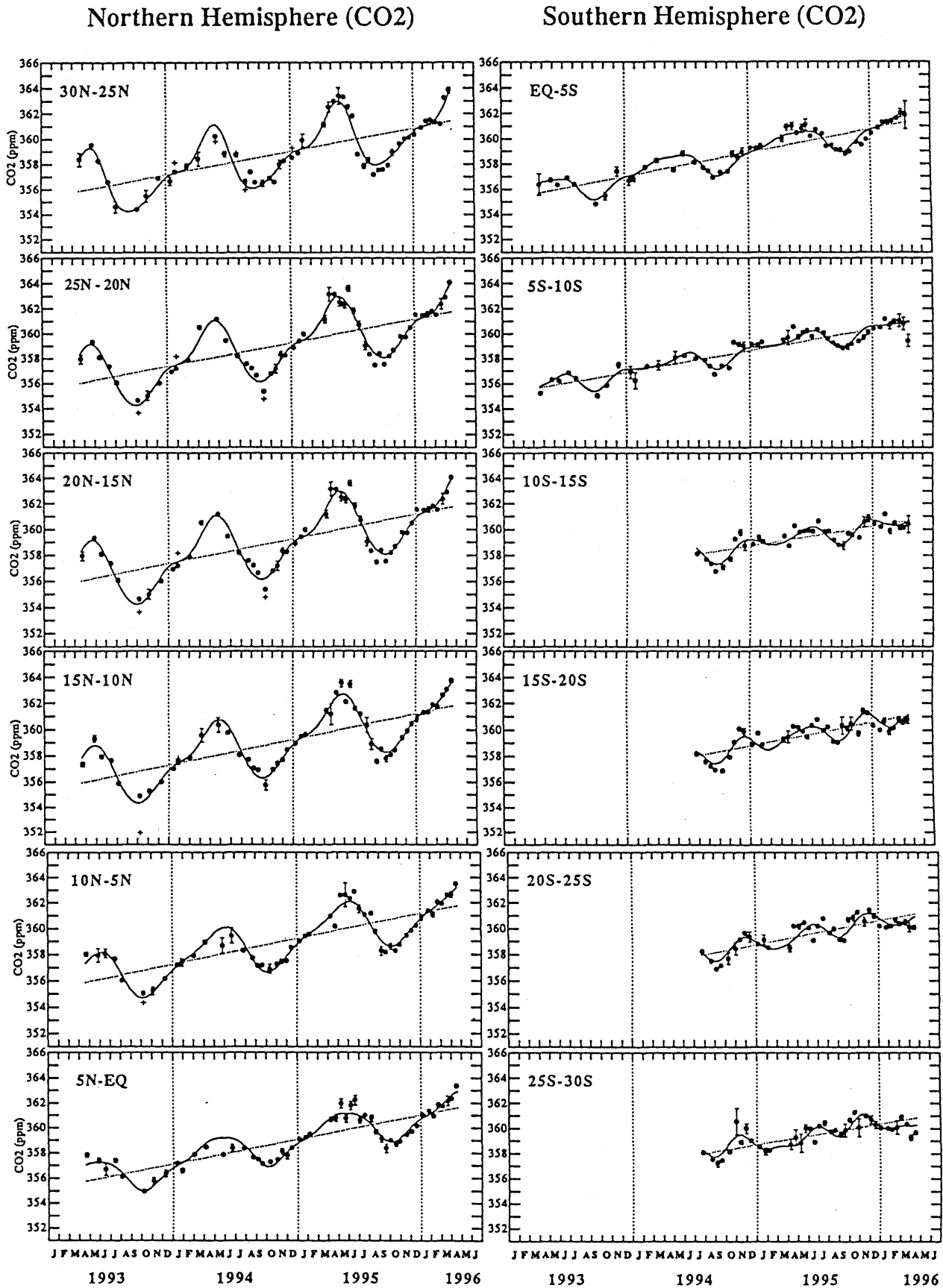


Fig. 96-2 Averaged CO<sub>2</sub> mixing ratios (closed circles) and SD (error bars) for 12 latitudinal bands between 30°N and 30°S at 9-13 km over western Pacific. Selected data presented as (+). Thick lines: best fit curve of data; dotted lines: fitted straight trend.

Northern Hemisphere (CH<sub>4</sub>)

Southern Hemisphere (CH<sub>4</sub>)

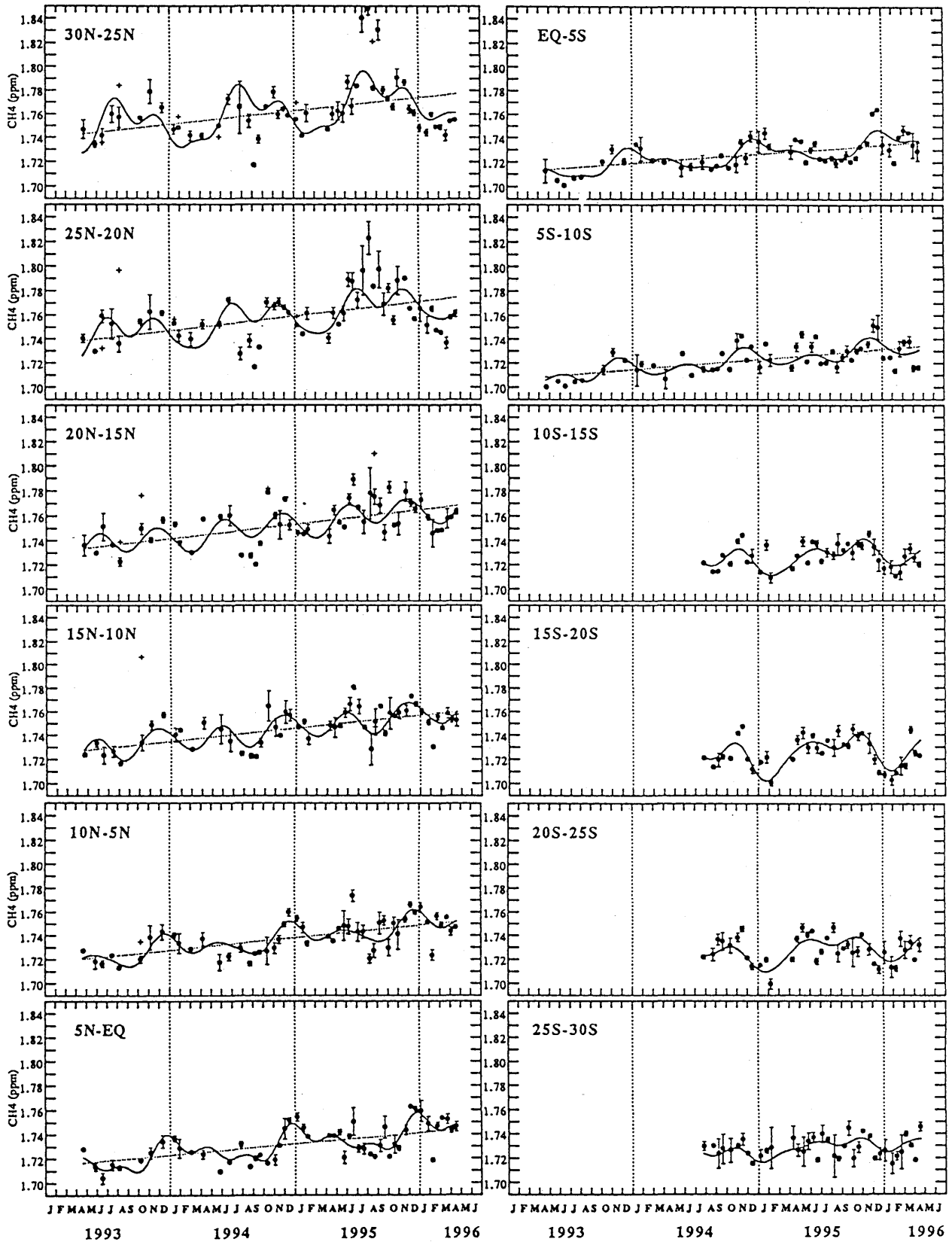


Fig. 96-3 As in Fig. 96-2 for CH<sub>4</sub>.

Air was sampled monthly over the western North Pacific between Narita (35°46'N, 140°23'E), Japan, and Cairns, (16°53'S, 145°45'E), Australia, during 1993-1994 (Figs. 1 and 2). Measurements of CO<sub>2</sub> and CH<sub>4</sub> in the Northern Hemisphere showed a clear seasonal cycle greatly influenced by the seasonal variation in the lower troposphere (Figs. 96-2 and 96-3). A significant decrease in mixing ratio during winter was observed in CH<sub>4</sub> variation, suggesting the intrusion of lower stratospheric air into the upper troposphere. The seasonal variation of both gases gradually decayed toward the equator, but a different seasonal cycle appeared in the Southern Hemisphere. This change indicated the significance of meridional transport of both gases through the upper troposphere into the Southern Hemisphere. The mixing ratio level of both gases showed a recent increase in the upper troposphere.

## 1.2 CO<sub>2</sub>, CH<sub>4</sub>, and CO in the upper troposphere from 1993 to 1996

Matsueda, Inoue, and Ishii (1997)

Matsueda *et al.* (1997) summarized observation results for CO<sub>2</sub>, CH<sub>4</sub> and CO in the upper troposphere observed using a commercial airliner from 1993 to 1996. To expand the observation region to the south, sampling flights after July 1994 were made using a different JAL airliner from Sydney (16°53'S, 145°45'E) to Narita, Japan. Sampling flight frequency was increased to about twice a month to obtain higher time resolution data.

The sampling system was operated regularly using a JAL airliner between Australia and Japan for 3 years from April 1993 to April 1996. A unique set of data for trace gases has been obtained in the upper troposphere at 9-13 km over the western Pacific. Data analysis of the observed results indicated they were successful in observing recent trends and seasonal cycles of CO<sub>2</sub>, CH<sub>4</sub>, and CO between 30°N and 30°S (Figs. 96-2, 96-3 and 96-4). The recent trend indicated recovery in the rate of CO<sub>2</sub> and CH<sub>4</sub> increase after the great anomaly around 1992. Seasonal cycles showed a large difference between the Northern and Southern Hemispheres. The northern seasonal cycle was influenced by lower tropospheric variations and mixing processes in stratospheric air, while upper tropospheric transport was identified as an important process for the seasonal cycle in the Southern Hemisphere. In addition, biomass burning in the Southern Hemisphere was identified as an additional source of trace gases in the upper troposphere.

More long-term observation is necessary in this program to gain a better understanding of the global cycle of trace gases in the upper troposphere. Special attention should be paid to the impact of widespread biomass burning on the upper atmospheric environment.

Northern Hemisphere (CO)

Southern Hemisphere (CO)

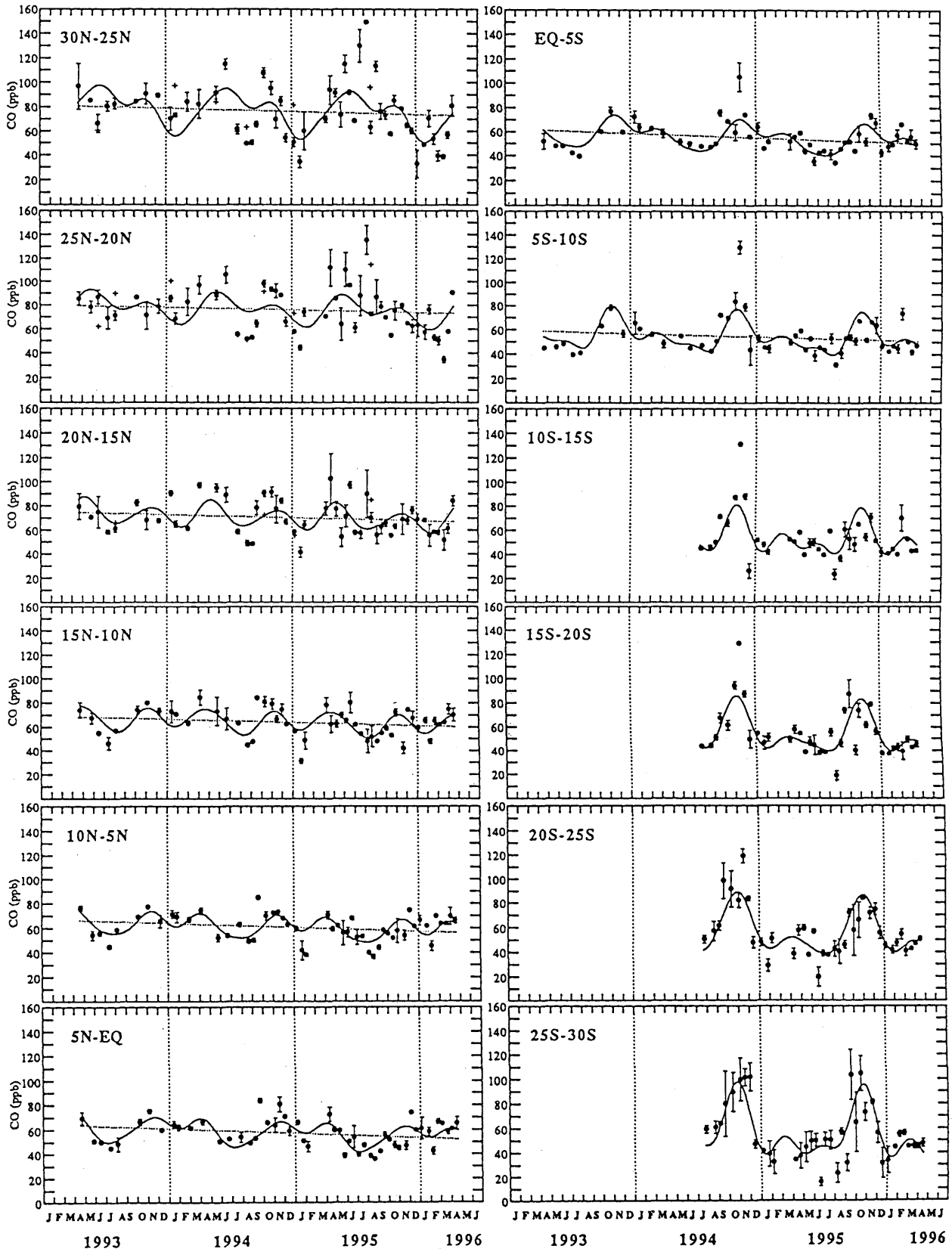


Fig. 96-4 As in Fig. 96-2 for CO.

## 2. Greenhouse Gas Behavior in Western and Central Pacific Ocean

### 2.1 Evaluation of CO<sub>2</sub> exchange at sea surface in western North Pacific: ΔpCO<sub>2</sub> distribution and CO<sub>2</sub> flux

Murata, Fushimi, Inoue, Hirota, Nemoto, Okabe, Yabuki, and Asanuma (1996)

We conducted repeated observation of carbon dioxide partial pressure (pCO<sub>2</sub>) in the western North Pacific since 1981. The increasing trend of pCO<sub>2</sub> in surface water in the region north of 10°N at 137°E was reported for the first time by Inoue *et al.* (1995) as described in 1995 ACTIVITIES. This result suggests that the middle latitude of the western North Pacific is a sink for atmospheric CO<sub>2</sub> and pCO<sub>2</sub> is increasing.

To evaluate CO<sub>2</sub> exchange at the sea surface in the western North Pacific (130°E-160°E, 30°N-0°) throughout one year, Murata *et al.* (1996) mapped the ΔpCO<sub>2</sub> using data observed from 1987 to 1993 by the JMA and the MRI on board several research vessels (Fig. 96-5). They calculated the CO<sub>2</sub> flux based on surface seawater CO<sub>2</sub> normalized, interpolated, and extrapolated using the temperature dependence of dissolved CO<sub>2</sub> determined empirically (Fig. 96-6).

They obtained the following results:

- (1) The ΔpCO<sub>2</sub> map shows that the region north of 10°N is a sink of <-70 μatm at a maximum in winter and a source of >40 μatm at a maximum in summer. This demonstrates a large seasonal change in ΔpCO<sub>2</sub> reaching 90 μatm.
- (2) The region south of 10°N is a source of 40 μatm in winter and is almost at equilibrium with atmospheric CO<sub>2</sub> in summer. This seasonal tendency is the reverse of that in the region north of 10°N.
- (3) Integrated annual net CO<sub>2</sub> flux is -22.4/-48.6 MtC (ocean influx) in the region north of 10°N and 3.7/5.4 MtC (ocean efflux) south of it, depending on the wind-dependent transfer velocity and exchange coefficient (Table 96-1).

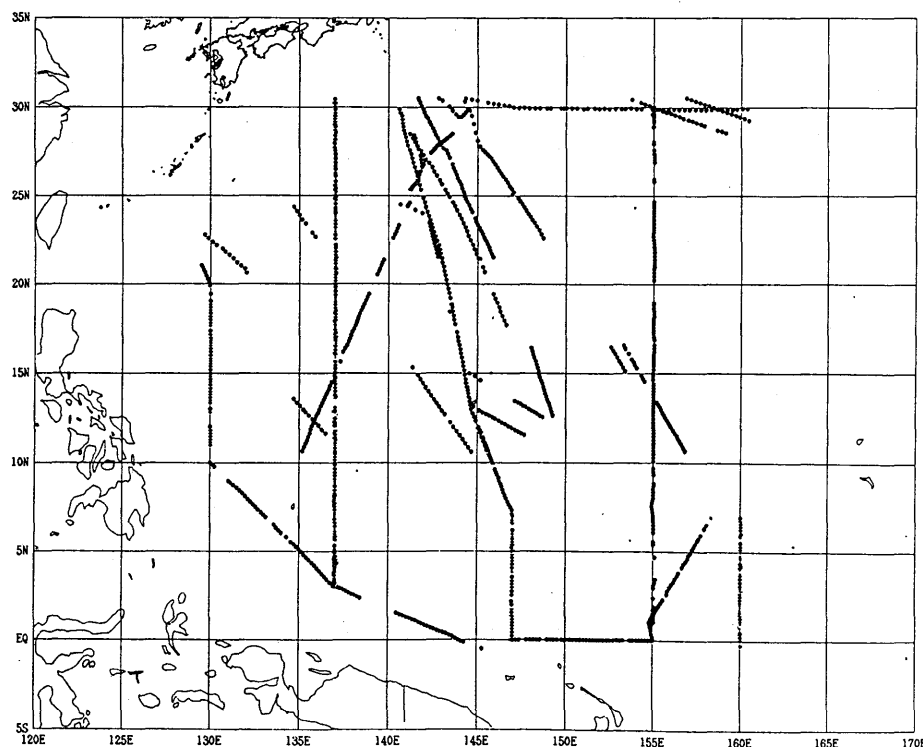
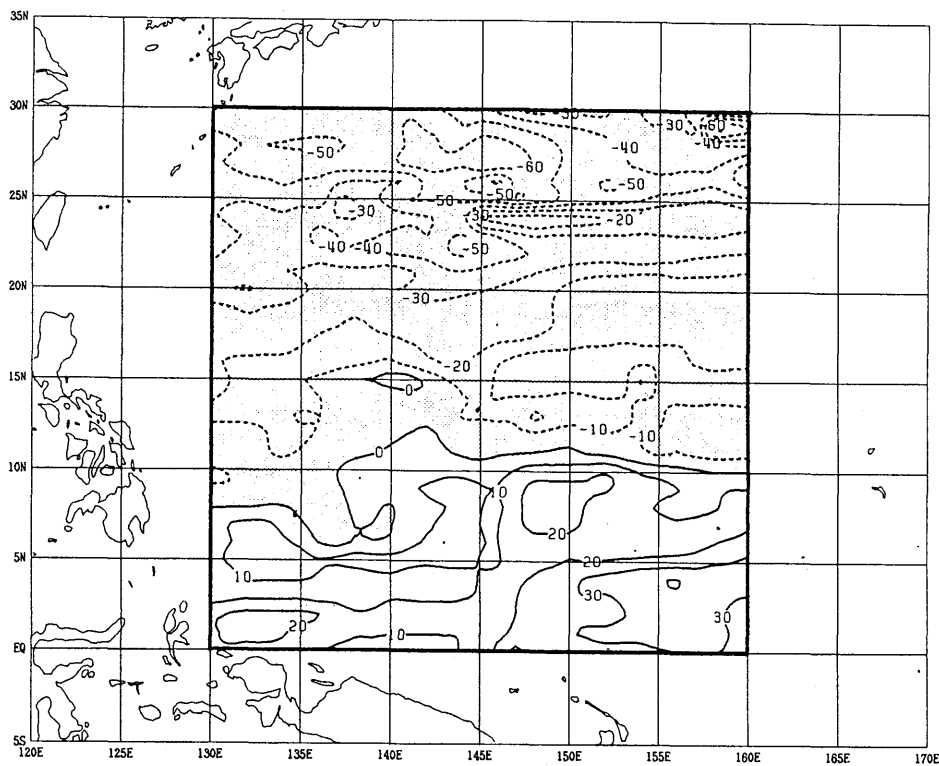


Fig. 96-5 Surface seawater CO<sub>2</sub> data points observed from 1987 to 1993 by JMA and MRI.

$\Delta pCO_2$  ( $\mu atm$ ): January



$\Delta pCO_2$  ( $\mu atm$ ): February

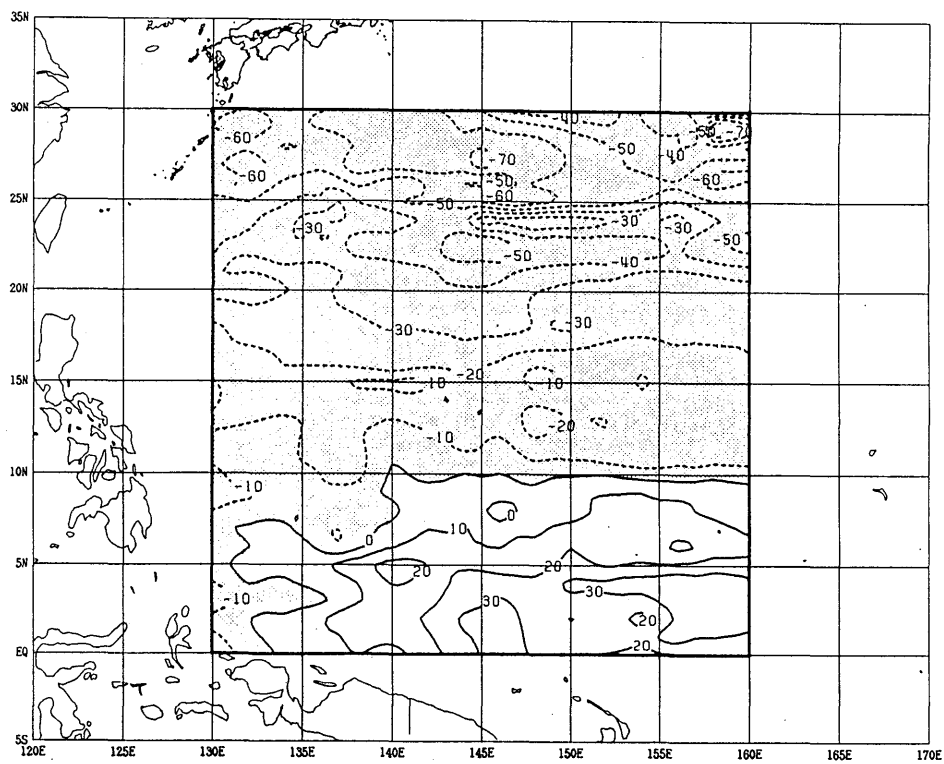
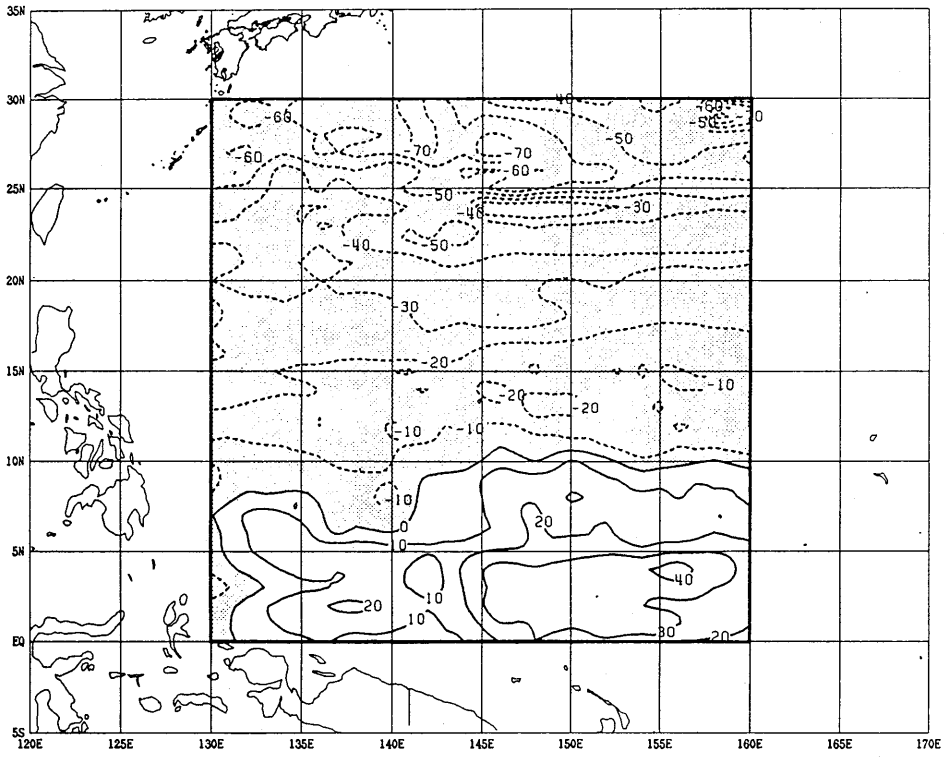


Fig. 96-6 Distribution of reconstructed  $\Delta pCO_2$  ( $\mu atm$ ) from January to December 1990. The dotted pattern indicates negative (air-to-sea)  $\Delta pCO_2$ .

$\Delta p\text{CO}_2$  ( $\mu\text{atm}$ ): March



$\Delta p\text{CO}_2$  ( $\mu\text{atm}$ ): April

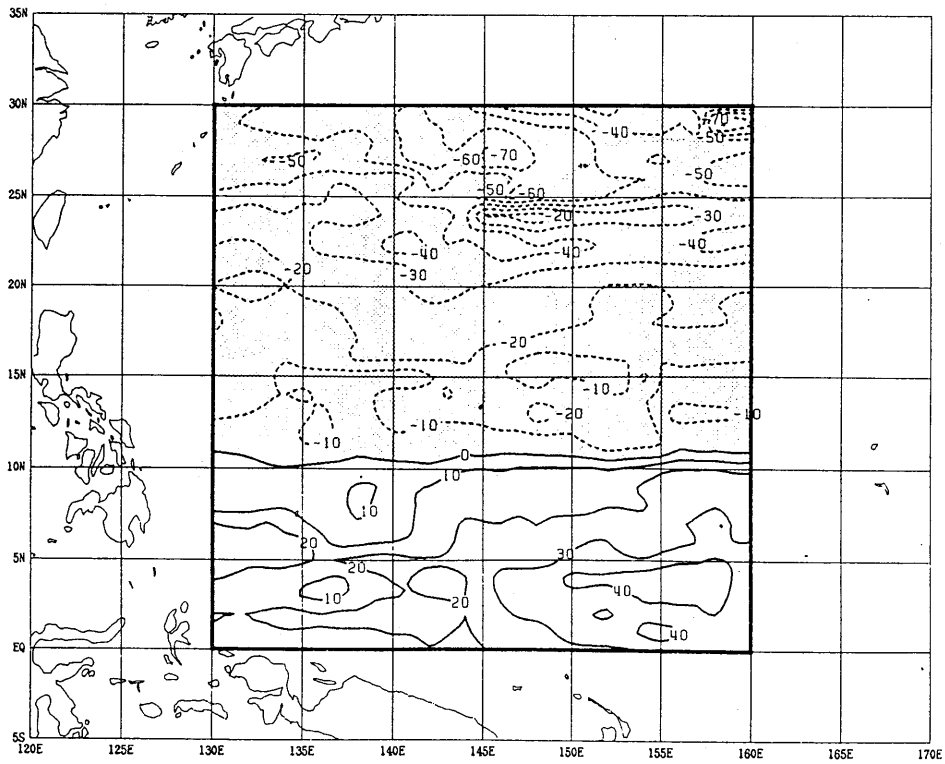
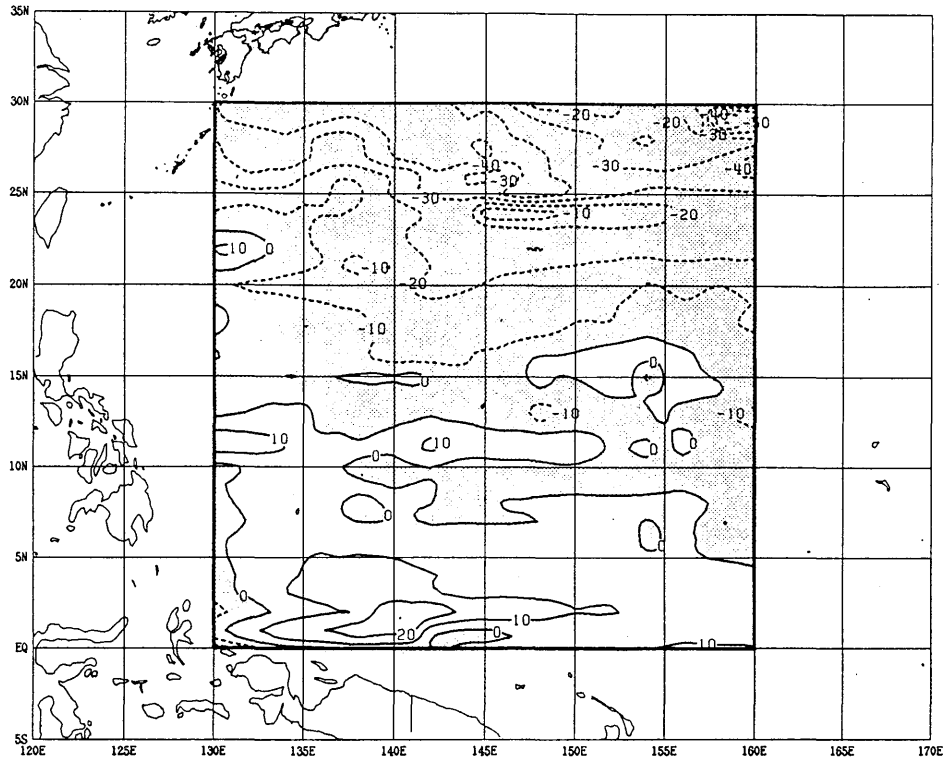


Fig. 96-6 Continued.

$\Delta p\text{CO}_2$  ( $\mu\text{atm}$ ): May



$\Delta p\text{CO}_2$  ( $\mu\text{atm}$ ): June

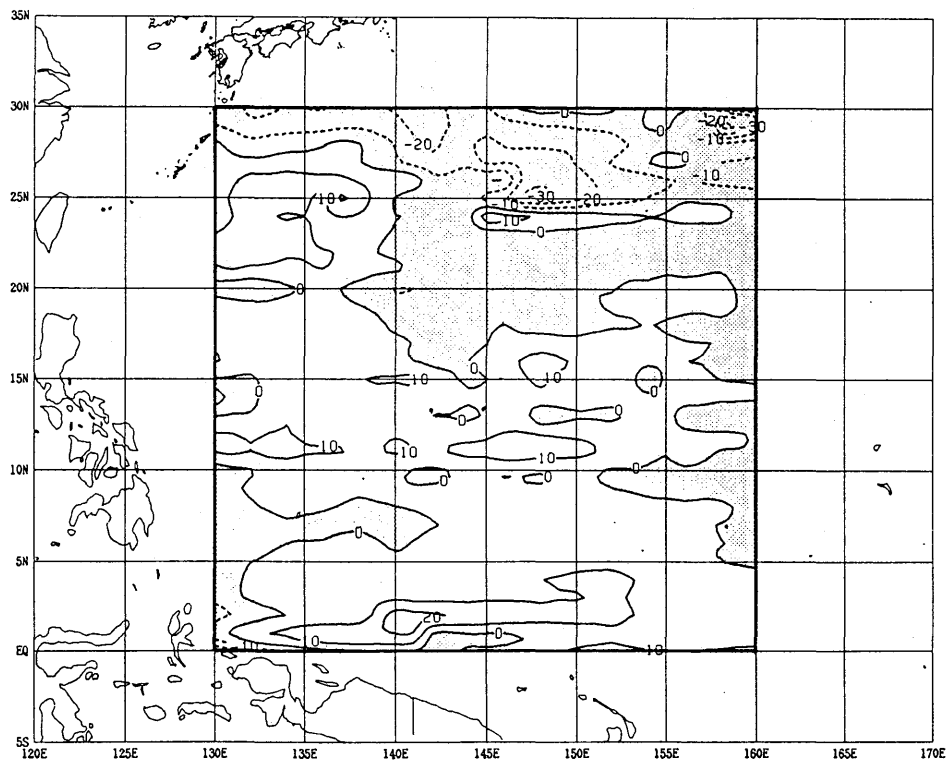
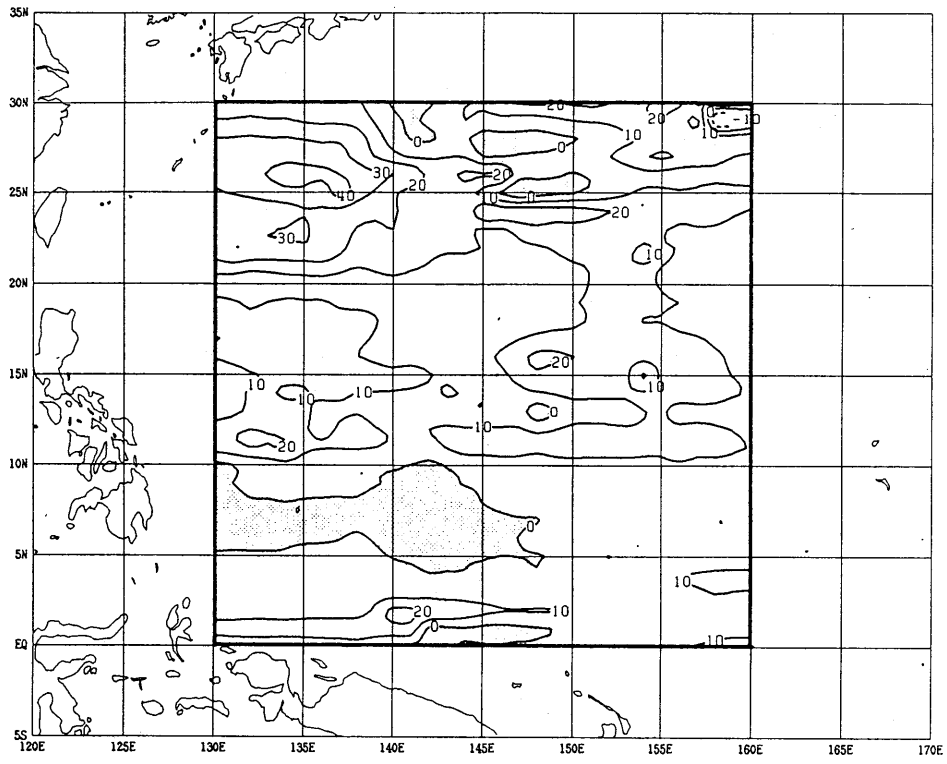


Fig. 96-6 Continued.

$\Delta p\text{CO}_2$  ( $\mu\text{atm}$ ): July



$\Delta p\text{CO}_2$  ( $\mu\text{atm}$ ): August

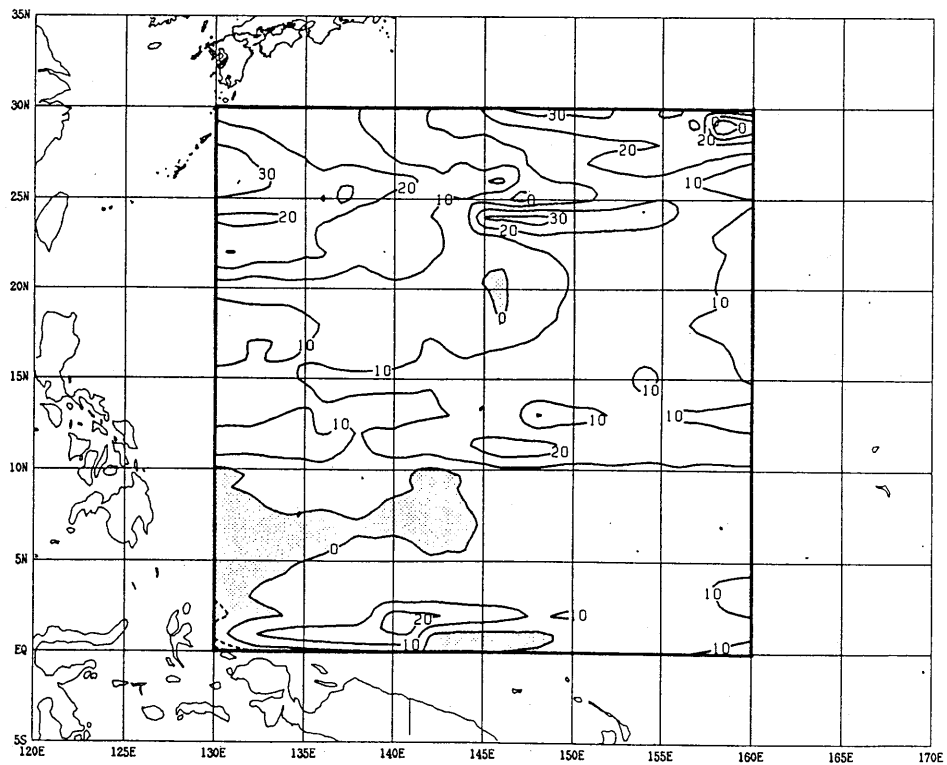
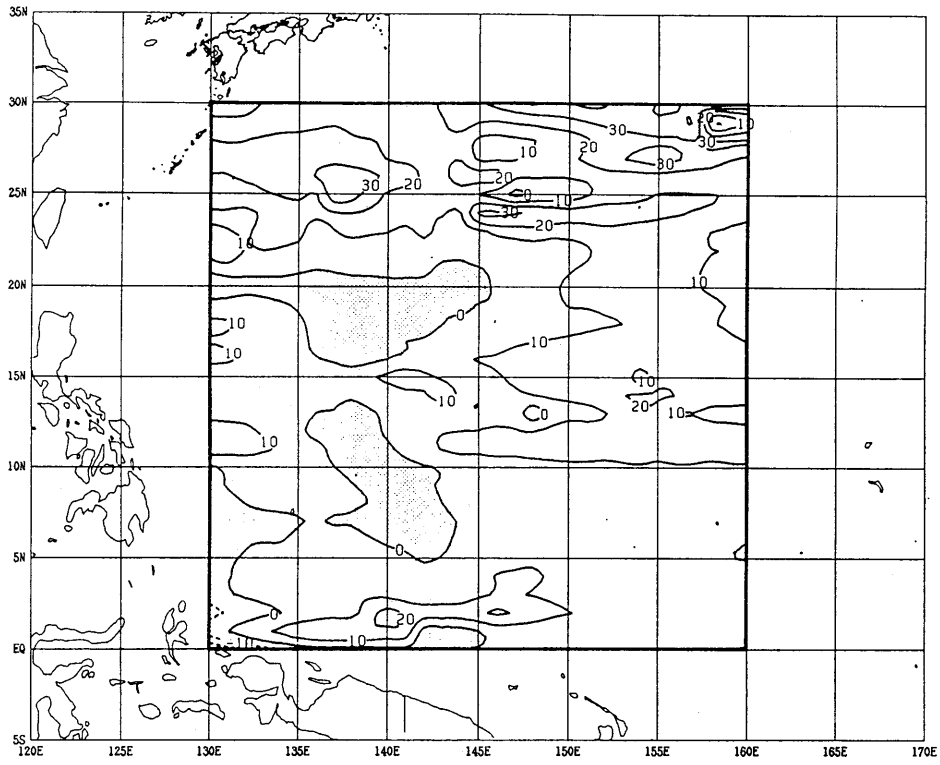


Fig. 96-6 Continued.

$\Delta pCO_2$  ( $\mu atm$ ): September



$\Delta pCO_2$  ( $\mu atm$ ): October

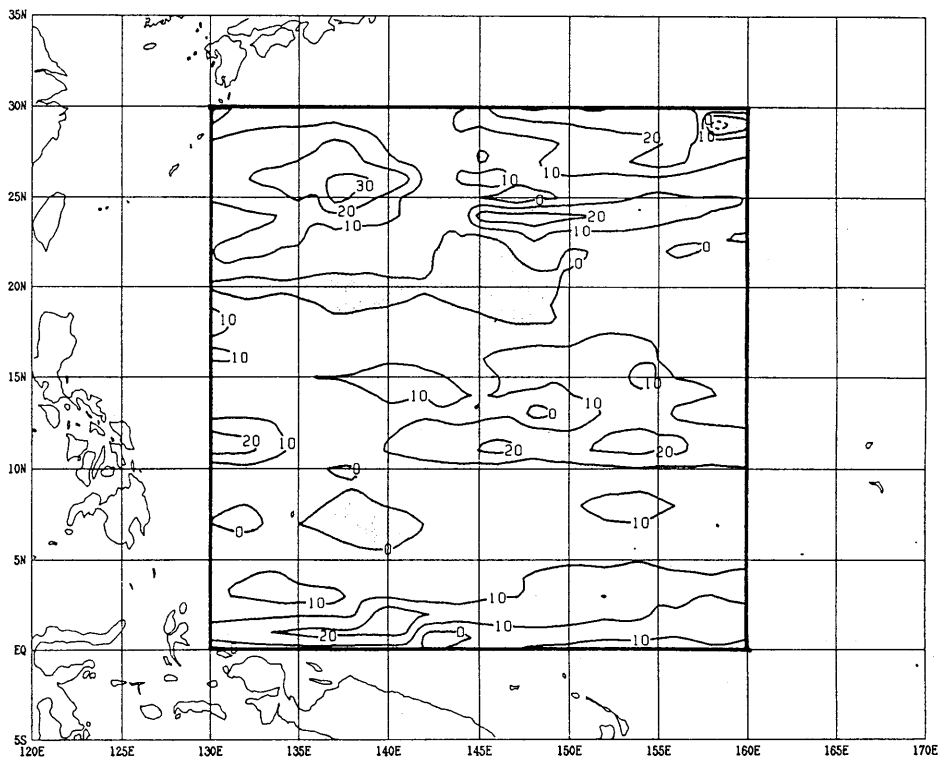
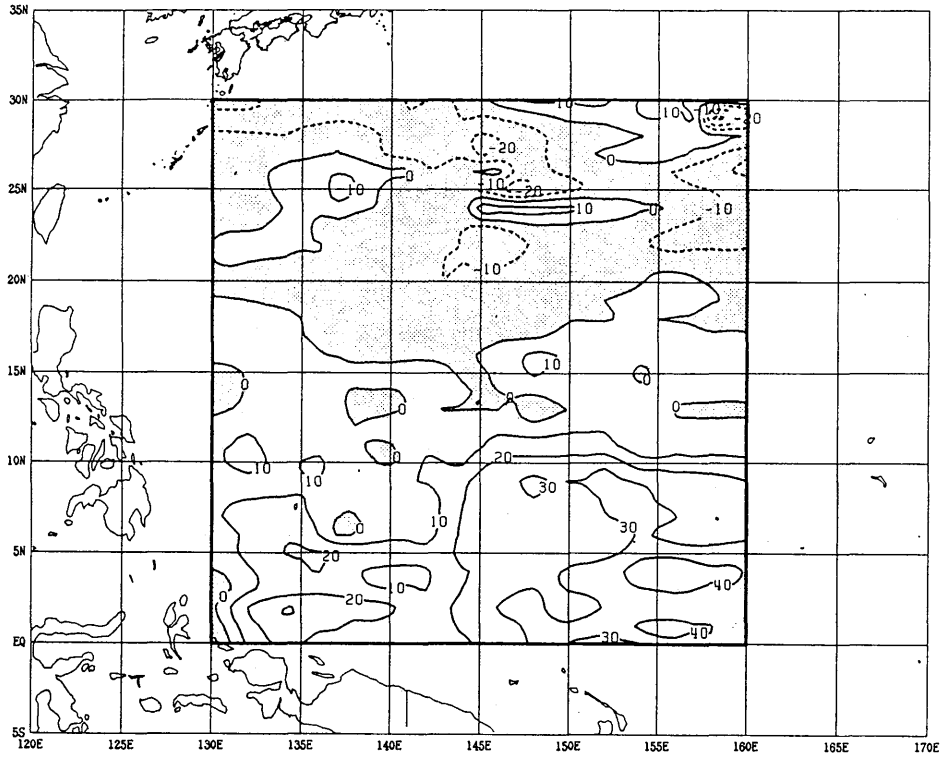


Fig. 96-6 Continued.

$\Delta p\text{CO}_2$  ( $\mu\text{atm}$ ): November



$\Delta p\text{CO}_2$  ( $\mu\text{atm}$ ): December

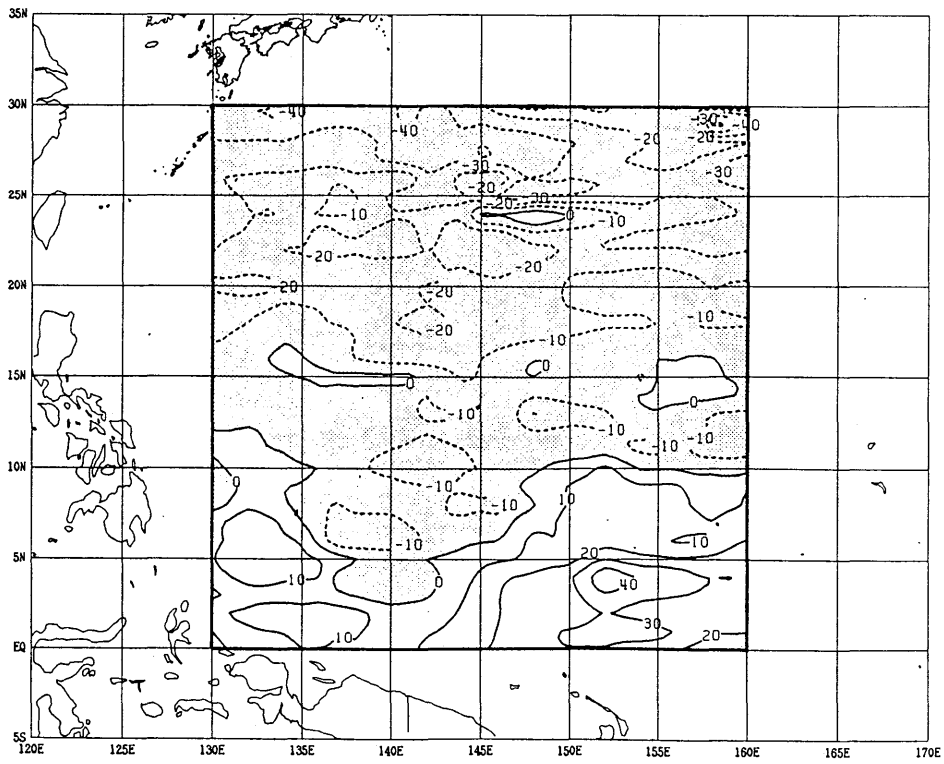


Fig. 96-6 Continued.

Table 96-1 Estimates of sea-to-air CO<sub>2</sub> flux (Mt of C) in the regions north and south of 10°N for each month, separated for (a) LM and (b) TFT formula.

(a)													
	J	F	M	A	M	J	J	A	S	O	N	D	Total
> 10°N	-7.2	-5.6	-6.3	-4.0	-2.1	0.0	1.2	2.6	1.9	1.3	-0.5	-3.5	-22.4
≤ 10°N	0.6	0.3	0.3	0.3	0.1	0.2	0.0	0.1	0.1	0.1	1.3	0.3	3.7

(b)													
	J	F	M	A	M	J	J	A	S	O	N	D	Total
> 10°N	-15.1	-12.3	-13.4	-8.7	-4.7	0.0	2.3	5.2	3.9	2.7	-1.1	-7.3	-48.6
≤ 10°N	1.1	0.6	0.3	0.4	0.0	0.2	0.0	0.1	0.1	0.1	2.1	0.3	5.4

## 2.2 Changes in longitudinal distribution of CO<sub>2</sub> partial pressure in central and western equatorial Pacific, west of 160°W

Inoue, Ishii, Matsueda, Aoyama, and Asanuma (1996)

We focused our study on pCO<sub>2</sub> distribution variation in the western and central equatorial Pacific with relation to El Niño/Southern Oscillation (ENSO) phenomena. The equatorial Pacific is known as a strong oceanic source of atmospheric CO<sub>2</sub>. CO<sub>2</sub> is supplied to the atmosphere mostly in the eastern and central equatorial Pacific due to upwelling containing CO<sub>2</sub>-rich water.

Inoue *et al.* (1996) described spatial and temporal variations in pCO<sub>2</sub> in the central and western equatorial Pacific based on measurements conducted between 1987 and 1994. Surface water pCO<sub>2</sub> data indicate significant differences in longitudinal distribution depending on ocean conditions (Figs. 96-7 and 96-8). They examined the relationship between the area showing higher surface pCO<sub>2</sub> and ENSO phenomena by using the Southern Oscillation Index (SOI) (Fig. 96-9). Results indicate that the area showing higher surface pCO<sub>2</sub> correlates with the SOI, and the western edge of the higher pCO<sub>2</sub> area moves eastward with increasing SOI, which suggests significant intra- and interannual fluctuations of CO<sub>2</sub> outflux from the central and western equatorial Pacific (Fig. 96-10).

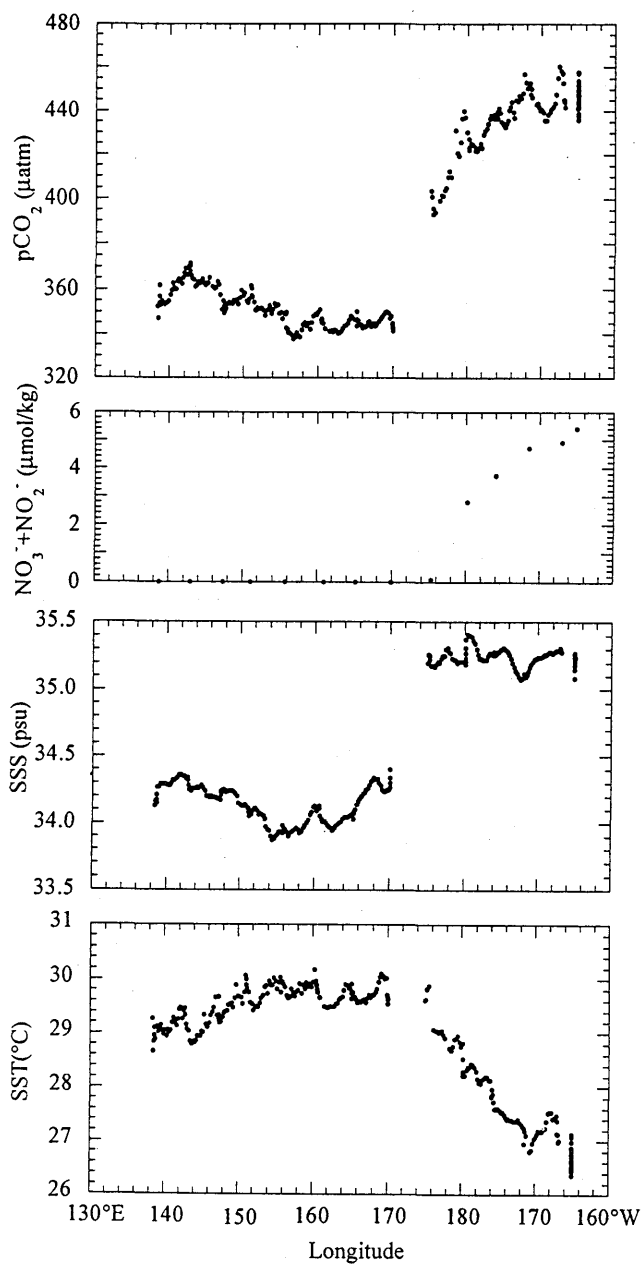


Fig. 96-7 Longitudinal distributions of pCO<sub>2</sub> (top), concentration of nitrate and nitrite (upper middle), SSS (lower middle), and SST (bottom) along equator for January-February 1994.

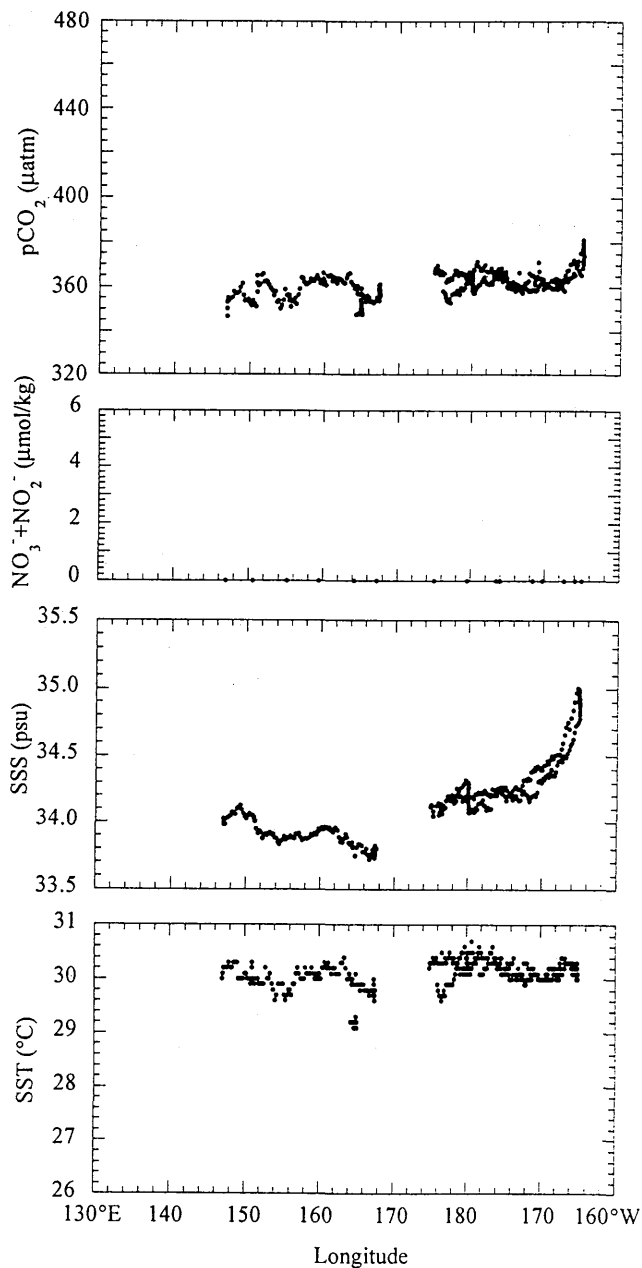


Fig. 96-8 Same as in Fig. 96-7 except for November-December 1994.

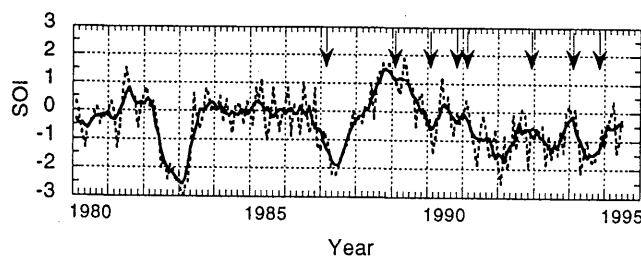


Fig. 96-9 SOI times series. Dotted line: monthly mean SOI; solid line: 5-month running mean. Arrows: pCO<sub>2</sub> observation times. Cruises in western and central equatorial Pacific were conducted January-February 1987, January-February 1989, January-February 1990, September-December 1990, January-February 1991, November-December 1992, January-February 1994, and November-December 1994.

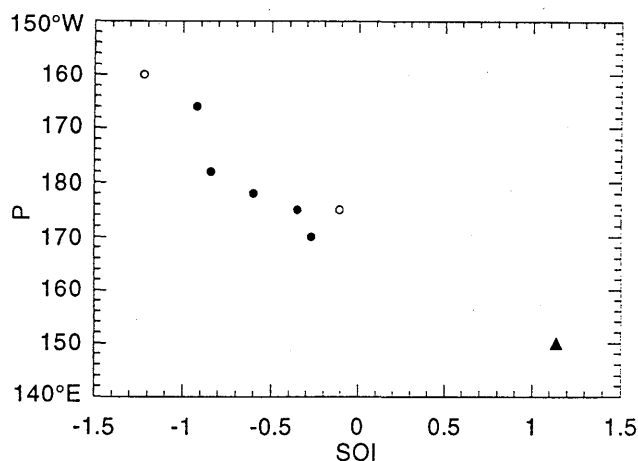


Fig. 96-10 Position (P) of abrupt change in pCO<sub>2</sub> and SOI. SOI during observation was calculated based on a 5-months running mean. pCO<sub>2</sub> data from September-October 1990 was not used because data around P (170°E-180°) was insufficient. Open circle: P along 5°S. During January-February 1989, P was estimated based on SST data (solid triangle).

### 2.3 Temporal and spatial variations in atmospheric and oceanic CO<sub>2</sub> in western North Pacific From 1990 to 1993: Possible link to 1991/92 ENSO event

Murata and Fushimi (1996)

Murata and Fushimi (1996) presented the results of atmospheric and oceanic CO<sub>2</sub> observations conducted by the JMA at 137°E in the western North Pacific for 1990 - 1993, covering an ENSO event (onset: spring 1991; disappearance: summer 1992) (Fig. 96-11). The atmospheric CO<sub>2</sub> concentration over the region south of 30°N increased drastically between 1990 and 1991 during winter (4.0 ppmv) and summer (4.5 ppmv), although values are not seasonally adjusted. Over the other two years of observation, growth rates were smaller or even negative (Figs. 96-12 and 96-13).

Oceanic CO<sub>2</sub>, expressed in units of the mole fraction (ppmv) in dry air equilibrated with seawater, significantly increased, especially in low latitudes during both seasons of 1991 - 1993, compared to 1990 (Fig. 96-14). Oceanic CO<sub>2</sub>, normalized at a constant temperature, also significantly increased, with larger magnitudes for winter and smaller for summer. This implies that increased summer oceanic CO<sub>2</sub> results mostly from changes in surface seawater temperature, while for that in winter, other factors, unknown at present, are more related to increased oceanic CO<sub>2</sub>.

Calculated  $\Delta p\text{CO}_2$  and CO<sub>2</sub> flux at the air-sea interface reveal that in winter, the region north for 10°N acts

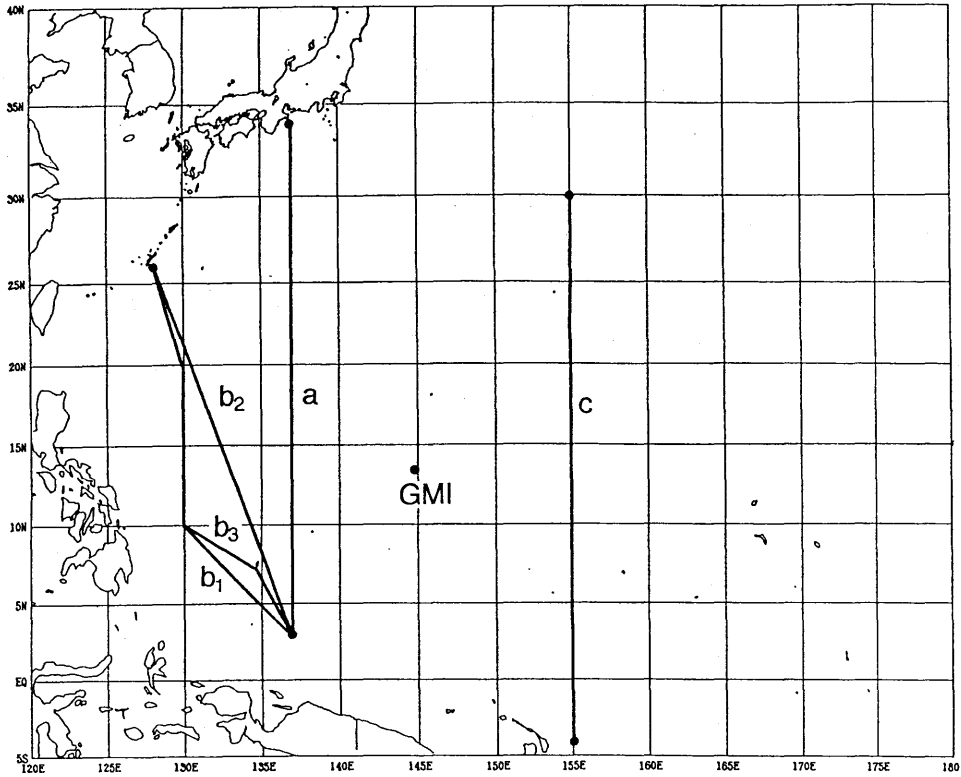


Fig. 96-11 Location of observational lines indicated as a 137°E,  $b_{1-3}$  lines west of 137°E, and c 155°E. The NOAA/CMDL GMI site (Guam, 13°26'N, 144°47'E) is also indicated.

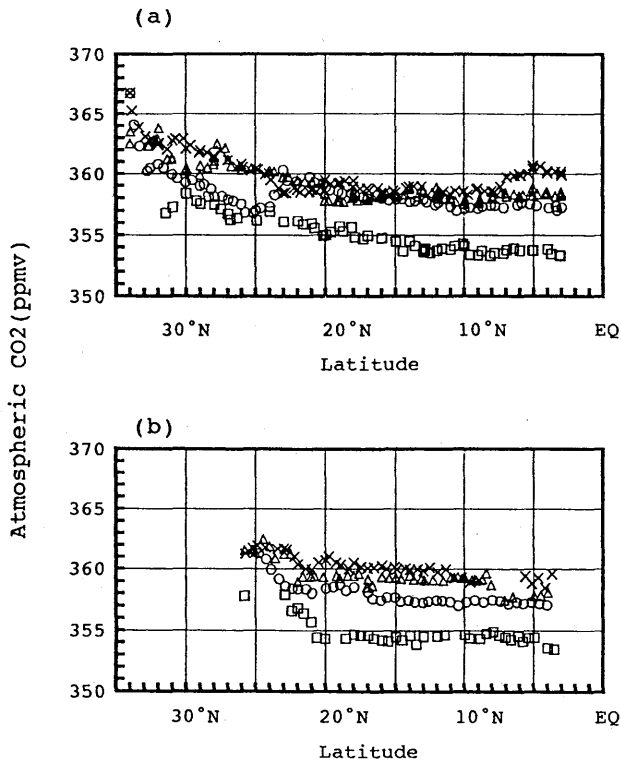


Fig. 96-12 Latitudinal distributions of atmospheric CO<sub>2</sub> during winter from 1990 to 1993, for (a) observational line along 137°E and (b) lines west of 137°E. Letters at upper left of panels correspond to observational lines in Fig. 96-11. Squares: 1990; circles: 1991; triangles: 1992; crosses: 1993.

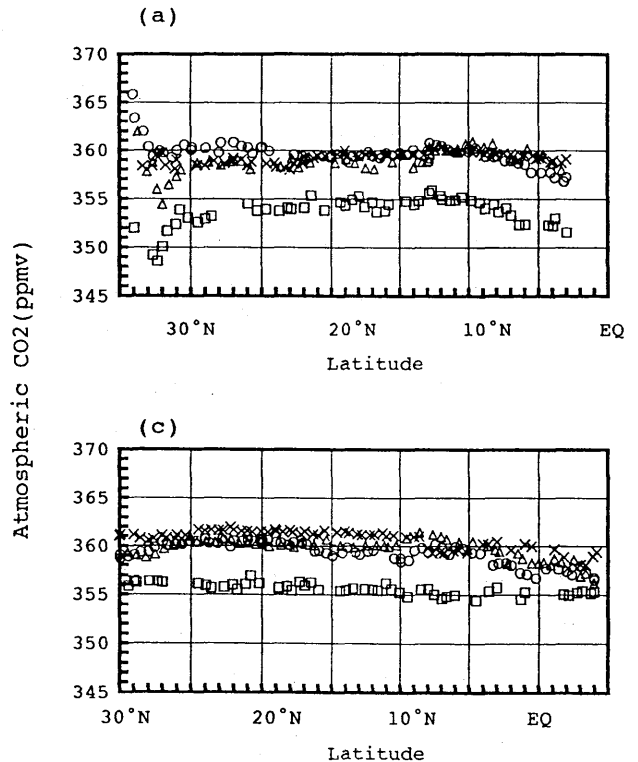
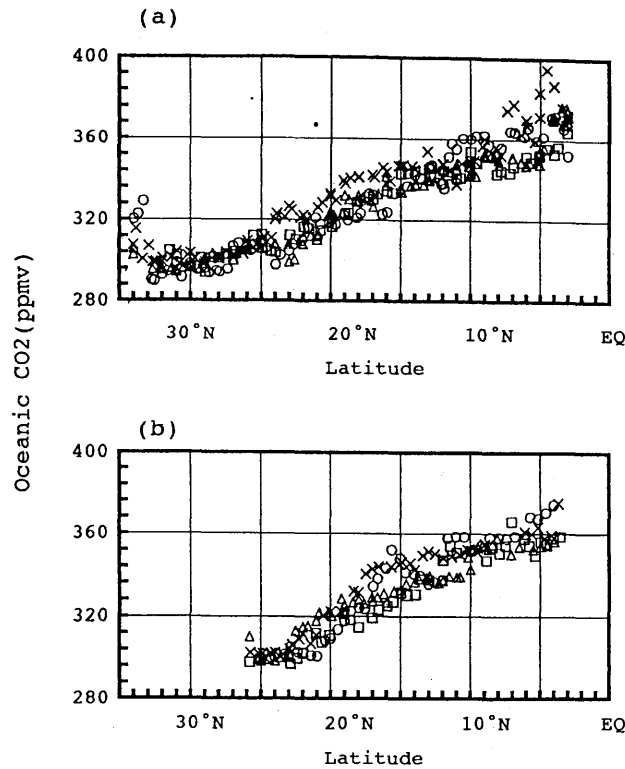


Fig. 96-13 Same as in Fig. 96-12 except for (a) observational line along 137°E and (c) that along 155°E during summer.


 Fig. 96-14 Same as in Fig. 96-12 except for oceanic CO<sub>2</sub>.

as a sink for CO<sub>2</sub>, with a maximum net flux of  $\sim -10.0 \text{ mmol} \cdot \text{m}^{-2} \cdot \text{d}^{-1}$ . The region south of 10°N, however, at times becomes a weak source of CO<sub>2</sub>, with a maximum net flux of  $2.4 \text{ mmol} \cdot \text{m}^{-2} \cdot \text{d}^{-1}$ . In summer, the western North Pacific becomes a weak source or is almost in equilibrium with atmospheric CO<sub>2</sub>.

The increase in winter oceanic CO<sub>2</sub> or  $\Delta p\text{CO}_2$ , related to the 1991/92 ENSO event, is not as distinct as in the 1982/83 ENSO event, although lower temperatures and higher salinity in surface seawater were commonly found during both events. The response of CO<sub>2</sub> flux in the tropical western North Pacific to the 1991/92 ENSO event was rather small compared to the magnitude of rate changes obtained in previous results for the central or eastern tropical Pacific.

#### 2.4 Atmospheric methane over North Pacific from 1987 to 1993

Matsueda, Inoue, Ishii, and Nogi (1996)

Atmospheric methane is known as an important greenhouse gas that influences the radiative balance and climate of the earth. Methane has accumulated in the atmosphere since the Industrial Revolution, but it is known that the recent global rate of increase shows large interannual variations in both hemispheres. Such growth rate variations are caused by a change in the relative strength between sources and sinks, but a particular cause cannot be quantitatively identified at the moment. A long-term record of atmospheric methane measurements is necessary to better understand recent growth rate variation.

Matsueda *et al.* (1996) continued to collect air samples over the western North Pacific region and measured atmospheric methane mixing ratios during winter from 1987 to 1993 to extend their methane record since 1978 (Matsueda *et al.*, 1992) (Fig. 96-15). The meridional distribution of methane showed a yearly north-to-south gradient from midlatitudes to the equator (Fig. 96-16). A sharp mixing ratio gradient often appeared at the boundary between the winter monsoon and trade wind regions around 20°N. No significant longitudinal gradient

was found during winter, although methane levels along the equator showed a large difference between the western and eastern Pacific.

The overall methane increase rate in the western Pacific was estimated at 13 ppb/yr based on the long-term record for 15 years from 1978 to 1993. This record indicates that the methane growth rate over this Pacific region gradually slowed until 1990, followed by no significant increase in the 1990s. The overall deceleration of the growth rate was more rapid in the middle latitudinal zone (20°N - 30°N) than in the lower latitudinal zone (3°N - 20°N) (Fig. 96-17a). This latitudinal difference suggests a rapid reduction of methane emission from continent. The methane growth rate showed an interannual variation with an increasing trend around 1983 and 1987, roughly related to El Niño events (Fig. 96-17b). The methane growth rate thus appears to have been affected by a change in interhemispheric transport due to the ENSO events.

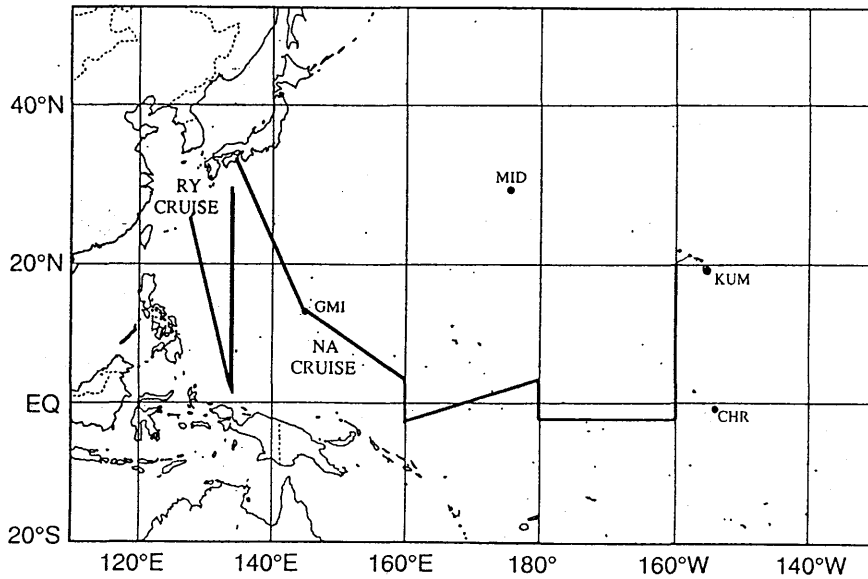


Fig. 96-15 Tracks of R/V *Ryofu Maru* (RY) and R/V *Natsushima* (NA) during January-February 1987. The sampling area of NA cruises was almost the same in 1989, 1990, and 1991, although tracks in these years were slightly different from that used in 1987.

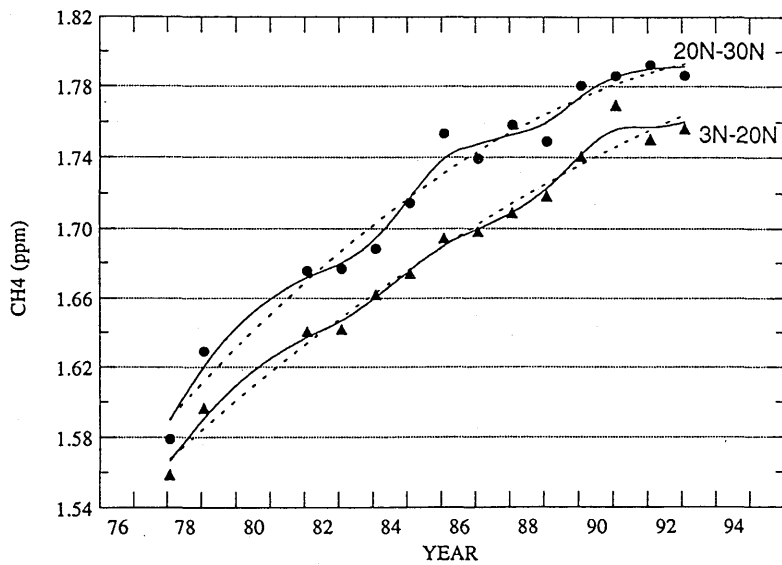


Fig. 96-16 Averaged methane mixing ratio in middle (20°N-30°N) and lower (3°N-20°N) latitudinal zones along 137°E in western Pacific from 1978 to 1993. Dashed lines: quadratic equation  $f(t)$ ; solid lines: function  $F(t)$ ; fitted to averaged data.

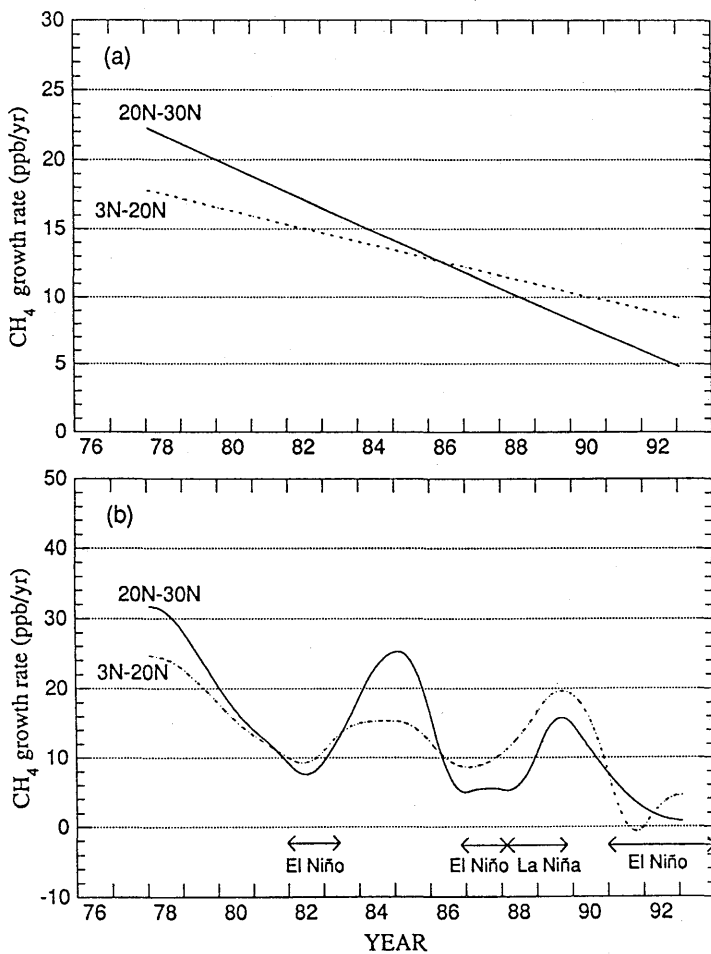


Fig. 96-17 Growth rate variations of atmospheric methane in middle (20°N-30°N) and lower (3°N-20°N) latitudinal zones along 137°E in western North Pacific from 1978 to 1993. (a) Overall trends and (b) interannual variation of growth rate were obtained by derivatives of  $f(t)$  and  $F(t)$  (Fig. 96-16).

## WATER MASS ANALYSIS

### 3. Western North Pacific

#### 3.1 Water masses between Mindanao and New Guinea

Kashino, Aoyama, Kawano, Hendiarti, Syaefudin, Anantasena, Munezama, and Watanabe (1996)

In the western equatorial Pacific, particularly in the southern Philippine Sea, there is an area called "water mass crossroads" where several water masses from the northern and southern hemispheres meet.

Kashino *et al.* (1996) investigated water masses between Mindanao and New Guinea, using hydrographic data, during two R/V *Kaiyou* WOCE expeditions conducted in October 1992 and February 1994 by the Japan Marine Science and Technology Center (JAMSTEC) to understand the Indonesian throughflow, which probably plays an important role in the global ocean circulation. It is important to identify which water masses enter the Indonesian Seas from the Pacific.

Conclusions are as follows:

1. South Pacific Tropical Water (SPTW), with a salinity maximum around  $25.0 \sigma_{\theta}$  reaches north of Morotai Island (Fig. 96-18).
2. Antarctic Intermediate Water (AAIW), with a salinity minimum around  $27.2 \sigma_{\theta}$  and high oxygen ( $>100 \mu\text{mol/kg}$ ), exists in the southwestern area of the southernmost Philippine Sea (Fig. 96-19).
3. North Pacific Tropical Water and the remnant of the North Pacific Intermediate Water originating in the North Pacific return from the Celebes/Maluku Seas with the low salinity water via the northeastward flow between Talaud Islands and Morotai Island. They found that this northeastward flow, which was shown to exist in the upper 100 m by Lukas *et al.* (1991), extended to at least a depth of 300-400 m. This finding suggests that retroflexion of the Mindanao Current (MC) occurs in the Celebes Sea.
4. The New Guinea Coastal Undercurrent, transporting SPTW and AAIW from the southern hemisphere, is divided into at least two parts because the retroflexion of the MC prevents its shallow part from reaching farther north; the shallower SPTW turns eastward as a source of the North Equatorial Countercurrent and retroflects toward the southeast. AAIW and the lower part of SPTW flow northward and appear to be linked to the Mindanao Undercurrent.

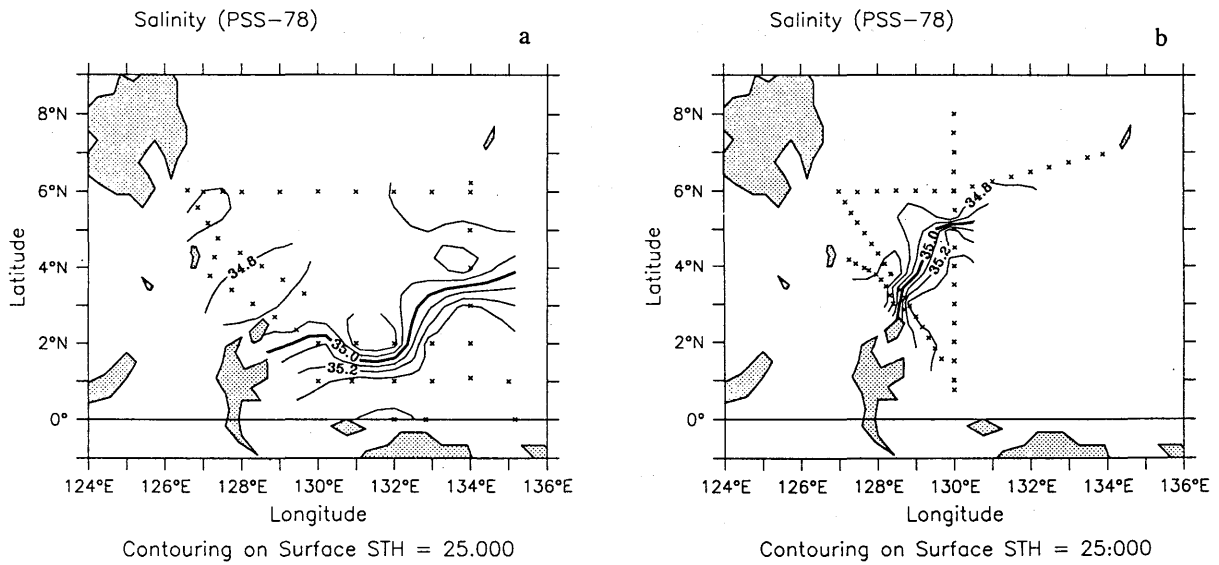


Fig. 96-18 Salinity distributions at surface  $\sigma_\theta = 25.0$  during (a) *Kaiyo* WOCE I and (b) *Kaiyo* WOCE II. Contour interval: 0.1 PSS.

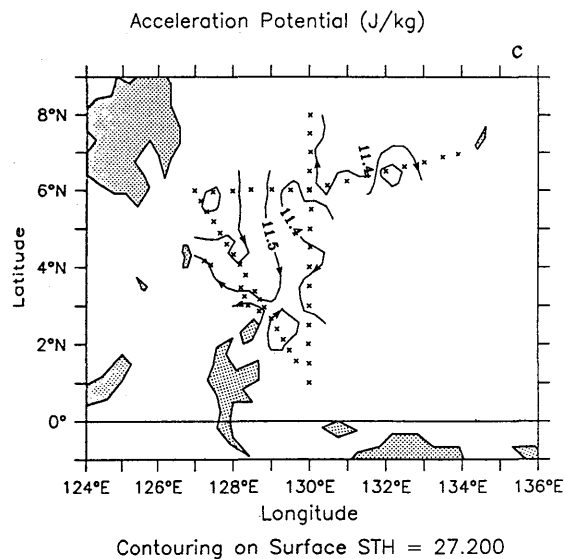
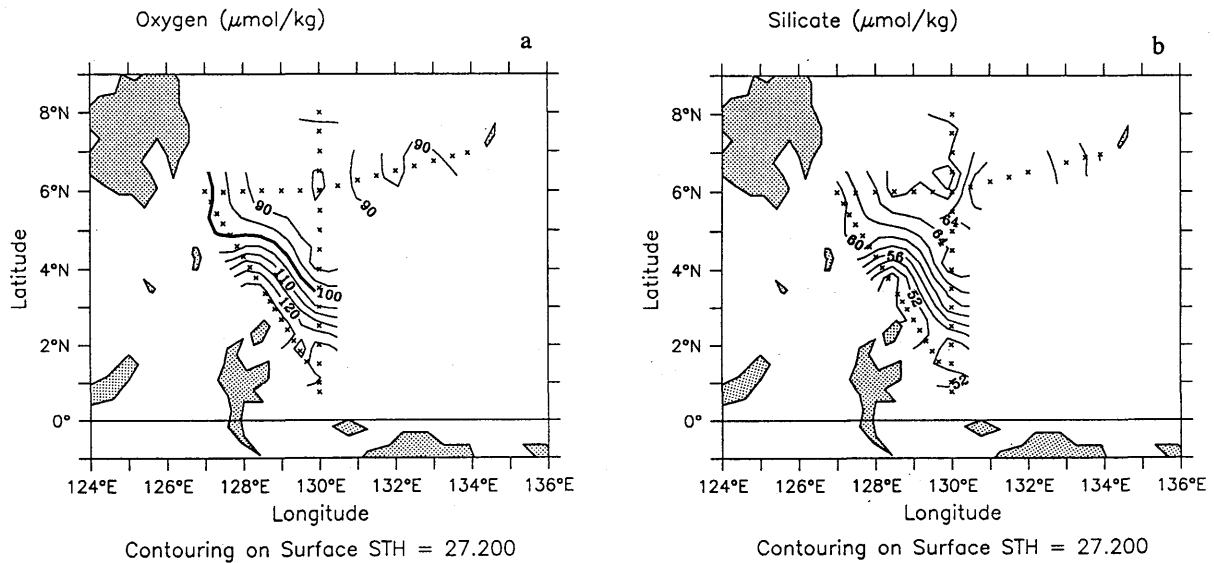


Fig. 96-19 (a) Dissolved oxygen, (b) silicate, and (c) acceleration potential relative to 1500 dbar on the surface  $\sigma_\theta = 27.2$  during *Kaiyo* WOCE II. Contour intervals are 5.0  $\mu\text{mol/kg}$ , 2.0  $\mu\text{mol/kg}$ , and 0.1 J/kg.

### 3.2 Preliminary study of in the north central Japan Sea temperature structure

Hirose, Hong, and Miyao (1996)

The north Japan sea is significant because of the formation of upper Japan Sea Proper Water (JSPW), which occupies most of the deep waters in the Japan Sea and is extremely homogeneous in salinity, temperature, and higher oxygen in winter due to deep convection. Little observational data has been collected, however, especially in winter.

In March 1994, a Japan-Korea-Russia Expedition was conducted in the north central Japan Sea, the main purpose of which was to determine the radioactive contamination of seawater, biota, and sediment from radioactive waste dumping by Russia (and the former USSR). During the expedition, Hirose *et al.* (1996) conducted CTD and XBT measurements to determine hydrographic features of the area surveyed (Fig. 96-20).

Water mass in early spring in the north central Japan Sea (north of 40°N) was characterized as cold (less than 2.5°C) and salinity-homogeneous ( $34.07 \pm 0.02$ ). Vertical profiles of seawater temperature suggest that the water mass can be divided into at least two parts: surface water and JSPW. The spatial distributions of seawater temperature suggest that an anticyclonic eddy coupled with a cyclonic eddy was present in the north central Japan Sea (Fig. 96-21). Hydrographic information is important to understanding the distribution of radionuclides in the north central Japan Sea.

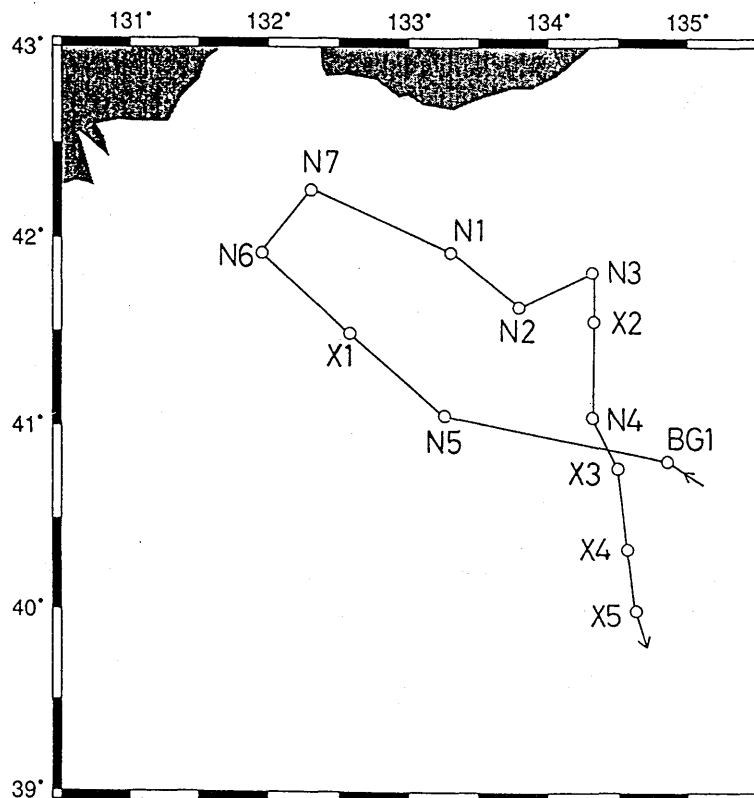


Fig. 96-20 Track and sampling points in central Japan Sea.

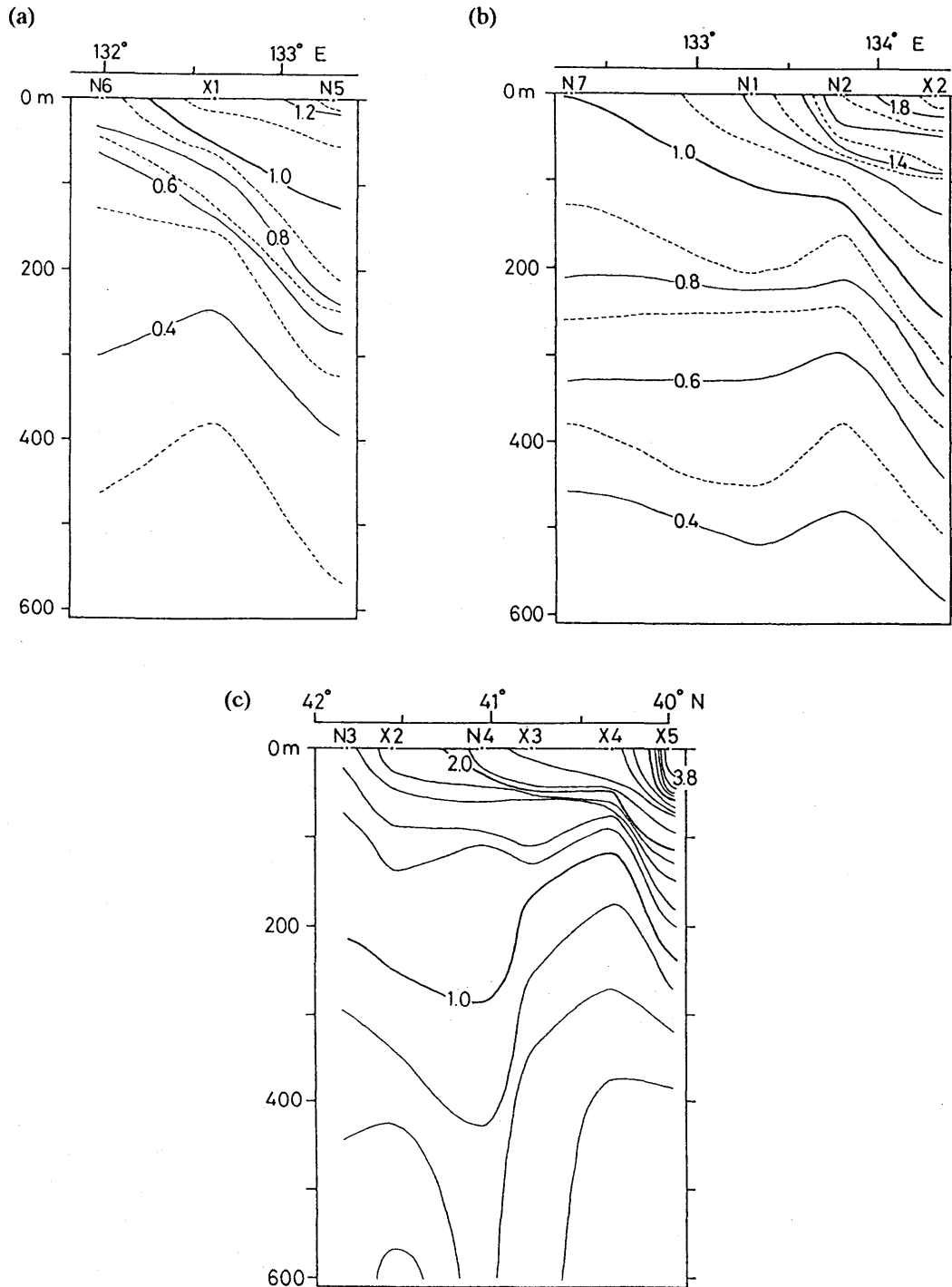


Fig. 96-21 Seawater temperature cross sections from surface to 600 m depth. a: N6-N5, b: N7-X2, c: N3-X5.

## RADIOACTIVE NUCLIDES

### 4. Anthropogenic Radionuclide Geochemical Studies and Analysis in Fallout Samples

Aoyama, Hirose, Igarashi, and Miyao (1996)

Since 1957, GRD scientists of the MRI have measured anthropogenic radionuclides in fallout samples collected in Japan — over 40 years. In the series of studies, we obtained information useful to understanding the behavior of anthropogenic radionuclides in connection with meteorology and atmosphere dynamics and on the atmospheric contamination level.

In the Meteorological Research Institute Technical Report No.36, Aoyama *et al.* (1996) described a detailed radiochemical analysis of long-lived anthropogenic radionuclides (i.e.,  $^{90}\text{Sr}$ ,  $^{137}\text{Cs}$  and plutonium isotopes) in fallout samples together with a data set of monthly deposition rates of  $^{137}\text{Cs}$  and  $^{90}\text{Sr}$  at 12 stations in Japan (Fig. 96-22 and Table 96-2). To control the fallout sample quality in radiochemical analysis, a fallout reference was prepared based on deposition samples collected at 14 stations throughout Japan during 1963–1979 as referenced in the 1995 ACTIVITIES (Otsuji-Hatori *et al.*, 1995). Using this reference, several independent institutions determined the activities of  $^{137}\text{Cs}$ ,  $^{90}\text{Sr}$ , and plutonium isotopes. The results show good agreement among individual institutions, meaning that the fallout reference is useful in guaranteeing the quality of radiochemical analysis for anthropogenic radionuclides.

The Report discusses the geochemical behavior of anthropogenic radionuclides in deposition samples originating from atmospheric nuclear testing and nuclear reactor accidents such as the Chernobyl accident (Fig. 96-23). The major processes controlling the behavior of radioactive deposition are stratospheric fallout, tropospheric fallout, and resuspension. Resuspended radionuclides are considered a major source of recent  $^{90}\text{Sr}$  and  $^{137}\text{Cs}$  deposition observed at MRI.

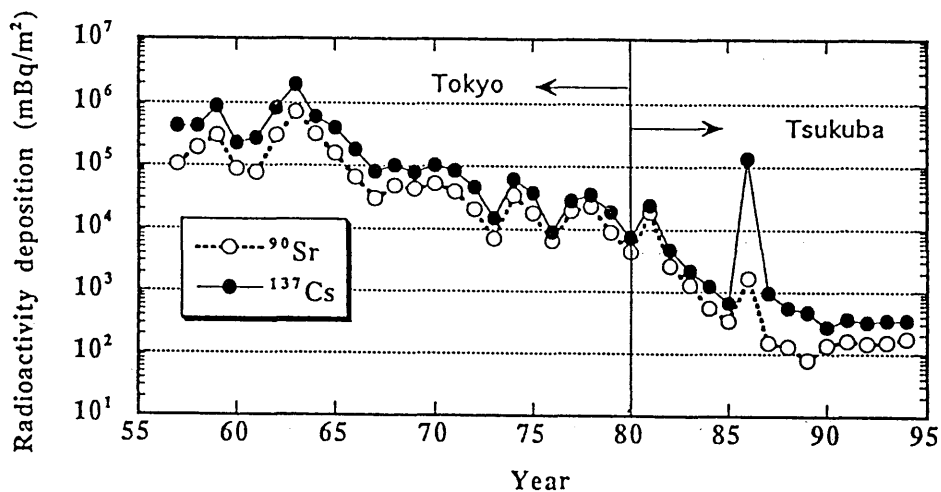


Fig. 96-22 Temporal variation in annual radioactivity deposition observed at MRI.

Table 96-2 Annual deposition of <sup>90</sup>Sr, <sup>137</sup>Cs and plutonium observed in MRI. (1958-1994)

Year	<sup>90</sup> Sr Bq m <sup>-2</sup>	<sup>137</sup> Cs Bq m <sup>-2</sup>	<sup>239,240</sup> Pu Bq m <sup>-2</sup>	Amount of ppt mm
1958	386	1092		1796
1959	219	692	3.59	1612
1960	64.9	168	1.6	1176
1961	56.8	197	1.37	1232
1962	219	592	4.06	1153
1963	516	1414	7.41	1657
1964	232	435	6.85	1136
1965	116	286	4.47	1761
1966	48.6	135	2.71	1796
1967	21.6	59.5	0.78	1208
1968	35.1	75.7	0.93	1644
1969	32.4	59.5	0.44	1472
1970	52.9	102	0.22	1082
1971	39.6	84	0.48	1396
1972	20.4	45.9	0.19	1701
1973	7.0	14.8	0.096	1207
1974	34	61.6	0.23	1757
1975	18.1	37.4	0.24	1621
1976	6.7	8.9	0.034	1559
1977	19.6	28.1	0.2	1617
1978	22.9	34.8	0.27	1064
1979	8.9	18.9	0.15	1575
1980	4.4	7.4	0.036	1479
1981	18.9	24.1	0.26	1222
1982	2.6	4.8	0.052	1324
1983	1.3	2.1	0.0136	1362
1984	0.56	1.2	0.0079	1826
1985	0.33	0.67	0.0026	1374
1986	1.7	135	0.0032	1182
1987	0.15	0.96	0.0032	1098
1988	0.13	0.56	0.0038	1296
1989	0.079	0.47	0.0017	1520
1990	0.19	0.29	0.0021	1284
1991	0.16	0.36	0.0030	1841
1992	0.15	0.32	0.0044	1282
1993	0.15	0.35	0.0078	1381
1994	0.18	0.42		

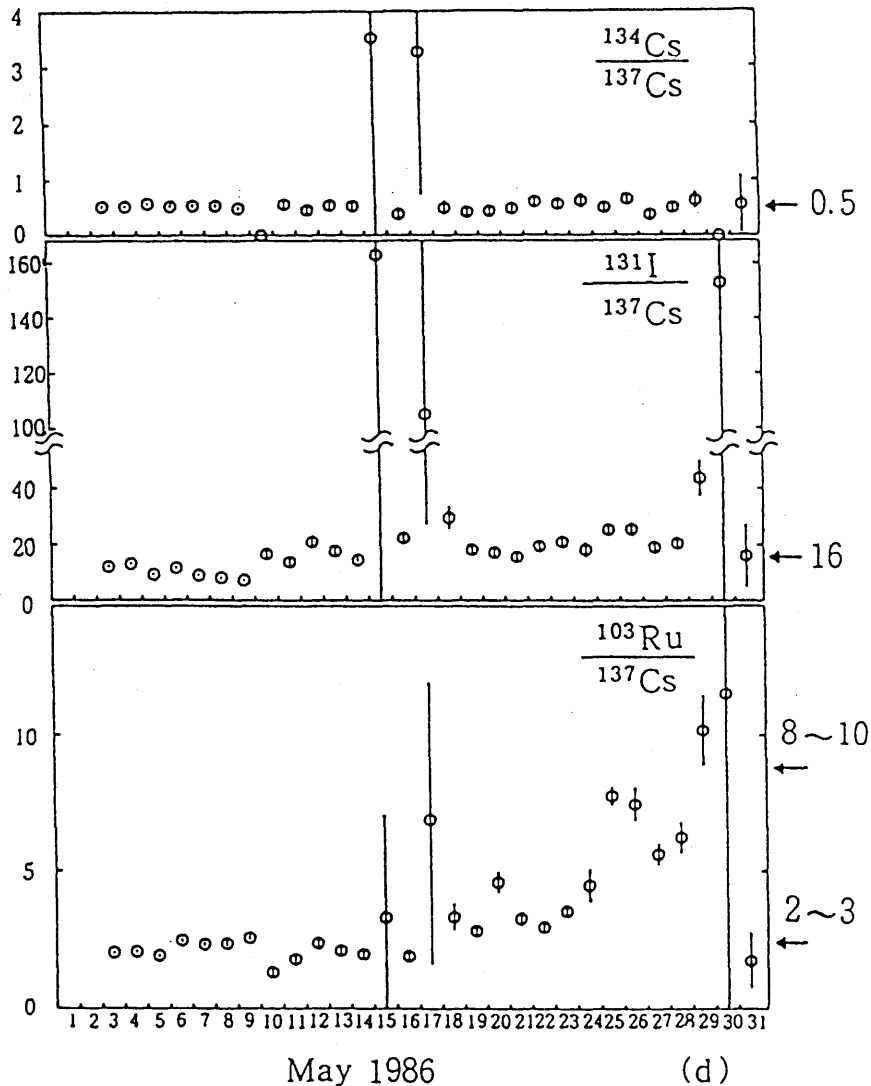


Fig. 96-23 Temporal variation of activity ratios of Chernobyl-derived radionuclides in surface air at Tsukuba.

## ORGANIC MATTER AND LIGANDS

### 5. Ocean Biogeochemistry

#### 5.1 Characterization of particulate protein in Pacific surface waters

Tanoue (1996)

Dissolved organic matter (DOM) is one of the largest but most poorly understood active reservoirs of organic matter on the planet. Although most DOM is marine in origin, its sources and sinks are not well known. As referenced in the 1995 ACTIVITIES, Tanoue extracted dissolved proteins from seawater and found that a limited number of protein species accounted for most of the dissolved proteins and that proteins contributed quantitatively to dissolved organic N throughout the water column.

Protein is the major cellular constituent of phytoplankton and 85% of phytoplankton nitrogen is in the form of protein (e.g., Billen, 1984). Cellular proteins in living organisms may be converted to detrital "combined amino acids" or "proteinaceous compounds" through biogeochemical processes. Particulate-combined amino acids (PCAA), the largest identified fraction of particulate organic matter (POM) in oceanic surface waters, represent a mixture of cellular proteins of organisms and of detrital combined amino acids. The dynamics of the

two types of PCAA are expected to be quite different, but have not been distinguished in previous PCAA studies.

Tanoue (1996) reported the molecular characteristics of particulate proteins in surface waters along transects from 45°N to 25°S in the central Pacific (Fig. 96-24). The majority of PCAA was in the form of protein molecules in samples from the northern Pacific and Equatorial regions, namely, productive areas, while PCAA was mainly present as nonproteinaceous amino acid in subtropical regions, namely, oligotrophic areas (Fig. 96-25). Thus, it appears that the chemical form of PCAA, one of the major constituents of POM, varies meridionally.

Two typical groups of particulate protein were identified from meridional differences in molecular distribution (Fig. 96-26). The first group, derived directly from cellular proteins of living organisms, was made up of a large number of proteins, each present at a relatively low level, which gave smeared electrophoretograms

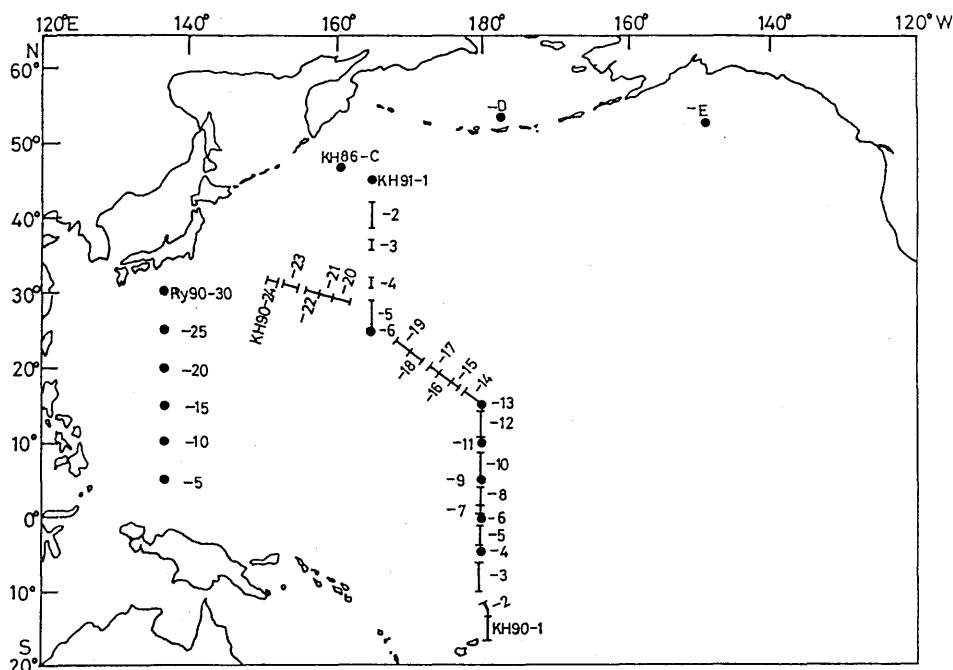


Fig. 96-24 Locations at which particulate matter in surface waters was sampled during cruises Ry90-01 (sample nos. Ry90-5 to Ry90-30), KH90-2 (KH90-1 to KH90-24), and KH91-3 (KH91-1 to KH91-6). Stations (KH86-C, -D and -E) in northern North Pacific and in Bering Sea for which SDS-PAGE patterns of particulate proteins were previously reported (KH86-D and -E; Tanoue, 1992) are also shown.

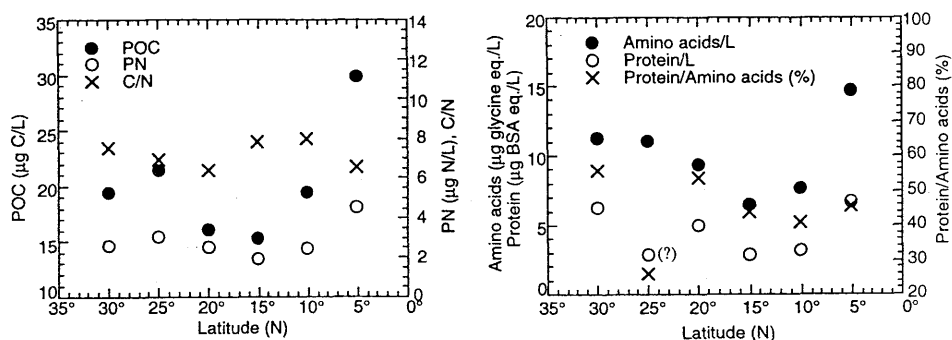


Fig. 96-25 Concentrations of POC ( $\mu\text{g C/l}$ ), PN ( $\mu\text{g N/l}$ ), PCAA ( $\mu\text{g}$  relative to a glycine standard/l) and particulate proteins ( $\mu\text{g}$  relative to a BSA standard/l), and C/N and Protein/PCAA (%) along 137°E (Ry90-01).

and were considered to be "background" proteins that contributed greatly to both total protein and PCAA, and appeared to be readily remineralized. The second group included a small number of specific proteins with a limited range of molecular mass. This group was prevalent in oligotrophic areas, an indication that proteins from specific sources survive and accumulate due to their resistance to degradation.

A protein with an apparent molecular mass of 45 kilodaltons (kDa), a member of the second group, was commonly found at low latitudes and the partial N-terminal amino acid sequence indicated that the 45 kDa protein was a single protein species that has not previously been reported (Table 96-3). Thus, a single identifiable protein molecule appears to be very widespread at low latitudes.

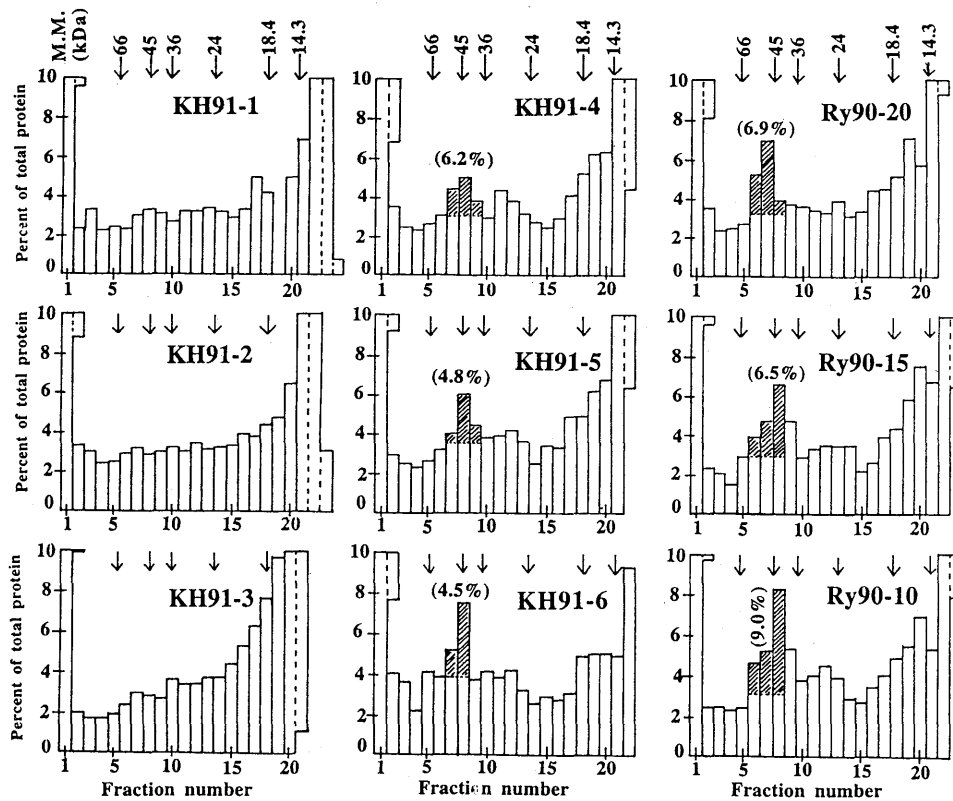


Fig. 96-26 Relative abundance of proteins in 5-mm pieces of gel for samples collected along 165°E and 137°E. Shaded fractions represent contribution (%) of proteins in distinct bands to total protein.

Table 96-3 N-terminal amino acid sequence of the 45-kDa protein obtained by automated Edman degradation.

Cycle	1	2	3	4	5	6	7	8	9	10	11	12
45-kDa protein	Gly	Thr	Gln	Pro	Asn	Pro	Ser	Pro	Ala	Ser	Pro	Val

## 5.2 Discrete dissolved and particulate proteins in oceanic waters

Tanoue, Ishii, and Midorikawa (1996)

Tanoue *et al.* (1996) extracted dissolved and particulate proteins from samples of surface seawater collected from the equatorial area, through the Indian Ocean, to the Antarctic Ocean (Fig. 96-27). Dissolved proteins were also observed in waters of the equatorial Pacific. They detected dissolved and particulate proteins with a wide range of molecular masses by sodium dodecylsulfate-polyacrylamide gel electrophoresis (SDS-PAGE). The particulate proteins were made up of many background proteins of overlapping molecular weight, which caused uniform staining in gel. However, distinct bands of individual proteins with apparent molecular masses of ~66 and 45 kDa were evident among background proteins (Fig. 96-28).

Electrophoretograms of dissolved proteins were quite different from those of the particulate proteins. Dissolved background proteins were not significant, and fewer than 30 proteins were clearly visualized as major dissolved proteins. Dissolved proteins with apparent molecular masses of 48 and 37 kDa were commonly found as major proteins in all samples examined.

Such molecular characteristics of dissolved and particulate proteins are consistent with previous results from the North Pacific. It thus appears that processes by which specific proteins from marine organisms are transferred to and accumulated in pools of dissolved and particulate organic matter are identical throughout the world's oceans.

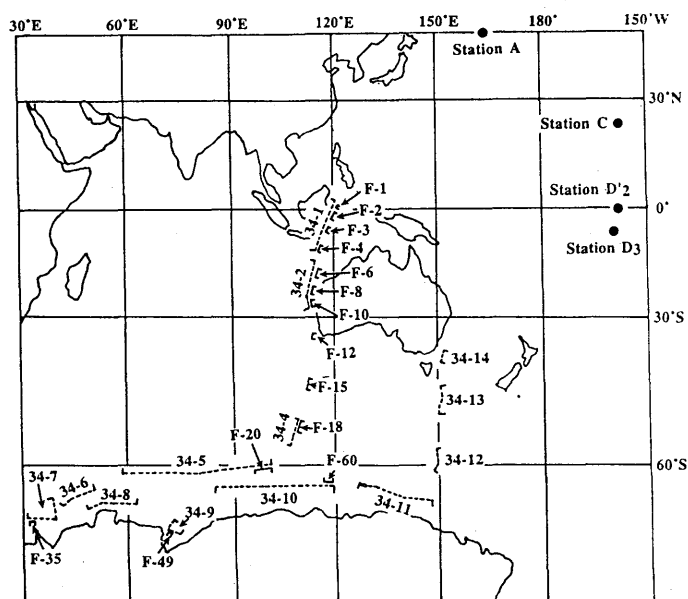


Fig. 96-27 Distribution of sampling locations of composite samples of surface seawater for extraction of dissolved proteins (broken lines: sample 34-1 to 34-14) and samples of surface POM for particulate proteins (solid lines: F-1 to F-60) along the track of JARE 34, and locations of depth stations A, C, D<sub>2</sub>, and D<sub>3</sub> for extraction of dissolved proteins during cruise KH 93-4.

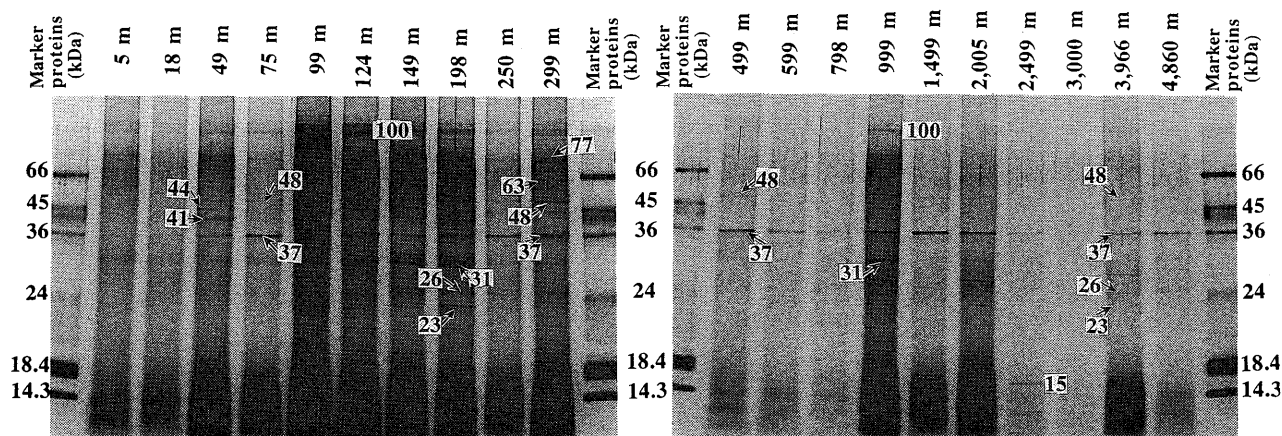


Fig. 96-28 Depth profiles of dissolved proteins at station D'2. Proteins were, visualized by silver staining. Amounts of sample loaded on gel were equivalent to 100 ml of original seawater in each case. Each marker protein was loaded at 25 ng in each left- and 50 ng in each right-hand lane of each gel. Electrophoretograms of samples from depths of 18, 2005, and 3996 m were reported elsewhere (Tanoue 1995).

### 5.3 Abundance of viruses in deep oceanic waters

Hara, Koike, Terauchi, Kamiya, and Tanoue (1996)

Viruses are recognized as important members of the marine surface water ecosystem due to their role as decomposers of bacterial and protistan biomasses. The concentration of viruses is information essential to the ecological study of the aquatic environment.

Hara *et al.* (1996) investigated vertical distributions of bacteria and viruses at oceanic stations located in subarctic (Stn A) and subtropical (Stn B) areas of the Pacific using direct count and transmission electron microscopy (Table 96-4). Small DAPI-positive, virus-like particles (VLP) were found to be distributed throughout the water column down to 5000 m depth at both stations. The abundance of VLP ranged from  $38 \times 10^5 \text{ ml}^{-1}$  at 50 m depth to  $0.6 \times 10^5 \text{ ml}^{-1}$  at 5000 m depth at Stn A (Fig. 96-29). The ratio of VLP to bacteria-like particle (BLP) ranged from 1.1 to 7.4 at Stn A and 1.0 to 8.7 at Stn B in the entire water column. The maximum ratio was recorded at Stn B from the deepest sample, collected at a depth of 5000 m. The electron microscopic investigation indicated that the majority of VLP were probably viruses.

Table 96-4 Abundances of bacteria and viruses in Nan-wan (Taiwan) samples enumerated with direct and film counts. Cells were collected with different filters; 0.2  $\mu\text{m}$  Poretics (P), 0.2  $\mu\text{m}$  and 0.02  $\mu\text{m}$  Anodisc (A) and 0.015  $\mu\text{m}$  Nuclepore (N)

Filter	Abundance at each depth ( $10^5 \text{ ml}^{-1}$ )			
	0 m	5 m	10 m	20 m
<b>Bacteria (direct count)</b>				
0.2 $\mu\text{m}$ P	$5.22 \pm 0.37$	$5.02 \pm 0.19$	$4.33 \pm 0.18$	$4.40 \pm 0.41$
0.2 $\mu\text{m}$ A	$5.01 \pm 0.07$	$5.60 \pm 0.17$	$5.23 \pm 0.23$	$5.64 \pm 0.27$
0.02 $\mu\text{m}$ A	$5.30 \pm 0.08$	$5.42 \pm 0.38$	$5.82 \pm 0.28$	$5.54 \pm 0.16$
0.015 $\mu\text{m}$ N	$4.76 \pm 0.01$	$5.11 \pm 0.26$	$5.75 \pm 0.30$	$4.86 \pm 0.26$
<b>Bacteria (film count)</b>				
0.2 $\mu\text{m}$ P	$4.94 \pm 0.03$	$4.94 \pm 0.42$	$4.64 \pm 0.18$	$4.44 \pm 0.52$
0.2 $\mu\text{m}$ A	$5.43 \pm 0.30$	$5.42 \pm 0.20$	$6.43 \pm 0.31$	$5.66 \pm 0.42$
0.02 $\mu\text{m}$ A	$5.86 \pm 0.13$	$5.04 \pm 0.57$	$5.91 \pm 1.10$	$4.99 \pm 0.95$
0.015 $\mu\text{m}$ N	4.74	4.92	5.00	4.76
<b>Viruses (film count)</b>				
0.2 $\mu\text{m}$ P	$2.67 \pm 0.43$	$2.38 \pm 0.21$	$2.53 \pm 0.27$	$2.59 \pm 0.20$
0.2 $\mu\text{m}$ A	$11.37 \pm 4.85$	12.76	$11.23 \pm 3.44$	$12.92 \pm 2.93$
0.02 $\mu\text{m}$ A	$4.91 \pm 0.38$	$4.43 \pm 0.93$	$4.55 \pm 1.99$	$3.27 \pm 0.79$
0.015 $\mu\text{m}$ N	21.63	18.56	17.61	17.57

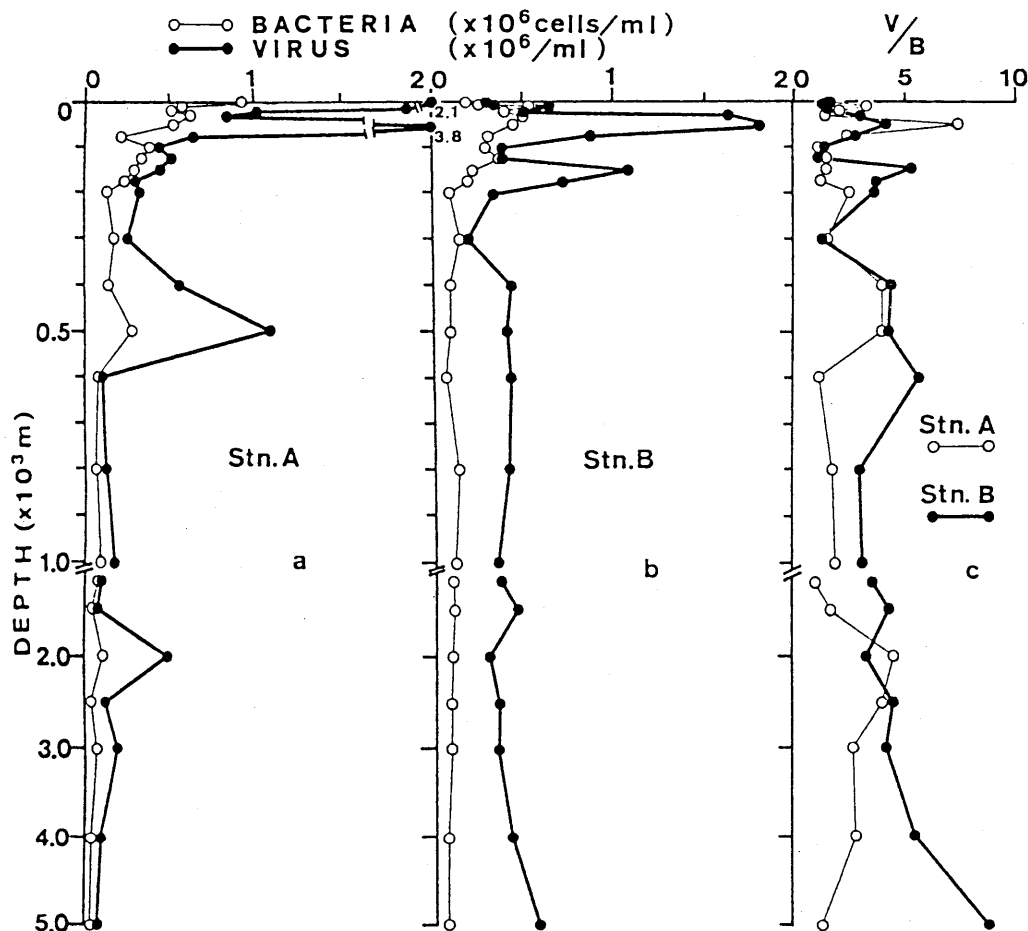


Fig. 96-29 Vertical distributions of bacteria and viruses at (a) Stn. A and (b) Stn. B, and (c) viruses/bacteria ratios at Stn. A and B.

#### 5.4 Extraction and characterization of organic ligands from oceanic water columns by immobilized metal ion affinity chromatography

Midorikawa, and Tanoue (1996a)

Studies on the association of metals and organic compounds in natural waters have focused on metal speciation in situ. Our present understanding of copper speciation is that organic ligands exist in seawater and that more than 99% of Cu(II) in surface water is present in organic complexes.

Midorikawa and Tanoue (1996a) extracted organic ligands for Cu(II) from oceanic water columns using immobilized metal ion affinity chromatography (IMAC) (Fig. 96-30). Separation of organic ligands from bulk dissolved organic matter (DOM) enabled organic ligands to be chemically clarified. Measurements of complexing abilities and fluorescence and chemical analyses indicated that natural ligands were a mixture of, at least, two different types of organic ligands (Table 96-5). One type, prominent in surface water; was weakly fluorescent but rich in both primary amines and carbohydrates. The other type predominant in deep water, had converse characteristics, namely, low levels of both primary amines and carbohydrates, but relatively strong fluorescence. The measurement of organic ligand complexing ability from surface waters suggested the existence of a natural ligand ( $\log K'_{CuL} \sim 9$ ) that has one or two primary amines as copper-binding sites.

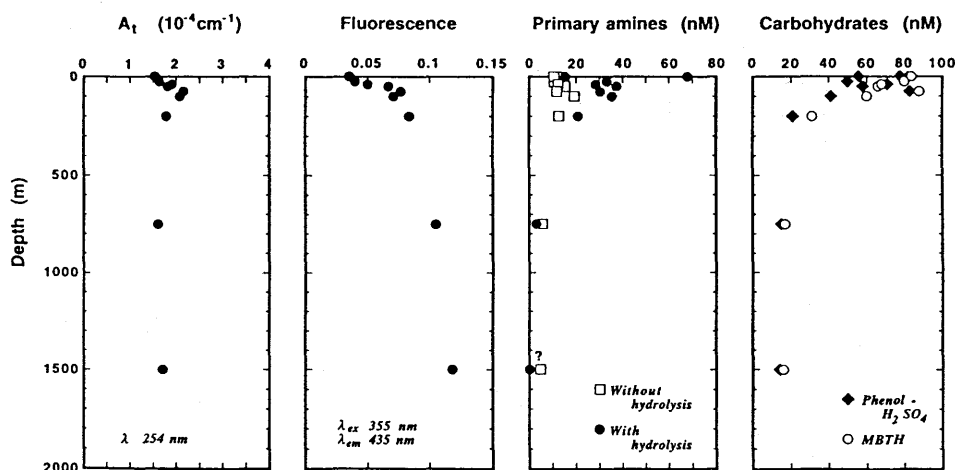


Fig. 96-30 Vertical profiles of organic-chemical characteristics of organic ligand fraction extracted by IMAC in equatorial Pacific. Water samples at Stations N-12 and M-2 were combined. Values are those in original seawater. Fluorescence is expressed in arbitrary units. Concentrations of primary amines with and without hydrolysis are given as nmol/l of glycine equivalents. The carbohydrate concentration was measured by phenol sulfuric acid and MBTH after hydrolysis and is given as nmol/l of glucose equivalents.

Reprinted from *Marine Chemistry*, 52, Midorikawa and Tanoue, Extraction and characterization of organic ligands from oceanic water columns by immobilized metal ion affinity chromatography, 157-171, Copyright (1996), with kind permission from Elsevier Science.

Table 96-5 Results of copper titration and chemical analysis of the EDTA eluate of samples of surface seawater <sup>a</sup> after demetalization

Station	Column	Conditional stability constant <sup>c</sup>		Concentration (nM) <sup>b</sup>					$A_1$ <sup>b,f</sup> ( $10^{-4}$ $\text{cm}^{-1}$ )	Recovery of UV absorbance <sup>g</sup> (%)
		$\log K'_{\text{CuL}_1}$	$\log K'_{\text{CuL}_2}$	Ligand <sup>c</sup>		Primary amine <sup>d</sup>	Carbohydrate <sup>e</sup>			
				$C_{L_1}$	$C_{L_2}$		P	M		
M-2	Upper	9.22	7.08	1.0	4.6	2.2	35	42	0.37	24
M-4	Upper	8.93	7.08	2.2	15	9.1	39	26 (?)	0.67	37
	Lower	8.92	7.44	0.5	3.1	3.8	17	16	0.16	25

<sup>a</sup> Seawater samples of 2.5 l (Station M-2) and 1.1 l (Station M-4) were each concentrated to titrated solutions of 10 ml.

<sup>b</sup> The respective values are expressed as those in the original seawater.

<sup>c</sup> The values represent values with respect to free copper under the conditions at  $I = 0.7$  M ( $\text{KNO}_3$ ), pH 8.15 (EPPS) and 25°C. The values for the ligand  $L_2$  are preliminary because  $L_2$  was detected but its precise quantification was hampered by the column blank.

<sup>d</sup> The values obtained without hydrolysis are given as nmol/l of glycine equivalents.

<sup>e</sup> The values were obtained by the phenol sulfuric acid method (P) and the MBTH method (M), and are given as nmol/l of glucose equivalents.

<sup>f</sup> The values for the total UV absorbance at 254 nm ( $A_1$ ) of the EDTA-eluted fraction after demetalization were converted to those in the original seawater.

<sup>g</sup> The values were estimated as the ratio of the  $A_1$  value for the EDTA-eluted fraction after demetalization (i.e., ligand fraction with a molecular mass of more than 1000 Da) to that for the acidic eluate fraction without demetalization.

Reprinted from *Marine Chemistry*, **52**, Midorikawa and Tanoue, Extraction and characterization of organic ligands from oceanic water columns by immobilized metal ion affinity chromatography, 157-171, Copyright (1996), with kind permission of Elsevier Science - NL, Sara Burgerhartstraat 25, 1055 KV Amsterdam, The Netherlands.

### 5.5 Effects of ligand speciation on complexing abilities of strong ligands in natural waters

Midorikawa, and Tanoue (1996b)

The presence, in oceanic waters, of organic ligands (L) whose conditional stability constants ( $K'_{\text{ML}}$ ) are strong enough to allow them to form complexes with copper has been reported, but no general consensus has been reached on the distribution of such strong ligands in the water column.

Midorikawa and Tanoue (1996b) found that these inconsistencies were derived from different analytical methods employed for their detection and different oceanographic conditions. In particular, the nature and quantity of detectable natural ligands are affected by the form the ligands are present in situ in different marine environments, that is, chemical speciation of natural ligands (ligand speciation), which depends strongly on the variations in concentrations of coexisting trace metals.

Using published data from observations in the laboratory and the field, they provided limits to the ranges of conditional stability constants of organic ligands for copper, zinc, and cadmium detectable by extensively used direct metal titration (Figs. 96-31 and 96-32). Their model indicates, for example, that organic ligands for copper with  $\log K'_{\text{CuL}(\text{Cu})} > 12.4$  in surface water and with  $\log K'_{\text{CuL}(\text{Cu})} > 9.9$  in deep water may not have been detected because stronger ligands formed complexes with ambient metals in situ at a station in the North Pacific.

The estimation suggests that there is a basin-scale difference in speciation of natural organic ligands and, moreover, that this difference influences metal speciation. They applied their ideas to more common oceanographic variations between the Pacific and Atlantic Oceans. There exist two remarkable differences in the respective vertical profiles of concentrations of total and inorganic copper in the two oceans: each level of copper in surface waters in the North Atlantic is not as greatly depleted as that in the North Pacific, whereas each copper level in the lower water column in the North Pacific is essentially about twice that in the North Atlantic (Fig. 96-33). Thus, these distributions have a major influence on ligand speciation in both oceans. In surface

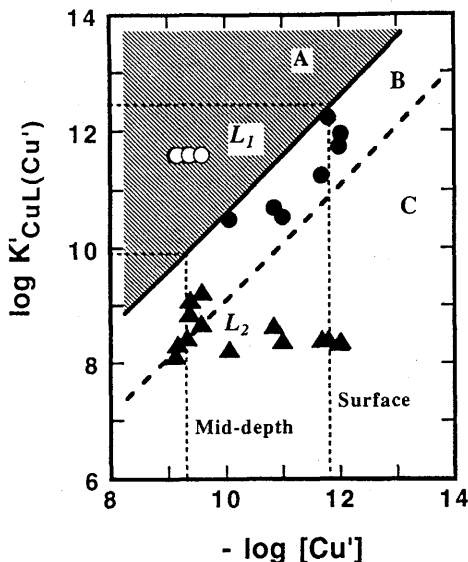


Fig. 96-31  $[Cu']$  and  $K'_{CuL(Cu')}$  for ligands  $L_1$  (circles) and  $L_2$  (triangles) in original samples of seawater (20-1,400 m) from eastern North Pacific (VERTEX seasonal station:  $33^\circ N$ ,  $139^\circ W$ ): solid symbols: observed ligands; open symbols: hypothetical ligands (not observed: assuming  $\log K'_{CuL_1(Cu')} = 11.6$  for ligand  $L_1$  at depths of 200-1,400 m). All data was from Coale and Bruland (1988). Solid line shows Eq. (5) for  $R = 80\%$  and dashed line that for  $R = 10\%$ ; area A,  $R > 80\%$ ; area B,  $10\% < R < 80\%$ ; area C,  $R < 10\%$ . Dotted lines show average ligand speciation under conditions in surface water (pH 8.2 and  $25^\circ C$ ) and at mid-depth (pH 7.5 and  $5^\circ C$ ).

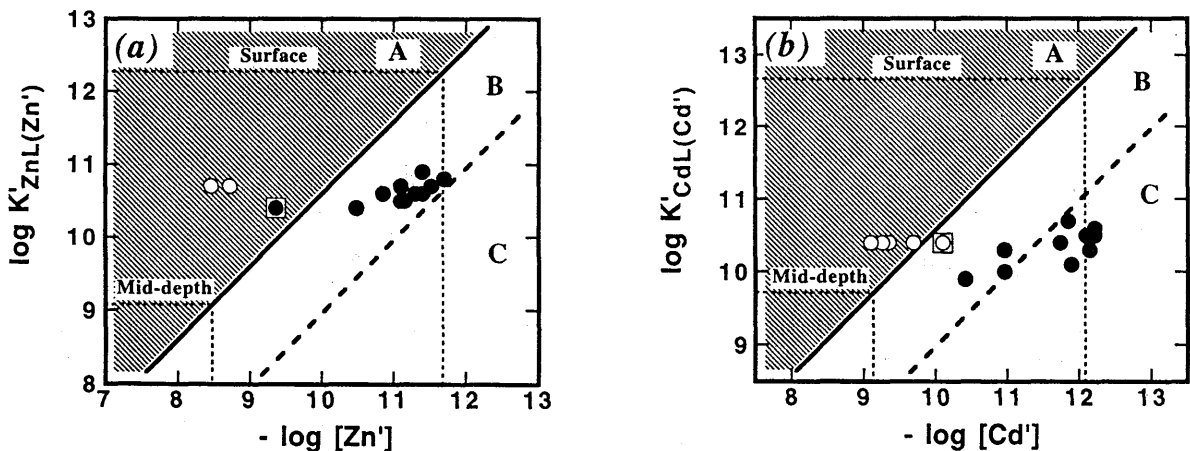


Fig. 96-32  $\log K'_{ML(M')}$  and  $-\log [M']$  for (a) zinc and (b) cadmium in original samples of seawater (22-600 m) from central North Pacific (VERTEX IV station:  $28^\circ N$ ,  $158^\circ W$ ) based on results of Bruland (1989, 1992): solid symbols: observed ligands; open symbols: hypothetical ligands (not observed; assuming  $\log K'_{ZnL(Zn')} = 10.7$  at depths of 500-600 m for zinc and  $\log K'_{CdL(Cd')} = 10.4$  at depths of 200-600 m for cadmium). Solid line shows Eq. (5) for  $R = 80\%$  and dashed line that for  $R = 10\%$ ; area A,  $R > 80\%$ ; area B,  $10\% < R < 80\%$ ; area C,  $R < 10\%$ . Dotted lines show average ligand speciation under conditions in surface water and at mid-depth, calculated for each metal.

waters in the North Atlantic, in contrast with the North Pacific, the R for ligand  $L_1$  and  $L_2$  was more than 98% and that for ligand  $L_2$  8-16%. (R is the percentage of complex between metal and ligand in total ligand concentration;  $R (\%)/100 = [ML]/C_L$ ) Thus, it could be predicted that the stronger ligand  $L_1$  would be undetectable but the weaker ligand, corresponding to  $L_2$ , would be detectable in Atlantic surface water. It is postulated that comparisons of the occurrence and levels of organic ligands might not be possible among spatially and temporally different observations without reconciliation of the effects of ligand speciation, even if an identical method is used in all cases.

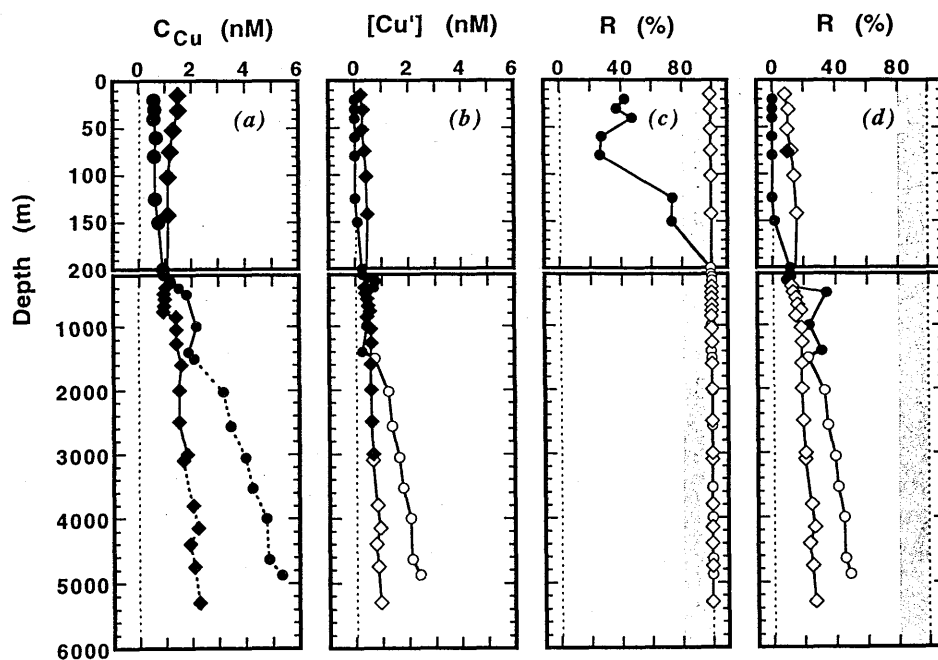


Fig. 96-33 Vertical profiles of copper concentrations and ligand speciation in North Pacific (circles) and the North Atlantic (diamonds): total copper (a), inorganic copper (b), R values for ligand  $L_1$  (c), and  $L_2$  (d). All solid symbols represent observed values and open symbols hypothetical, calculated values. Hatching shows the region (corresponding to area A in Fig. 96-31) in which the ligand cannot be detected by direct metal titration.

### 5.6 Determination of strong organic ligand dissolved in seawater: Thorium-complexing capacity of oceanic matter dissolved in oceans

Hirose (1996)

Oceanic organic matter, consisting of dissolved and particulate forms, is considered one of the important factors controlling the trace element composition of seawater and plays an essential role in the marine environment carbon cycle. To understand the biogeochemical role of organic matter in the marine environment, it is important to specify and identify chemical constituents of oceanic organic matter. The composition of organic matter in seawater is extremely complicated. As a choice among many methodologies, the natural organic matter can be analyzed by functional group such as ligands related to metal complexation.

Hirose (1996) developed a way to measure strong ligands in oceanic DOM by Th complexation in acidic media and the adsorption of the Th complex onto XAD-2 resin. Th reacts quantitatively with the organic binding site of DOM in strong acid media (around 0.1 M H<sup>+</sup> solution), which is equilibrated within 24 hours. According to mass action analysis, Th forms a 1 : 1 complex with the binding site in DOM, whose conditional stability constant is 10<sup>6.7</sup> M<sup>-1</sup>. The conditional stability constant of the Th complex in DOM is in good agreement with that determined for oceanic particulate matter (PM) under similar experimental conditions.

This finding suggests that the chemical properties of the strong ligand in DOM are similar to these in biogenic PM. The Th complexing capacity in DOM, which corresponds to the total concentration of the strong organic ligand, can be determined (2-3 nM in surface waters) in a small volume (about 200 ml) (Fig. 96-34 and Table 96-6). The method has a detection limit of about 0.05 nM for thorium complexing capacity of DOM by using <sup>230</sup>Th.

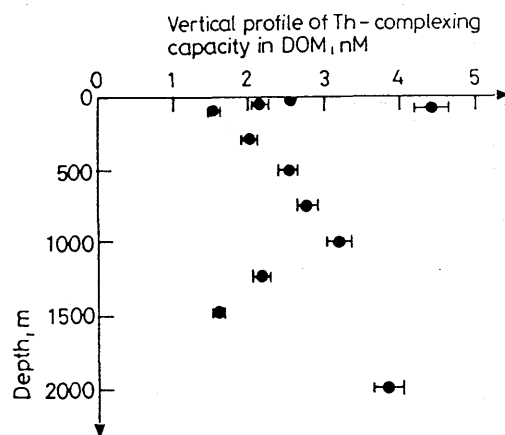


Fig. 96-34 Vertical distribution of Th complexing capacity of DOM in Japan Sea. (Sampling site: 38°11'N, 132°37'E)

Table 96-6 The vertical distribution of Th complexing capacity in DOM. (Sampling location: 38°11'N, 132°37'E; depth: 2354 m; sampling date: Oct. 1994)

Depth, m	T, °C	S, ‰	ThCC, nM
0	19.6	33.42	2.56 ± 0.10
50	17.6	33.67	2.13 ± 0.10
75	9.95	34.23	4.41 ± 0.13
100	6.02	34.13	1.53 ± 0.06
300	0.76	34.07	2.00 ± 0.08
500	0.40	34.07	2.51 ± 0.13
750	0.27	34.07	2.77 ± 0.12
1000	0.21	34.07	3.18 ± 0.16
1250	0.18	34.07	2.16 ± 0.11
1500	0.16	34.07	1.59 ± 0.06
2000	0.17	34.07	3.86 ± 0.14

Uncertainties quoted are at a level of one estimated standard deviation for counting only.

## INTERNATIONAL ACTIVITIES

### II. Participation in At-Sea Intercomparison of Underway pCO<sub>2</sub> Systems During *Meteor* Cruise 36-1

H. Y. Inoue and M. Ishii participated in the At-Sea Intercomparison of Underway pCO<sub>2</sub> Systems during German research vessel *Meteor* Cruise 36-1, June 6-19, 1996, organized by the marine CO<sub>2</sub> project at the Institute for Marine Research, Department of Marine Chemistry, Kiel, Germany. The purpose was to provide insights into the performance and comparability of seagoing CO<sub>2</sub> systems under typical identical working conditions to establish a database for use in understanding the basin and global scale distributions of pCO<sub>2</sub> and its influence on the oceanic uptake of anthropogenic CO<sub>2</sub>.

Fifteen scientists from nine research institutions in six countries joined the international exercise, conducted on board R/V *Meteor* between Bermuda and Gran Canaria in the North Atlantic. H.Y. Inoue and M. Ishii contributed to the intercomparison exercise using the underway MRI pCO<sub>2</sub> system.

### III. Contribution to WOCE Hydrographic Program – Pacific Data QA Activity

M. Aoyama was engaged in data quality evaluation (DQE) of Pacific WOCE data as an evaluator with the region study to assess data quality and make suggestions for improving it. He worked for the WHP Office in the Physical Oceanography Department of the Woods Hole Oceanographic Institution as a guest investigator from March 1, 1996 to May 31, 1996.

Aoyama applied original methods and compared data at crossing one-time survey lines in the North Pacific to assess the degree to which data is selfconsistent and examined individual datasets for data quality.

Details of his contribution to the Pacific Data QA Activity are given in the WHP Office Status Report, No. 19.

## 1995 PUBLICATIONS

- Aoyama M. and K. Hirose, 1995: The temporal and spatial variation of  $^{137}\text{Cs}$  concentration in the western North Pacific and its marginal seas during the period from 1979 to 1988. *J. Env. Radioact.*, **29**, 57-74.
- Dokiya Y., K. Tsuboi, H. Sekino, T. Hosomi, Y. Igarashi, and S. Tanaka, 1995: Acid deposition at the summit of Mt. Fuji: Observations of gases, aerosols, and precipitation in summer, 1993 and 1994, *Water, Air, and Soil Pollut.*, **85**, 1967-1972.
- Hirose K., 1995a: Geochemical studies on the Chernobyl radioactivity in environmental samples. *J. Radioanalyt. and Nucl. Chem., Arts.*, **197**, 331-342.
- Hirose K., 1995b: The relationship between particulate uranium and thorium-complexing capacity of oceanic particulate matter. *Sci. of Tot. Env.*, **173/174**, 195-201.
- Inoue H.Y., H. Matsueda, K. Fushimi, M. Hirota, I. Asanuma, and Y. Takasugi, 1995: Long-term trend of the partial pressure of carbon dioxide ( $p\text{CO}_2$ ) in surface water of the western North Pacific, 1984-1993. *Tellus*, **47B**, 391-413.
- Ishii M. and H.Y. Inoue, 1995: Air-sea exchange of  $\text{CO}_2$  in the central and western equatorial Pacific in 1990. *Tellus*, **47B**, 447-460.
- Takaku Y., T. Shimamura, K. Masuda, and Y. Igarashi, 1995: Iodine determination in natural and tap water using inductively coupled plasma mass spectrometry. *Analyt. Sci.*, **11**, 823-827.
- Tanoue E., 1995: Detection of dissolved protein molecules in oceanic water. *Marine Chem.*, **51**, 239-252.
- Tanoue E. and T. Midorikawa, 1995: Detection, characterization and dynamics of dissolved organic ligands in oceanic waters. *Biogeochemical Processes and Ocean Flux in the Western Pacific*, Eds. H. Sakai and Y. Nozaki, Terra Scientific Publishing Co. Ltd. Tokyo, pp. 201-224.
- Tanoue E., S. Nishiyama, M. Kamo, and A. Tsugita, 1995: Bacterial membranes: Possible source of a major dissolved protein in seawater. *Geochim. et Cosmochim. Acta*, **59**, 2643-2648.
- Weisburd R.S.J., M. Ishii, T. Fukushima, and A. Otsuki, 1995: Methods for measurement of dissolved inorganic carbon in natural water. *Jpn. J. Limnol.*, **56**, 221-226.

## 1996 PUBLICATIONS

- Aoyama M., K. Hirose, Y. Igarashi, and T. Miyao, 1996: Geochemical studies and analytical methods of anthropogenic radionuclides in fallout samples. *Tech. Rep. of MRI, No. 36* (in Japanese with English abstract).
- Hara S., I. Koike, K. Terauchi, H. Kamiya, and E. Tanoue, 1996: Abundance of viruses in deep oceanic waters. *Marine Ecology Progress Series, 145*, 269-277.
- Hirose K., 1996: Determination of a strong organic ligand dissolved in seawater: Thorium-complexing capacity of oceanic dissolved organic matter. *J. Radioanal. Nucl. Chem., Articles, 204*, 193-204.
- Hirose K., G-H. Hong and T. Miyao, 1996: A preliminary study of the temperature structure in the North Central Japan Sea. *Oceanogr. Mag., 45*, 1-8.
- Igarashi Y., M. Otsuji-Hatori, and K. Hirose, 1996: Recent deposition of  $^{90}\text{Sr}$  and  $^{137}\text{Cs}$  observed in Tsukuba. *J. Environ. Radioact., 31*, 157-169.
- Inoue H.Y., M. Ishii, H. Matsueda, M. Aoyama, and I. Asanuma, 1996: Changes in longitudinal distribution of partial pressure of  $\text{CO}_2$  ( $\text{pCO}_2$ ) in the central and western equatorial Pacific, west of  $160^\circ\text{W}$ . *Geophys. Res. Lett., 23*, 1781-1784.
- Inoue H.Y. and H. Matsueda, 1996: Variations in atmospheric  $\text{CO}_2$  at the Meteorological Research Institute, Tsukuba, Japan. *J. Atmospher. Chem., 23*, 137-161.
- Kashino Y., M. Aoyama, T. Kawano, N. Hendiarti, Syaefudin, Y. Anantasena, K. Muneyama, and H. Watanabe, 1996: The water masses between Mindanao and New Guinea. *J. Geophys. Res., 101*, 12, 391-12, 400.
- Matsueda H. and H.Y. Inoue, 1996: Measurements of atmospheric  $\text{CO}_2$  and  $\text{CH}_4$  using a commercial airliner from 1993 to 1994. *Atmospher. Environ., 30*, 1647-1655.
- Matsueda H., H.Y. Inoue, M. Ishii and Y. Nogi, 1996: Atmospheric methane over the North Pacific from 1987 to 1993. *Geochem. J., 30*, 1-15.
- Matsueda H., H.Y. Inoue, and M. Ishii, 1997:  $\text{CO}_2$ ,  $\text{CH}_4$  and  $\text{CO}$  in the upper troposphere observed using a commercial airliner from 1993 to 1996. *Summ. Rep. 1996, JAL Foundation*, February 1997.
- Midorikawa T. and E. Tanoue, 1996a: Extraction and characterization of organic ligands from oceanic water columns by immobilized metal ion affinity chromatography. *Marine Chem., 52*, 157-171.
- Midorikawa T. and E. Tanoue, 1996b: Effects of ligand speciation on determinations of the complexing abilities of strong ligands in natural waters. *J. Oceanogr., 52*, 421-439.
- Murata A.M. and K. Fushimi, 1996: Temporal and spatial variations in atmospheric and oceanic  $\text{CO}_2$  in the western North Pacific from 1990 to 1993: Possible link to the 1991/92 ENSO event. *J. Meteorol. Soc. of Jpn, 74*, 1-20.
- Murata A.M., K. Fushimi, H.Y. Inoue, M. Hirota, K. Nemoto, M. Okabe, M. Yabuki, and I. Asanuma, 1996: Evaluation of the  $\text{CO}_2$  exchange at sea surface in the western North Pacific: Distributions of the  $\Delta\text{pCO}_2$  and the  $\text{CO}_2$  flux. *J. Meteorol. Res., 48*, 33-58 (in Japanese with English abstract).
- Otsuji-Hatori M., Y. Igarashi, and K. Hirose, 1996: Preparation of a reference fallout material for activity measurements. *J. Environ. Radioact., 31*, 143-155.
- Tanoue E., 1996: Characterization of the particulate protein in Pacific surface waters. *J. Marine Res., 54*, 967-990.

Tanoue E., M. Ishii, and T. Midorikawa, 1996: Discrete dissolved and particulate proteins in oceanic waters.  
*Limnol. and Oceanogr.*, **41**, 1334-1343.

## 気象研究所技術報告一覧表

- 第1号 バックグラウンド大気汚染の測定法の開発 (地球規模大気汚染特別研究班, 1978)  
Development of Monitoring Techniques for Global Background Air Pollution. (MRI Special Research Group on Global Atmospheric Pollution, 1978)
- 第2号 主要活火山の地殻変動並びに地熱状態の調査研究 (地震火山研究部, 1979)  
Investigation of Ground Movement and Geothermal State of Main Active Volcanoes in Japan. (Seismology and Volcanology Research Division, 1979)
- 第3号 筑波研究学園都市に新設された気象観測用鉄塔施設 (花房龍男・藤谷徳之助・伴野 登・魚津 博, 1979)  
On the Meteorological Tower and Its Observational System at Tsukuba Science City. (T. Hanafusa, T. Fujitani, N. Banno, and H. Uozu, 1979)
- 第4号 海底地震常時観測システムの開発 (地震火山研究部, 1980)  
Permanent Ocean-Bottom Seismograph Observation System. (Seismology and Volcanology Research Division, 1980)
- 第5号 本州南方海域水温図-400m (又は500m) 深と1,000m 深- (1934-1943年及び1954-1980年) (海洋研究部, 1981)  
Horizontal Distribution of Temperature in 400m (or 500m) and 1,000m Depth in Sea South of Honshu, Japan and Western-North Pacific Ocean from 1934 to 1943 and from 1954 to 1980. (Oceanographical Research Division, 1981)
- 第6号 成層圏オゾンの破壊につながる大気成分及び紫外日射の観測 (高層物理研究部, 1982)  
Observations of the Atmospheric Constituents Related to the Stratospheric ozon Depletion and the Ultraviolet Radiation. (Upper Atmosphere Physics Research Division, 1982)
- 第7号 83型強震計の開発 (地震火山研究部, 1983)  
Strong-Motion Seismograph Model 83 for the Japan Meteorological Agency Network. (Seismology and Volcanology Research Division, 1983)
- 第8号 大気中における雪片の融解現象に関する研究 (物理気象研究部, 1984)  
The Study of Melting of Snowflakes in the Atmosphere. (Physical Meteorology Research Division, 1984)
- 第9号 御前崎南方沖における海底水圧観測 (地震火山研究部・海洋研究部, 1984)  
Bottom Pressure Observation South off Omaezaki, Central Honsyu. (Seismology and Volcanology Research Division and Oceanographical Research Division, 1984)
- 第10号 日本付近の低気圧の統計 (予報研究部, 1984)  
Statistics on Cyclones around Japan. (Forecast Research Division, 1984)
- 第11号 局地風と大気汚染質の輸送に関する研究 (応用気象研究部, 1984)  
Observations and Numerical Experiments on Local Circulation and Medium-Range Transport of Air Pollutions. (Applied Meteorology Research Division, 1984)
- 第12号 火山活動監視手法に関する研究 (地震火山研究部, 1984)  
Investigation on the Techniques for Volcanic Activity Surveillance. (Seismology and Volcanology Research Division, 1984)

- 第13号 気象研究所大気大循環モデル-I (MRI・GCM-I) (予報研究部, 1984)  
A Description of the MRI Atmospheric General Circulation Model (The MRI・GCM-I). (Forecast Research Division, 1984)
- 第14号 台風の構造の変化と移動に関する研究-台風7916の一生- (台風研究部, 1985)  
A Study on the Changes of the Three-Dimensional Structure and the Movement Speed of the Typhoon through its Life Time. (Typhoon Research Division, 1985)
- 第15号 波浪推算モデルMRIとMRI-IIの相互比較研究-計算結果図集- (海洋気象研究部, 1985)  
An Intercamparison Study between the Wave Models MRI and MRI-II -A Compilation of Results-. (Oceanographical Research Division, 1985)
- 第16号 地震予知に関する実験的及び理論的研究 (地震火山研究部, 1985)  
Study on Earthquake Prediction by Geophysical Method. (Seismology and Volcanology Research Division, 1985)
- 第17号 北半球地上月平均気温偏差図 (予報研究部, 1986)  
Maps of Monthly Mean Surface Temperature Anomalies over the Northern Hemisphere for 1891-1981. (Forecast Research Division, 1986)
- 第18号 中層大気の研究 (高層物理研究部・気象衛星研究部・予報研究部・地磁気観測所, 1986)  
Studies of the Middle Atmosphere. (Upper Atmosphere Physics Research Division, Meteorological Satellite Research Division, Forecast Research Division, MRI and the Magnetic Observatory, 1986)
- 第19号 ドップラーレーダによる気象・海象の研究 (気象衛星研究部・台風研究部・予報研究部・応用気象研究部・海洋研究部, 1986)  
Studies on Meteorological and Sea Surface Phenomena by Doppler Radar. (Meteorological Satellite Research Division, Typhoon Research Division, Forecast Research Division, Applied Meteorology Research Division, and Oceanographical Research Division, 1986)
- 第20号 気象研究所対流圏大気大循環モデル (MRI・GCM-I) による12年間分の積分 (予報研究部, 1986)  
Mean Statistics of the Tropospheric MRI・GCM-I based on 12-year Integration. (Forecast Research Division, 1986)
- 第21号 宇宙線中間子強度1983-1986 (高層物理研究部, 1987)  
Multi-Directional Cosmic Ray Meson Intensity 1983-1986. (Upper Atmosphere Physics Research Division, 1987)
- 第22号 静止気象衛星「ひまわり」画像の噴火噴煙データに基づく噴火活動の解析に関する研究 (地震火山研究部, 1987)  
Study on Analysis of Volcanic Eruptions based on Eruption Cloud Image Data obtained by the Geostationary Meteorological satellite (GMS). (Seismology and Volcanology Research Division, 1987)
- 第23号 オホーツク海海洋気候図 (篠原吉雄・四竈信行, 1988)  
Marine Climatological Atlas of the sea of Okhotsk. (Y. Shinohara and N. Shikama, 1988)
- 第24号 海洋大循環モデルを用いた風の応力異常に対する太平洋の応答実験 (海洋研究部, 1989)  
Response Experiment of Pacific Ocean to Anomalous Wind Stress with Ocean General Circulation Model. (Oceanographical Research Division, 1989)
- 第25号 太平洋における海洋諸要素の季節平均分布 (海洋研究部, 1989)  
Seasonal Mean Distribution of Sea Properties in the Pacific. (Oceanographical Research Division, 1989)
- 第26号 地震前兆現象のデータベース (地震火山研究部, 1990)  
Database of Earthquake Precursors. (Seismology and Volcanology Research Division, 1990)

- 第27号 沖縄地方における梅雨期の降水システムの特性 (台風研究部, 1991)  
Characteristics of Precipitation Systems During the Baiu Season in the Okinawa Area. (Typhoon Research Division, 1991)
- 第28号 気象研究所・予報研究部で開発された非静水圧モデル (猪川元興・斉藤和雄, 1991)  
Description of a Nonhydrostatic Model Developed at the Forecast Research Department of the MRI. (M. Ikawa and K. Saito, 1991)
- 第29号 雲の放射過程に関する総合的研究 (気候研究部・物理気象研究部・応用気象研究部・気象衛星・観測システム研究部・台風研究部, 1992)  
A Synthetic Study on Cloud-Radiation Processes. (Climate Research Department, Physical Meteorology Research Department, Applied Meteorology Research Department, Meteorological Satellite and Observation System Research Department, and Typhoon Research Department, 1992)
- 第30号 大気と海洋・地表とのエネルギー交換過程に関する研究 (三上正男・遠藤昌宏・新野 宏・山崎孝治, 1992)  
Studies of Energy Exchange Processes between the Ocean-Ground Surface and Atmosphere. (M. Mikami, M. Endoh, H. Niino, and K. Yamazaki, 1992)
- 第31号 降水日の出現頻度からみた日本の季節推移-30年間の日降水量資料に基づく統計- (秋山孝子, 1993)  
Seasonal Transition in Japan, as Revealed by Appearance Frequency of Precipitating-Days. -Statistics of Daily Precipitation Data During 30 Years- (T. Akiyama, 1993)
- 第32号 直下型地震予知に関する観測的研究 (地震火山研究部, 1994)  
Observational Study on the Prediction of Disastrous Intraplate Earthquakes. (Seismology and Volcanology Research Department, 1994)
- 第33号 各種気象観測機器による比較観測 (気象衛星・観測システム研究部, 1994)  
Intercomparisons of Meteorological Observation Instruments. (Meteorological Satellite and Observation System Research Department, 1994)
- 第34号 硫黄酸化物の長距離輸送モデルと東アジア地域への適用 (応用気象研究部, 1995)  
The Long-Range Transport Model of Sulfur Oxides and Its Application to the East Asian Region. (Applied Meteorology Research Department, 1995)
- 第35号 ウィンドプロファイラーによる気象の観測法の研究 (気象衛星・観測システム研究部, 1995)  
Studies on Wind Profiler Techniques for the Measurements of Winds. (Meteorological Satellite and Observation System Research Department, 1995)
- 第36号 降水・落下塵中の人工放射性核種の分析法及びその地球化学的研究 (地球化学研究部, 1996)  
Geochemical Studies and Analytical Methods of Anthropogenic Radionuclides in Fallout Samples. (Geochemical Research Department, 1996)

# 気象研究所

1946 (昭和21) 年 設立

所 長 : 長谷川 隆 司

予報研究部 部長 : 理博 吉住 禎夫  
気候研究部 部長 : 近藤 洋輝  
台風研究部 部長 : 八木 正允  
物理気象研究部 部長 : 白崎 航一  
環境・応用気象研究部 部長 : 理博 花房 龍男  
気象衛星・観測  
システム研究部 部長 : 田中 豊顯  
地震火山研究部 部長 : 望月 英志  
海洋研究部 部長 : 理博 宇治 豪  
地球化学研究部 部長 : 理博 伏見 克彦

## 気象研究所技術報告

編集委員長 : 近藤 洋輝

編集委員 : 加藤 政勝 山崎 信雄 村田 昭彦  
深堀 正志 堤 之智 鈴木 修  
上垣 内修 山中 吾郎 松枝 秀和  
事務局 : 佐藤 博 岡田 孝文

気象研究所技術報告は、1978 (昭和53) 年の初刊以来、気象研究所が必要の都度発行する刊行物であり、原則として気象研究所職員及びその共同研究者による気象学、海洋学、地震学その他関連の地球科学に関する技術報告、資料報告及び総合報告 (以下報告という) を掲載する。

気象研究所技術報告の編集は、編集委員が行う。編集委員会は原稿の掲載の可否を判定する。

本誌に掲載された報告の著作権は気象研究所に帰属する。本誌に掲載された報告を引用する場合は、出所を明示すれば気象研究所の許諾を必要としない。本誌に掲載された報告の全部又は一部を複製、転載、翻訳、あるいはその他に利用する場合は気象研究所の許諾を得なければならない。個人が研究、学習、教育に使用する場合は、出所を明示すれば気象研究所の許諾を必要としない。

気象研究所技術報告 ISSN 0386-4049

第 37 号

平成11年2月26日 発行

編集兼  
発行者 気象研究所

〒305-0052 茨城県つくば市長峰1-1

TEL. (0298) 53-8535

印刷所 株式会社 イセブ

〒305-0005 茨城県つくば市天久保2-11-20